2019-01-01

Damage Quantification Of Energy Developing Areas Of South Texas Using The Axle Load Spectra

Carlos Licon
University of Texas at El Paso

DAMAGE QUANTIFICATION OF ENERGY DEVELOPING AREAS OF SOUTH TEXAS USING THE AXLE LOAD SPECTRA

CARLOS LICON JR.

Master's Program in Civil Engineering

APPROVED:

Reza Ashtiani, Ph.D., P.E., Chair,

Ruey Cheu, Ph.D. P.E.

Diane Doser, Ph.D.

Yirong Lin, Ph.D.

Stephen L. Crites, Jr., Ph.D.
Dean of the Graduate School

DEDICATION

I dedicate this thesis to my parents, Carlos Licon and Maria Licon, my brother, Kevin Licon, and the love of my life, Nancy Gutierrez; whose continuous support and words of encouragement helped push me to complete this thesis.

DAMAGE QUANTIFICATION OF ENERGY DEVELOPING AREAS OF SOUTH TEXAS USING THE AXLE LOAD SPECTRA

by

CARLOS LICON JR., BSCE, EIT

THESIS

Presented to the Faculty of the Graduate School of

The University of Texas at El Paso

in Partial Fulfillment

of the Requirements

for the Degree of

MASTER OF SCIENCE

Department of Civil Engineering

THE UNIVERSITY OF TEXAS AT EL PASO

August 2019

ACKNOWLEDGEMENTS

I would like to express my sincere gratitude to my graduate advisor and committee chairman Dr. Reza Ashtiani for his guidance, support, and mentorship. His dedication and passion for teaching and inspiring his students is unparalleled. I would also like to thank Dr. Cesar Tirado for always being accessible and willing to provide valuable feedback. His challenging courses pushed me to become a better student. I thank Sergio Rocha for always accompanying me and working with my schedule to conduct all our field trips. There was never a dull moment travelling in the car with him. I also want to extend my gratitude to Dr. Ruey Cheu, Dr. Diane Doser, and Dr. Yirong Lin for being part of my thesis committee.

Moreover, I would also like to acknowledge the support and assistance from my peers and colleagues Ali Morovatdar, Mohammed Rashidi, Jesus Baca, Hector Lopez, German Garay, and Margarita Ordaz. Finally, I would also like to thank The Texas Department of Transportation for providing the funds and support to conduct this research.

ABSTRACT

Advances in technology, particularly in crude oil extraction, natural gas production, wind energy farms, and other pertinent industries have contributed to exponential growth in energy development activities. In Texas, this energy boomed created large volumes of Over-Size/Over-Weight (OS/OW) truck traffic operations that adversely affected the service life of the transportation infrastructure in the network. This study focused on characterizing the traffic operations in overweight corridors and energy sector zones of South Texas in order to properly quantify the damage induced by overweight vehicles on the pavement structures. To achieve this, the Axle Load Spectra (ALS) database was developed through deployment of portable Weigh-in-motion (WIM) devices on ten selected highways. In addition, nondestructive tests such as Ground Penetrating Radar (GPR) and Falling Weight Deflectometer (FWD) test were conducted on the representative pavement sections to obtain site-specific pavement characteristics. The data collected from portable WIM devices, FWD, and GPR tests were incorporated into the Texas Mechanistic-Empirical pavement design (TxME) to run numerical simulations to predict the service life of each highway. The different methods used to incorporate the traffic information (i.e. Axle Load Spectra, ESALs, and Default TxME traffic values) showed significant differences in the predicted service life of the representative highways. The results showed that utilizing the Axle Load Spectra of a site-specific highway in the service life analysis led to the most accurate prediction in service life, while using the default TxME traffic values led to the worst prediction in service life.

TABLE OF CONTENTS

LIST OF TABLES

LIST OF FIGURES

CHAPTER 1: INTRODUCTION

1.1 Problem Statement

Development of energy resources in energy sector zones will significantly contribute to the economy of the impacted counties and the state as a whole for many years to come. It provides employment for thousands of Texans, especially in economically disadvantaged areas in the region. Additionally, since the beginning of the drilling operations in the region, the influx of workforce and severance taxes has resulted in the generation of unprecedented tax revenue for many local government agencies in Texas energy sector zones. Despite many positive economic impacts, the development of energy resources has adversely impacted the transportation infrastructure systems such as pavements and bridges. Since the onset of energy activities in the region, damaged local and county roads have been a major source of inconvenience for the local residents. There are several reported cases of severely damaged pavements that prevented access by school buses and emergency vehicles. Deteriorated highway systems also have caused major operational and logistical concerns for the energy companies active in the energy development regions. More importantly, premature failure of the local and country roads due to the passage of heavy truck traffic also contributed to an increase in the number of accidents and fatalities in the region.

Due to the sudden explosion of drilling activities, the local governing agencies and TxDOT were not able to ramp up their pavement preservation and maintenance efforts to meet the unexpected demand. Lack of funding resources, coupled with unclear guidelines are among the many elements that contribute to the delay of the pavement maintenance and repair in several counties. The unaccounted number of load applications of permitted and unpermitted overweight vehicles can potentially reduce the service life of the pavements and bridges. In addition to damaging the highways designed to carry legal loads, up to 80,000 lb. gross weight, heavy trucks used by the energy companies are also traveling overload-zoned roads, which are designed to accommodate vehicles that weight less than 58,420 lb. These roads are not designed to withstand such heavy loads; therefore, even a few passages of heavy trucks will cause permanent damage and consumes the life of the pavement. The loss of serviceability of the pavements is more pronounced in Farm to Market (FM) roads at the local level in the energy development areas. Therefore, there is a pressing need to properly characterize the traffic and to quantify the damages

imparted by the energy-related vehicles to protect the taxpayers' investment in the transportation system. The first step for the mechanistic quantification of the damages relies on the accurate account of the traffic operations in impacted zones. For this reason, this study aims to explore a robust methodology to quantify the traffic operations in the impacted corridors in South Texas. The most promising approach, as adopted by the new Mechanistic-Empirical Pavement Design Guide (MEPDG), is the concept of axle load spectra. In this approach, the performance of the pavement sections is tied to the hourly, daily, seasonal, and annual distributions of different classes of traffic. The Texas Mechanistic-Empirical pavement design system (TxME), designed under TxDOT Project 0-6622, adopted the incremental damage concept for the characterization of the performance of flexible pavement structures. This will allow for the determination of incremental damage imparted by a specific class of truck at a specific timeframe on a pavement section. The axle load spectra characterization is an integral component for the calculation of the cumulative damage during the service life of pavements. Therefore, it is necessary to develop pertinent databases of traffic operations as a function of time and vehicle classification. This will allow for accurate assessment of the damage imparted to the highway pavement and the reduction in service life due to overload truck operations.

1.2 Objectives

The primary objectives of this study were twofold, the first objective was to develop the axle load spectra database for energy developing areas of South Texas by deployment of portable Weigh-in-Motion (WIM) devices. The secondary objective of this study was to properly quantify the damage induced by heavy and overweight vehicles operations in the network. The information development in axle load spectra section was incorporated into the TxME to run numerical simulations in order to study the predicted service life of the selected highways.

1.3 Organization of Report

The contents of this report are divided into the following eight chapters: Chapter 1 Introduction, Chapter 2 Literature Review, Chapter 3 Survey of TxDOT's District, Chapter 4 Development of the Axle Load Spectra, Chapter 5 Non-Destructive Testing, Chapter 6 Numerical Analysis Methodology, Chapter 7 Results and Discussion, Chapter 8 Conclusion and Recommendations, Appendix A, and Appendix B.

CHAPTER 2: LITERATURE REVIEW

2.1 Texas Energy Sector and Impact of State Infrastructure Network

2.1.1 Economic Impact

Advances in technology, particularly in crude oil extraction, natural gas production, wind energy farms, and other pertinent industries have yielded exponential growth in energy development. The development of these energy resources in the energy sector zones substantially contributes to the economy of the state as well as individual sectors. In Texas, it predominantly influences economically disadvantaged areas where it provides employment for thousands of Texans. In addition, such economic activities provide several forms of tax revenue due to the generation of sales taxes, hotel taxes, and severance taxes. Figure 2. 1 shows the different shale plays across the continental United States and more importantly across Texas, where it is observed that most of the state lies in regions with basins and active shale plays.

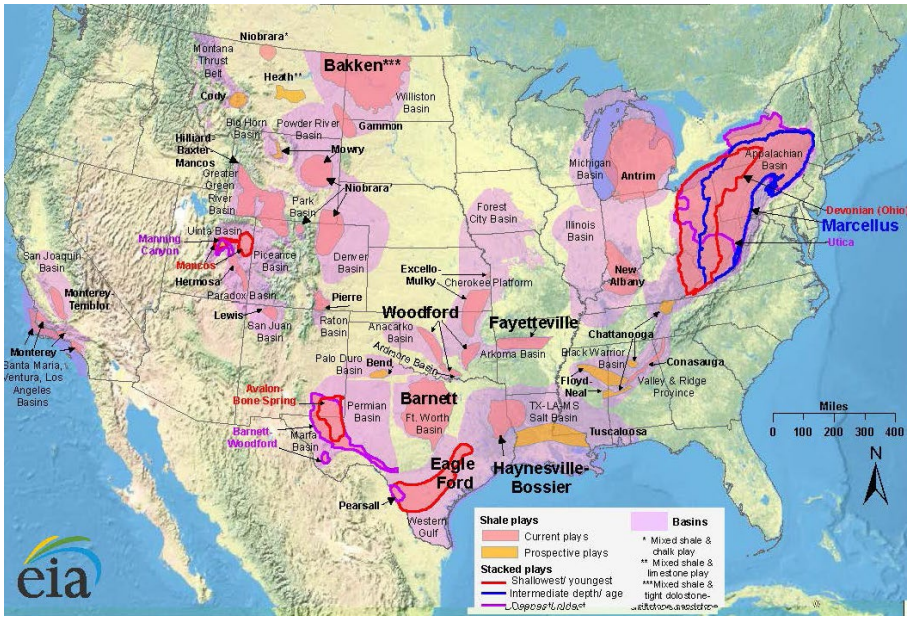

Figure 2.1 United States Oil and Gas Shale Regions (from U.S. Energy Information Administration, Drilling Productivity Report, 2011).

Energy development activities in the Eagle Ford Region alone have grown from 581 barrels per day in 2008, to over 1.1 million barrels per day as of June 2014, and over 4 billion cubic feet per day of natural gas (Turnstall et al., 2014). In the Permian Basin, the total crude oil production is estimated to be over 1.4 million barrels a day (Ewing et al., 2014). Figures 2.2 and 2.3 illustrate

the oil and natural gas production and the new-wells for oil and natural gas production for Eagle Ford Shale Region, respectively. Figures 2.4 and 2.5 show the oil and natural gas production and the new-wells for oil and natural gas production for the Permian Basin up to November 2017.

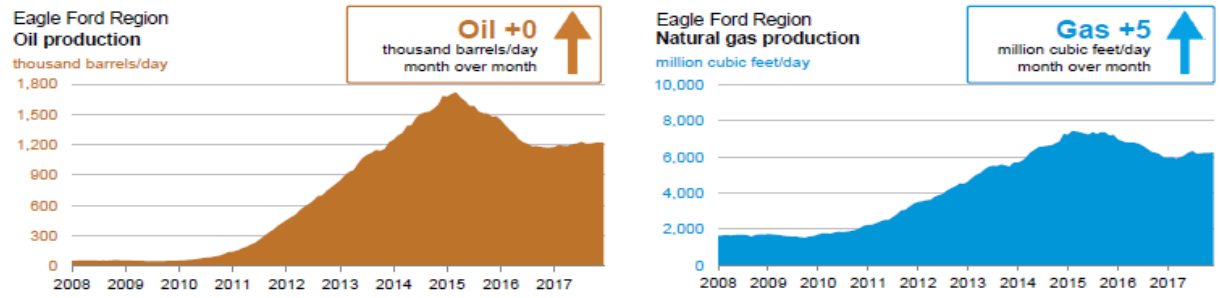

Figure 2.2 Oil and Natural Gas Production for the Eagle Ford Region (from U.S. Energy Information Administration, Drilling Productivity Report, 2017).

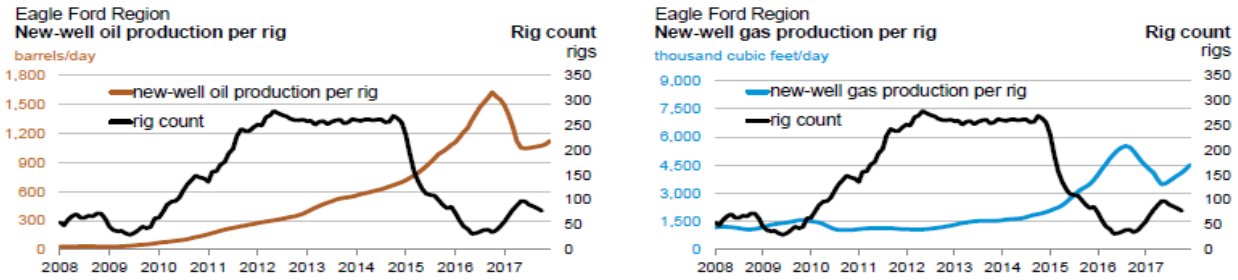

Figure 2.3 New-well Oil and Natural Gas Production for the Eagle Ford Region (from U.S. Energy Information Administration, Drilling Productivity Report, 2017).

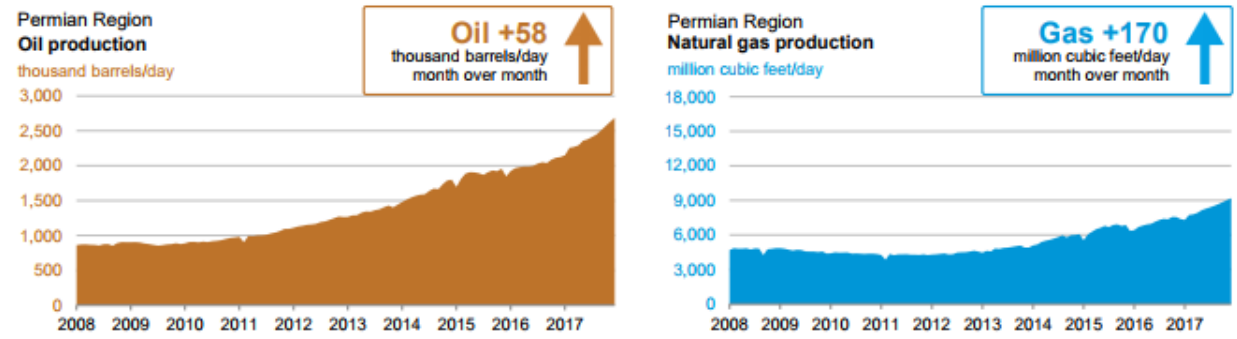

Figure 2.4 Oil and Natural Gas Production for the Permian Basin (from U.S. Energy Information Administration, Drilling Productivity Report, 2017).

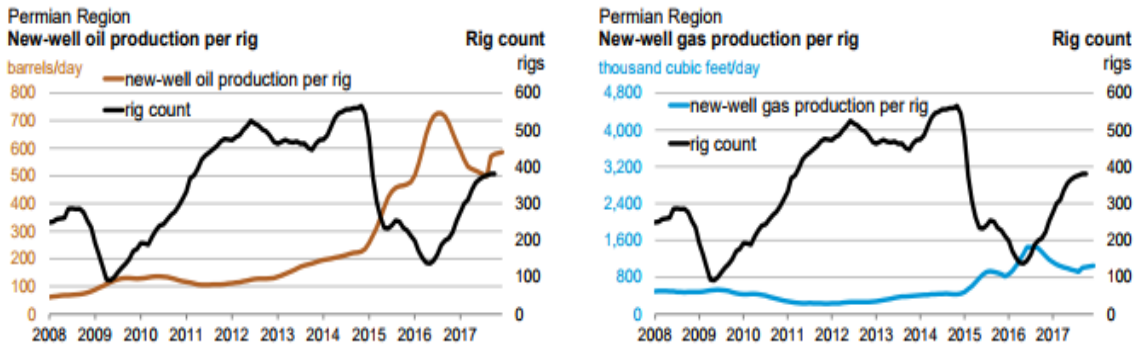

Figure 2.5 New-Well Oil and Natural Gas Production for the Permian Basin (from U.S. Energy Information Administration, Drilling Productivity Report, 2017).

The contributions of these energy development areas are excessively intriguing that several studies have been conducted to assess their socio-economic impacts in affected districts. A 2014 study conducted by the Rawls College of Business at Texas Tech University examined the economic impact of oil and gas industry in the Permian Basin (Ewing et al.,2014). The report maintains that in 2013, the Texas portion of the Permian Basin's oil and gas industry supported over 444,000 jobs, generated $113.6 billion in economic output, and contributed over $71.1 billion to the gross product of the state (Ewing et al., 2014). The detailed results of this study are tabulated in Table 2.1.

Table 2.1 Economic Impact of the Permian Basin in 2013, in Millions of USD (after Ewing et al., 2014)

Impact Type	Employment	Labor Income	Total Value Added	Output
Direct Effect	0.19	15,706.91	40,086.45	77,880.00
Indirect Effect	0.13	6,238.98	11,405.09	21,103.16
Induced Effect	0.12	4,297.03	8,724.07	14,646.35
Total Effect	0.44	26,242.09	60,215.61	113,629.51

Note: Labor income, total value added and output are measured in current USD.

In another study conducted by the Center of Community and Business Research (CCBR) at The University of Texas at San Antonio, the authors concluded that the Eagle Ford Shale is the largest single oil and gas development in the world based on capital expenditures (Turnstall et al., 2013). CCBR focused their study on the impacts of the 15 most active energy producing counties and their 6 neighboring counties. This study concluded that the economic impact in 2013 for the 21 county-area amounted to 155,000 jobs and $87 billion in total economic output (Turnstall et al., 2014). Total impacts for the Eagle Ford Shale are summarized in Table 2.2. The Eagle Ford

Shale paid nearly $5.6 billion in salaries and benefits to workers and provided over $2.2 billion for local and state governments (Turnstall et al., 2014). Additionally, the CCBR also made moderate predictions for the year 2023 in the 15-county area and the greater 21-county area that presented staggering revenue figures (Table 2.3). The 21-county area was estimated to employ 196,660 people, provide over $4 billion for local and state governments, and generate over $137 billion in economic output (Turnstall et al., 2014).

Table 2.2 Impacts of Eagle Ford Shale 21-County Area in 2013 (after Turnstall et al., 2014)

	Economic impact	**Direct**	**Indirect**	**Induced**	**Total**
Core 15-county area	Output	$61,470,280,412	$7,941,100,117	$2,418,234,050	**$71,829,614,579**
	Employment, full-time	42,607	52,333	19,375	**114,315**
	Payroll	$2,027,428,721	$1,539,076,337	$584,718,872	$4,151,223,930
	Gross regional product	$30,448,269,805	$4,333,962,004	$1,542,827,867	$36,325,059,676
	Local government revenues				$2,025,968,804
	State revenue, including severance taxes				$2,028,406,113
Core and neighboring 21-county area	Output	$70,725,115,021	$12,896,817,708	$4,135,496,654	**$87,757,429,382**
	Employment, full-time	51,652	71,648	31,684	**154,984**
	Payroll	$2,707,017,870	$2,036,271,899	$896,394,413	$5,639,684,182
	Gross regional product	$32,992,259,490	$7,199,851,186	$2,640,560,616	$42,832,671,293
	Local government revenues				$2,218,877,342
	State revenue, including severance taxes				$2,214,664,000

Table 2.3 Impacts of Eagle Ford Shale 21-County Area in 2023 (after Turnstall et al., 2014)

	Economic Impact	**Direct**	**Indirect**	**Induced**	**Total**
Core 15-county area	Output	$90,168,212,826	$10,893,464,660	$5,332,379,266	**$106,394,056,752**
	Employment, full-time	36,785	71,309	42,699	**150,793**
	Payroll	$6,311,816,751	$2,035,342,931	$1,289,319,720	$9,636,479,402
	Gross regional product	$52,608,595,765	$5,805,086,021	$3,402,243,230	$61,815,925,016
	Local government revenues				$3,741,688,868
	State revenue, including severance taxes				$3,774,006,283
Core and neighboring 21-county area	Output	$110,576,454,317	$19,636,284	$7,488,598,501	**$137,428,984,102**
	Employment, full-time	38,767	99,786	58,107	**196,660**
	Payroll	$6,718,204,896	$3,432,856,335	$1,927,647,160	$12,078,708,391
	Gross regional product	$57,330,415,830	$10,686,840,880	$4,777,170,284	$72,794,426,994
	Local government revenues				$4,073,239,614
	State revenue, including severance taxes				$4,098,369,070

2.1.2 Impact on Texas Infrastructure

Despite many positive economic impacts and benefits that energy companies generate; the development of these energy resources has significantly affected the state and local transportation infrastructure. This is more pronounced during oil and gas fracking operations where there is a large volume of truck traffic in a short timeframe associated with the transportation of fresh water, chemicals, and sand to the sites as well as the transportation of the wastewater from the sites (Bierling, et al., 2014). It is estimated that the volume of truck traffic to bring one gas well into production is equivalent to eight million cars and an additional two million cars per year to maintain one gas well (TxDOT, 2016). In addition to the substantial truck traffic operations, the transportation of heavy construction equipment and drilling rig components has also contributed to damages that local and county roads experience. These local and county roads were not designed or built to accommodate such high volumes of truck traffic or heavy loads. Therefore, even a few passages such as exceeding loading conditions can result in substantial damage and reduced service life of transportation facilities in the region. Moreover, these roads lack appropriate width to accommodate wider vehicles, thus increased truck traffic quickly deteriorates shoulders which in turn, contributes to the accelerated damage of the pavements and causes safety concerns for the travelling public (Bierling, et al., 2014). Damaged roads and bridges are also a major source of inconvenience for energy companies, local residents, school buses, and emergency vehicles. In the last five years of the state's ongoing drilling and fracking boom, Texas has become one of the deadliest states in total traffic fatalities, with over 3,120 fatalities in 2015 (Olsen, 2014). Table 2.4 provides information on motor vehicle crash deaths per state and highlights Texas as the state with the most fatal crashes, deaths, and deaths per 100 million vehicle miles travelled.

Table 2.4 Motor Vehicle Crash Deaths per State in 2015 (after Insurance Institute for Highway Safety, 2016)

State	Population	Vehicle miles traveled (millions)	Fatal crashes	Deaths	Deaths per 100,000 population	Deaths per 100 million vehicle miles travel
Alabama	4,858,979	67,257	783	849	17.5	1.26
Alaska	738,432	5,045	60	65	8.8	1.29
Arizona	6,828,065	65,045	810	893	13.1	1.37
Arkansas	2,978,204	34,897	472	531	17.8	1.52
California	39,144,818	335,539	2,925	3,176	8.1	0.95
Colorado	5,456,574	50,437	506	546	10.0	1.08
Connecticut	3,590,886	31,592	253	266	7.4	0.84
Delaware	945,934	9,931	122	126	13.3	1.27
D.C.	672,228	3,557	23	23	3.4	0.65
Florida	20,271,272	206,982	2,699	2,939	14.5	1.42
Georgia	10,214,860	118,107	1,327	1,430	14.0	1.21
Hawaii	1,431,603	10,301	86	94	6.6	0.91
Idaho	1,654,930	16,662	198	216	13.1	1.30
Illinois	12,859,995	105,223	914	998	7.8	0.95
Indiana	6,619,680	78,819	756	821	12.4	1.04
Iowa	3,123,899	33,161	282	320	10.2	0.96
Kansas	2,911,641	31,379	322	355	12.2	1.13
Kentucky	4,425,092	48,675	694	761	17.2	1.56
Louisiana	4,670,724	48,180	674	726	15.5	1.51
Maine	1,329,328	14,629	144	156	11.7	1.07
Maryland	6,006,401	57,516	472	513	8.5	0.89
Massachusetts	6,794,422	59,257	291	306	4.5	0.52
Michigan	9,922,576	97,843	893	963	9.7	0.98
Minnesota	5,489,594	57,395	375	411	7.5	0.72
Mississippi	2,992,333	39,890	604	677	22.6	1.7
Missouri	6,083,672	71,918	802	869	14.3	1.21
Montana	1,032,949	12,345	204	224	21.7	1.81
Nebraska	1,896,190	20,101	218	246	13	1.22
Nevada	2,890,845	25,925	296	325	11.2	1.25
New Hampshire	1,330,608	13,094	103	114	8.6	0.87
New Jersey	8,958,013	75,393	522	562	6.3	0.75
New Mexico	2,085,109	27,435	269	298	14.3	1.09
New York	19,795,791	127,230	1,046	1,121	5.7	0.88
North Carolina	10,042,802	111,879	1,275	1,379	13.7	1.23
North Dakota	756,968	10,036	111	131	17.3	1.31
Ohio	11,613,423	113,673	1,029	1,110	9.6	0.98
Oklahoma	3,911,338	47,713	588	643	16.4	1.35
Oregon	4,028,977	35,999	412	447	11.1	1.24
Pennsylvania	12,802,503	100,945	1,102	1,200	9.4	1.19
Rhode Island	1,056,298	7,833	41	45	4.3	0.57
South Carolina	4,896,146	51,726	909	977	20.0	1.89
South Dakota	858,469	9,324	115	133	15.5	1.43
Tennessee	6,600,299	76,670	884	958	14.5	1.25
Texas	27,469,114	258,122	3,124	3,516	12.8	1.36
Utah	2,995,919	29,604	256	276	9.2	0.93
Vermont	626,042	7,314	50	57	9.1	0.78
Virginia	8,382,993	82,625	711	753	9.0	0.91
Washington	7,170,351	59,653	516	568	7.9	0.95
West Virginia	1,844,128	19,827	246	268	14.5	1.35
Wisconsin	5,771,337	62,073	523	566	9.8	0.91
Wyoming	586,107	9,597	128	145	24.7	1.51
U.S total	321,418,821	3,095,373	32,166	35,092	10.9	1.13

There is no exact way to correlate deaths to energy development activities. However, the counties that experienced the largest increase in accidents were in the Permian Basin and the Eagle Ford Shale, as shown in Figure 2.6. In 2013, there were 3,430 traffic reported accidents in the energy development areas that resulted in serious injuries or fatalities. In addition, the 26-county area stretches from Laredo to Huntsville accounted for 236 of fatalities of the total reported accidents (TxDOT, 2014).

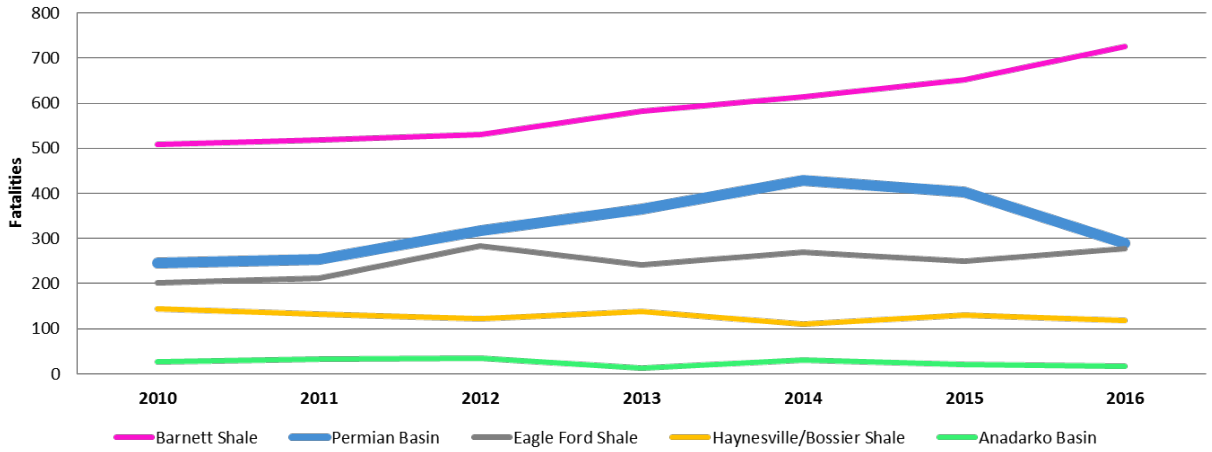

Figure 2.6 Safety Statistics in the Texas Energy Sectors in 2010 through 2016 (from TxDOT, Permian Road Safety Coalition Safety Forum, 2017).

2.1.3 Significance of the Research

TxDOT is currently seeking a methodology to assess the energy development impacts on the transportation infrastructure in energy development regions. The lack of a uniform and practical structure for dealing with the impacts of the energy development has resulted in unclear and even contradicting approaches. Given this situation, it is imperative to properly characterize the traffic distributions in the region to properly assess the damages imparted by heavy truck operations in the affected network. According to the Center for Community and Business Research (CCBR), it is estimated that roadways currently require $2 billion in total maintenance per year, $1 billion for damage to state highways and $1 billion for damages to local and county roads (Turnstall et al., 2013). However, many counties do not have the funding to address these damaged roads. Rebuilding a paved road can cost local agencies more than $1 million amounting to the total annual maintenance and construction budget that most of these departments can afford to allocate (TxDOT, 2016). Damaged roads also affect the energy development industry in the forms of

equipment damage and lower operating speeds due to poor road conditions amounting to $1.5 to 3.5 billion (Epps et al., 2013).

2.1.4 Strategies to Address Energy Development Impacts

Other state DOTs have implemented several policies and programs to help address the impacts of energy developments. For example, they have posted weight limits, created bonds and maintenance agreements. In addition to establishing active industry engagement and implementing provisional capital improvement programs (Bierling, et al., 2014). Several DOTs have also established a policy to reduce the allowable weight of roads and bridges to 10 tons or less per vehicle to preserve the service life of their transportation infrastructure. States such as Pennsylvania and West Virginia have created bond policies and road use agreements with the energy development users that places financial and roadway maintenance responsibility on them (Bierling, et al., 2014). One Pennsylvania DOT official reported that the energy development industries in their states have covered "tens to hundreds of millions of dollars" in roadway maintenance and upgrades.

Pennsylvania has also created highly active industry engagement programs such as the Governor's Marcellus Shale Advisory Commission and has enforced regular meetings with the Marcellus Shale Coalition. These meetings are regarded as highly effective because they allow Pennsylvania DOT officials to work alongside the industry to address roadway needs. The lack of such programs in most states leads to limited communication with energy companies, difficulties solving problems and poor planning of future developments. TxDOT has initiated this strategy by conducting workshops with energy sector stakeholders. Additionally, increases in transportation funding allow DOTs to create capital improvement programs that enhance the serviceability of roadway infrastructures in energy development areas. TxDOT has created capital improvement programs to target the energy development sectors with the House and Senate appropriations such as the HB 1025, 83R, 2015 - $225 million and the SB 1747, 83R, 2015 - $225 million (TxDOT, 2016).

In 2016, TxDOT created the Energy Sector Corridor Improvement program to strengthen pavements and provide safety enhancements on important roads. The program identified road projects by prioritizing corridors with high frequencies of injury or fatal crashes, segments that cross multiple districts, and segments that connect energy sector activity. TxDOT then identified and categorized these corridors into two priorities; Priority 1 and Priority 2. The Energy Sector

Corridor Improvement program proposed the corridor improvement estimates as displayed in Table 2.5. The results indicate that the largest dollar amount for the rehabilitation of pavements is associated with the Eagle Ford Shale ($596 million) and the Permian Basin ($676 million) (TxDOT, 2016). The total funding needs for Priority 1 corridors amounted to $1.8 Billion in projects, while an additional $1.25 Billion in projects was identified for Priority 2 corridors, as shown in Tables 2.5 and 2.6, respectively. The energy sector corridor improvements are allocated to the strengthening of 1,125 miles of pavement; adding 50 miles of shoulders, 20 miles of lanes and constructing 521 miles of passing lanes in Super-2 Corridors (TxDOT, 2016).

Table 2.5 Energy Sector Corridor Improvement Estimates (Reproduced from TxDOT, Transportation Planning and Programming Division)

Energy Play Energy Play	Priority 1 Corridor Estimate
Eagle Ford Shale	$596M
Permian Basin	$676M
Barnett Shale	$271M
Anadarko Basin	$97M
Haynesville-Bossier	$179M
Total	**$1.8 Billion**

Table 2.6 Energy Sector Corridor Improvement Miles (Reproduced from TxDOT, Transportation Planning and Programming Division)

Energy Sector Corridor Improvements Energy Sector Corridor Improvements	
Strengthening/ Reinforcing Pavement Structure	1,125 miles
Adding Shoulders to Protect Pavement Edges	50 miles
Adding/Widening lanes for Safety	20 miles
Constructing Passing Lanes on Super 2 Corridor	521 miles
Total Miles to Improve	**1,716 miles**

There is no doubt that energy development sectors have a positive economic impact on the local and state economies, and this impact is expected to continue for more than a decade. However, the damages that heavy truck volumes impart on the transportation's infrastructure are severe and cannot be neglected, Figure 2.7 illustrates a map of the major energy developing areas throughout Texas. It is estimated that between 12,000 to 24,000 oil and gas wells were permitted each year in Texas for the last decade (Railroad Commission of Texas, 2013). Figure 2.7 illustrates

the oil and gas wells permitted between 2010-2015. The truck traffic associated with each good development and production is estimated to range from 1,000 to 4,000 loaded trucks per well.

The total loaded trucks traveling to and from wells represents a significant amount of loaded truck volume that local and county roads were not designed to accommodate. As a result of the increased truck traffic, these roads quickly deteriorate and require substantial maintenance and reparations. In addition, maintenance costs on severely damaged Farm to Market roads has increased significantly from $500 - $1,500 per mile prior to oil and gas developments to $35,000 -$45,000 post-development (Epps and Newcomb, 2016). Local governments are expected to spend around $200 million per year for maintenance and rehabilitation. While at the state level, it is anticipated that TxDOT will invest $500 million per year for safety, maintenance and capacity need on the energy sector oil and gas impacted roadways (Epps and Newcomb, 2016). The authors also concluded that taking precautionary measures to address roadway conditions is a more cost-effective approach to protect the transportation infrastructure facilities

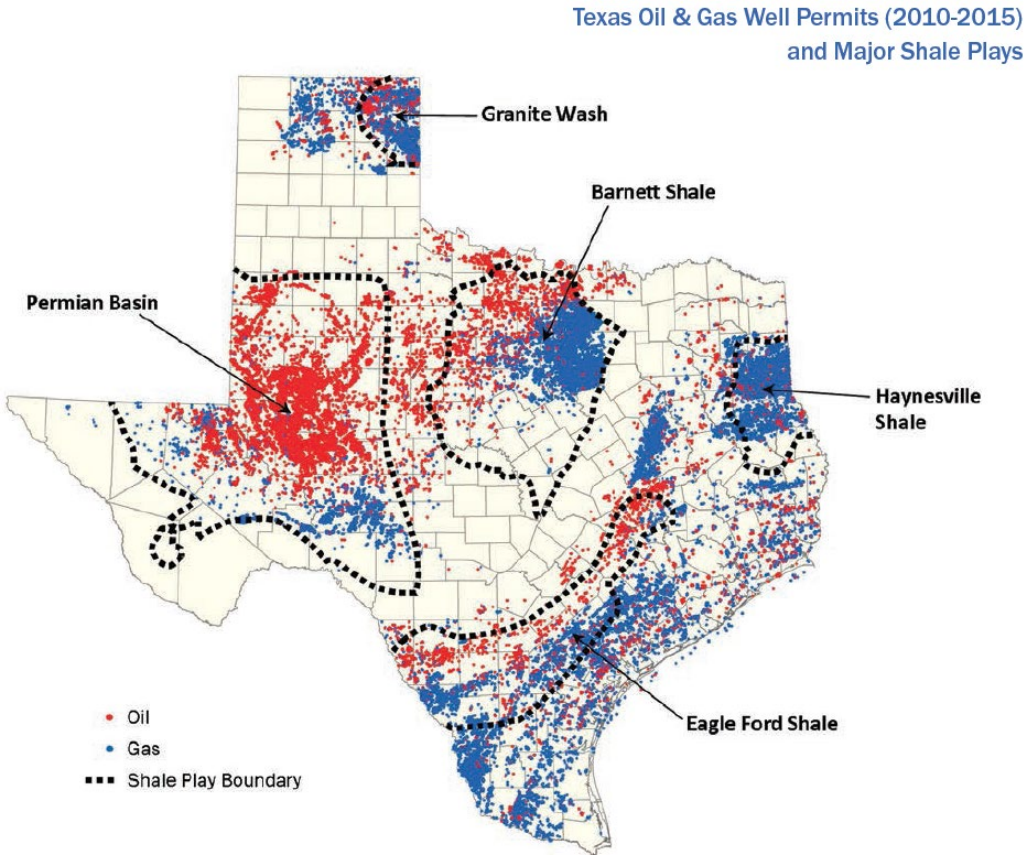

Figure 2.7 Texas Oil and Gas Well Permits from 2010 to 2015 (from TxDOT, 2016)

2.2 Traffic Characterization

2.2.1 FHWA Vehicle Classification

The Federal Highway Administration (FHWA) classifies vehicular traffic into 13 vehicle classifications beginning with motorcycles in Class 1 through trucks with seven or more axles in Class 13. The most prevalent commercial truck configuration is the five-axle tractor-semitrailer that belongs to Class 9. Figure 2.8 illustrates the FHWA Vehicle Classification Chart, while the following list provides a brief description of each vehicle class (FHWA, 2014).

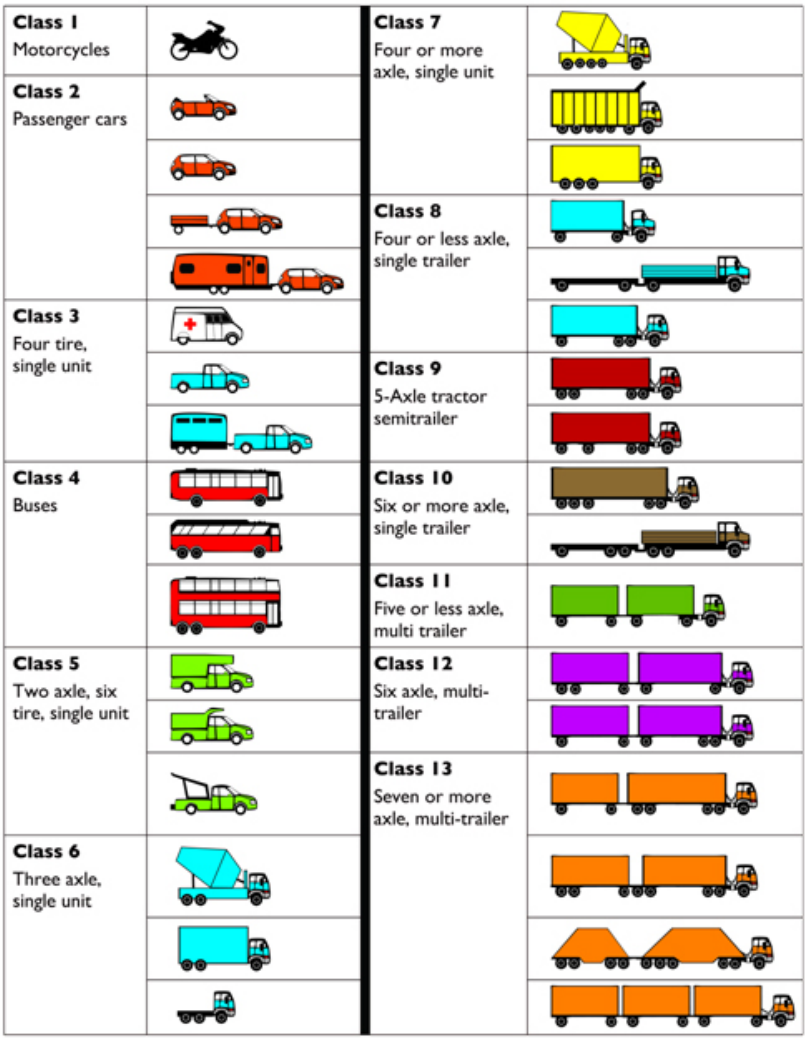

Figure 2.8 FHWA 13 Vehicle Classification Chart (from the Federal Highway Administration, 2014).

2.2.2 Texas's Current Axle and Weight Limits

Table 2.7 lists the maximum GVW limits, axle loads limits, and truck size limits that are allowed on Texas Highway without a permit. The Texas Transportation Code Chapter 621: "General provisions relating to vehicle size and weight" sets Texas's current Truck Size and Weight (TS&W) regulation. Table 2.8 provides the maximum legal weight as a function of a number of axles and distance any group of two or more consecutive axles. The maximum legal weights can be calculated using equation 2.1 as:

$$W = 500 \cdot \left[\frac{L \cdot N}{N-1} + 12 \cdot N + 36\right] \quad (2.1)$$

where W is the maximum overall Gross Vehicle Weight (GVW) of the group, L is the distance in feet between the axles of the group that are the farthest apart, and N is the number of axles in the group.

Table 2.7 Texas Permissible Truck Size and Weight Limits (after TxDOT)

Item/ Description	Limits	Illustrations
Weight		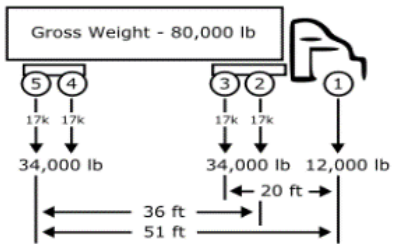
Gross Vehicle Weight	80,000 lb.	
Steering (Front) Axle	12,000 lb.	
Tandem Axle Group	34,000 lb.	
Tridem Axle Group	42,000 lb.	
Quad Axle Group	50,000 lb.	
Size		
Width	8.5 ft (8 ft 6 inches)	
Height	14.0 ft (14 ft 0 inches)	
Length		
Single-Motor Vehicle	45.0 ft (45 ft 0 inches)	
Truck-Tractor	Unlimited	
Semitrailer or two vehicle combination	59.0 ft (59 ft 0 inches)	
Two- or three-vehicle combination	65.0 ft (65 ft 0 inches)	
*A tire may not carry a heavier weight than the weight specified and marked on the sidewall of the tire.		

Table 2.8 Texas Current Texas Permissible Weight Table (after TxDOT and TxDMV)

Distance in Feet	Axles					
	2	3	4	5	6	7
4	34,000					
5	34,000					
6	34,000					
7	34,000					
8	34,000	34,000				
8+	38,000	42,000				
9	39,000	42,500				
10	40,000	43,500				
11		44,500				
12		45,000	50,000			
13		45,000	50,500			
14		46,500	51,500			
15		47,500	52,000			
16		48,000	52,500	58,000		
17		48,500	53,500	58,500		
18		49,900	54,000	59,000		
19		51,400	54,500	60,000		
20		52,800	55,500	60,500	66,000	
21		54,000	56,000	61,000	66,500	
22		54,000	56,500	61,500	67,000	
23		54,000	57,500	62,500	68,000	
24		54,000	58,700*	63,000	68,500	74,000
25		54,500	59,650*	63,500	69,000	74,500
26		55,500	60,600*	64,000	69,500	75,000
27		56,000	61,550*	65,000	70,000	75,500
28		57,000	62,500*	65,500	71,000	76,500
29		57,500	63,450*	66,000	71,500	77,000
30		58,500	64,000*	66,500	72,000	77,500
31		59,000	65,350*	67,500	72,500	78,000
32		60,000	66,300*	68,000	73,000	78,500
33			67,250*	68,500	74,000	79,000
34			68,200*	69,000	74,500	80,000
35			69,150*	70,000	75,000	
36			70,100*	70,500	75,500	
37			71,050*	71,000	76,000	
38			72,000*	72,000*	77,000	
39			72,000*	72,500	77,500	
40			72,000*	73,000	78,000	
41			72,000*	73,500	78,500	
42			72,000*	74,000	79,000	
43			72000*	75,000	80,000	
44			72000*	75,500		
45			72,000	76,000		
46			72,500	76,500		
47			73,500	77,500		
48			74,000	78,000		
49			74,500	78,500		
50			75,500	79,000		
51			76,000	80,000		

*These figures were carried forward from Article 6701d-11, Section 5(a)(4) when Senate Bill 89 of the 64th Texas Legislature amended it on December 16, 1974. The amendment provided that axle configurations and weights that were lawful as of that date would continue to be legal under the increased weight limits.

*These figures apply only to an axle spacing greater than 8 feet but less than 9 feet.

2.3 Pavement Design Approaches

2.3.1 AASHTO 1993 Pavement Design Guide

AASHTO's Guide for Design of Pavement Structures has been extensively used as a reference for the design of new and rehabilitated highways pavements. AASHTO's Guide was established based on empirical design approaches obtained from the AASHTO Road Test. The primary motivation for this design approach was to establish a uniform framework for the design and rehabilitation of rigid and flexible pavements (AASHTO, 1993). However, there are several drawbacks associated with the AASHTO's pavement design guide. The first problem that pavement designers and other professionals face is that accepted procedures rely on experimental information that was developed 50 to 60 years ago from field measurements in the late 1950s and early 1960s. Additionally, the Road Test was limited to one location, Ottawa in Illinois, with single subgrade type, specific climatic condition, and approximately 1.2 million load repetitions The relationships that were established from the AASHTO Road Test are more relevant to similar design parameters, vehicle characteristics, and climatic conditions. For instance, the data used to develop the actual AASHTO Guide equations were based on traffic loadings of approximately 1.2 million 18-kip ESALs. In contrast, pavements today are designed to carry loadings beyond 100 million 18-kip ESALs during their design life (Hallin et al., 2007). Consequently, designs based on projections that are beyond the dataset tend to be significantly inaccurate and untrustworthy. Additionally, limited material inputs into the design procedure of flexible pavements did not allow for new changes and improvements of materials. Listed below are some of the limitations associated with the nature of the AASHTO Road Test as follows (Highway Research Board, 1962).

1. The experiments were not inclusive of all the materials as they only tested materials and road soils related to that specific site.
2. The test site experienced environmental conditions not representative of conditions in all regions. The experiments were conducted at one specific site with unique environmental condition that are not representative of diverse climate of the US.
3. Relationships were extrapolated to longer design periods (15-30 years) using limited 2-year field test data.
4. Limited type of trucks used for trafficking the test sections.
5. The current construction equipment and techniques are vastly different from 1960s.

The traffic characterization in the AASHTO's Guide for Design of Pavement Structures relied on the Equivalent Single Axle Loads (ESAL's) concept. An ESAL is the number and weight of all axle loads from vehicles expressed as 18,000-lbs or 18kips, the reference axle load is an 18-Kip load carried by a single axle with dual tires (TxDOT, 2005). This concept was developed to establish a damage relationship for comparing the effects of axles carrying different weight. The design of ESALs is a traffic load summary statistic that represents a mixed stream of traffic with different axle configurations and axle loads estimated over an analysis period of a pavement and converted to an equivalent number of 18-Kip single axle loads (TxDOT, 2005). The procedure for calculating design ESALs are summarized in Table 2.9.

Table 2.9 Formulation for Determining ESALs.

Formulation	Equation	Variables
ESALs	$\sum ESALs = T_f TGDL(365)Y$	T_f = truck factor T = percentage of trucks in average daily traffic (ADT) G = growth factor D = directional distribution factor L = lane distribution factor Y = design period in years
Truck factor T_f	$T_f = \left(\sum_{i=1}^{m} p_i F_i \right) A$	p_i = percentage of total repetitions F_i = equivalent axle load factor for the i^{th} load group A = average number of axles per truck m = number of axle groups
Growth factor G	$G = \frac{(1+g)^n - 1}{g}$	g = annual growth rate n = analysis period in years

2.3.2 Mechanistic-Empirical Pavement Design Guide

The National Cooperative Highway Research Program (NCHRP) under Project 1-37A was established to improve the pavement design procedure. This updated Mechanistic-Empirical Pavement Design Guide (MEPDG) was based on an extensive assessment of previous research, practices, literature, and available databases relevant to pavement design. The MEPDG provided a uniform basis for the design of flexible, rigid, and composite pavements. This hierarchical design

methodology incorporated comprehensive traffic, climatic, and material properties of layers for reliable analysis and design of pavements. To aid in the implementation of the new design procedure the NCHRP created supporting software along with training documents. The following section provides detailed explanation regarding the use of axle load spectra for the characterization of the traffic information in the MEPDG.

2.3.3 Axle Load Spectra

The axle load spectra or axle load distribution factors are the percentage of the total axle applications within each weight interval for single, tandem, tridem, and quad axle configurations (Jiang et al, 2008). The axle load spectra approach was a major departure from the traditional ESAL quantification, explained in Chapter 4 of this report. According to Jiang et al. (2008), using the axle load spectra to represent vehicle loads as the traffic input in the MEPDG software will enable users to: analyze the impacts of different traffic loads on pavements, analyze the effects of different materials and impacts of seasons, perform forensic analysis of pavement conditions, and to provide an optimal pavement structure design. The load intervals for each axle configuration are defined as: single axles (3,000 lb. to 40,000 lb. at 1.000 lb. intervals), tandem axles (6,000 lb. to 80,000 lb. at 2,000 lb. intervals), and tridem and quad axles (12,000 lb. to 102,000 lb. at 3,000-lb. interval) (NCHRP 2004). Examples and figures are illustrated in Chapter 4 of this thesis.

Prozzi et al. (2005) conducted a study to assess the implications associated with the new axle load spectra methodology in the MEPDG guide. The research team conducted a sensitivity analysis and pavement evaluation from traffic data provided by TxDOT's Transportation Planning and Programming Division (TPP). In addition, researchers developed a methodology for specifying the accuracy of WIM equipment based on the effect that it has on pavement performance. The authors concluded that the use of continuous distribution functions is more advantageous than the proposed discrete axle load spectra. Analysis of traffic growth rate and growth factors were also conducted, and tables were prepared for the selection of both of these factors. The authors claimed the use of traffic growth rate and growth factors allow pavement

designers to select values based on the anticipated design reliability. The authors also highlighted the issues associated with non-uniform distribution of the WIM stations across Texas highways. Ultimately, the researchers reported the following outcomes and recommendations for their study:

1. Significant benefits could result from collecting WIM data at 12-week intervals that would allow capturing weekly, monthly, and seasonal variations.
2. Traffic loading data should be pre-processed and only four axle configurations should be used for pavement design (steering axles, single axles with dual wheels, tandem and tridem axles).
3. To increase accessibility of WIM data, TPP's should consider a complementary system of temporary WIM stations that operate across Texas environments and facilities that are under-represented by the network of permanent WIM stations.
4. Traffic volume seasonality and growth are best forecasted by models that jointly capture both aspects simultaneously.
5. A plan should be developed to collect the following data for supporting the ME Guide: differentiation between single axles with single wheels and single axles with dual wheels, distribution of tire inflation pressures, and distribution of vehicle speed.

Turochy et al. (2005, 2015) conducted a study to examine the differences among national-level traffic inputs developed from the MEPDG, and state-level traffic inputs developed from Alabama Department of Transportation (ALDOT) WIM sites from site-specific traffic data. Researchers divided the entire traffic input range considered in the MEPDG into 13 groups and evaluated the effects of the three levels of data independently for each group. In addition, an unbiased quality control procedure was developed and applied to the ALDOT WIM data to produce traffic inputs at levels 1, 2, and 3. The researchers also determined the sensitivity of the pavement thickness required for the flexible and rigid pavement to different levels of traffic data in Alabama. Furthermore, they provided axle load recommendations for future use by ALDOT for both rigid and flexible pavements.

Xiao and Wu (2016) conducted a study that presents a systematic index approach to relate the truckload spectra directly to pavement performance and characterizes traffic loadings for volume, load, and damage. This study investigated the following four summary indices: cumulative truck volume (CTV), cumulative truckload (CTL), equivalent single axle load (ESAL), and relative pavement performance impact (RPPI) (Xiao, 2016). According to Xiao, numerical evaluation analysis of 30 axle load spectra, 18 vehicle class distributions, 2 truck configurations, and 2 pavement types were conducted to illustrate how the summary indices could be used. Results suggested that the systematic indices used in the study had a clear correlation with pavement performance. In addition, the results can aid engineers by allowing them to compare different load spectra and allowing them to understand the relationship between pavement performance and traffic for any specific design at any desired time (Xiao, 2016).

Prozzi et al. (2017) reviewed the work previously done under TxDOT Project 0-6736, Rider 36 Oversize/Overweight (OS/OW) Vehicle Fees Study, and extended the work to evaluate the effects of different axle configurations on pavements and bridges. According to the researchers, an increase in the current GVW and axle load limits would yield reduced fuel consumption, reduced CO2 emissions, and reduced truck congestion. The authors proposed an increase in current GVW and axle load limits in Texas and indicated that it would not result in increased infrastructure consumption. In contrast, they suggested using innovative axle configurations that would allow trucks to carry heavier loads with no additional pavement consumption. Furthermore, the researchers developed guidelines for infrastructure friendly vehicle configurations based on different factors such as axle type, load per axle, and the distance between axles. In addition, a cost recovery method that adequately funds repairs to roads used by the overweight vehicles was also developed.

Walubita et al. (2019) aimed to generate statewide site-specific traffic data that served as input for ME pavement design purposes. In this study the authors also proposed to explore the use portable WIM units and pneumatic tube classifiers to serve as commentary data to the permanent WIM stations in Texas. The study included 39 permanent WIM stations, 11 portable WIM stations,

and 15 pneumatic tube stations from which the authors used clustering analysis to group the WIM data and estimate future ME traffic data. In addition, the authors created excel macros to analyze the traffic data and an access database to report all the gather data. Other prominent studies related to the advancements in characterizing axle load spectra are summarized in Table 2.10.

Table 2.10 Previous Studies for Characterizing Axle Load Spectra

Authors	Objective	Key Findings
Buchanan (2004)	The objective of this study was to assist the Mississippi Department of Transportation in developing traffic inputs and the axle load spectra for the new MEPDG guide.	Buchanan examined the WIM data that consisted of weight and axle distributions then determined the base annual axle load spectra for single, tandem, tridem, and quantum axle configurations for the Mississippi long-term pavement performance (LTPP) sites. The axle load spectra data that was developed helped them with the implementation of the new MEPDG.
Mohammad et al. (2005)	The primary objective of this study was to develop the axle load spectra for the state of Washington using axle load data collected from permanent WIM stations located throughout the state. The secondary objective was to compare the values from the developed load spectra to historical ESALs data.	Researchers were able to develop the axle load spectra that is compatible with the requirements of the MEPDG for the state of Washington. They concluded that for single axle configuration the values they obtained were fairly similar to the default values of the MEPDG and the MnROAD results. While in tandem and tridem axles the values they produce were more conservative than the default values.
Turochy et al. (2005)	The objectives of this study were to develop accurate truck factors for use in pavement design and to develop new statistical models for axle load distributions.	Researchers evaluated the effects of variation in axle load spectra on pavement design requirements from different locations using the 1993 AASHTO pavement design guide and the MEPDG guide. A statistical model of axle load distribution was also created using data from WIM sites. The authors also reported that the developed single axle models explained 98.6% of the total variation in the data while the developed tandem axle models explained 96.2% of the total variation
Hajek et al. (2005)	This study followed the results of Phase 1 by the authors to develop a methodology for estimating axle load spectra. The objective of Phase 2 was to apply the methodology developed in Phase 1 for 500 LTPP sites to obtain annual axle load spectra.	Researchers evaluated the overall quality of traffic data for 980 (LTPP) sites and the projection of the axle loads for all LTPP sites with satisfactory traffic data. Moreover, axle load projections were developed for 558 LTPP traffic sites from all available data up to 1998 that had adequate traffic monitoring data in the IMS database.
Prozzi and Hong (2006)	The objective of this study was to assess the implications associated with the new axle load spectra methodology	The research team conducted sensitivity analysis and pavement evaluation from traffic data provided by TxDOT's Transportation

	in the MEPDG guide. The authors also considered the evaluation of current equipment and methodology for data collection and evaluation of the structural design of pavements.	Planning and Programming Division (TPP). In addition, researchers developed a methodology for specifying the accuracy of WIM equipment based on the effect that it has on pavement performance. It was determined that the use of continuous distribution functions is more advantageous than the proposed discrete axle load spectra.
Haider and Harichandran (2007)	The objective of this study was to develop a methodology for modeling the axle load spectra based on axle loads from truck weight and volume data.	This study concluded that using truck weights and proportions on a highway can be used to determine the axle load spectra for the different axle configurations. Truck weights can be estimated for existing data or they can be easily measured if adequate models are developed from local truck traffic characteristics.
Swan et al. (2008)	The objective of this study was to obtain the best default values for traffic input parameters required by the MEPDG.	This study used periodic commercial traffic surveys to obtain the best default values for traffic input parameters required by the MEPDG. Researchers developed default input parameters in terms of axle load spectra for two Ontario regions and compared them to the default values of the traffic input parameters required by the MEPDG. In addition, researchers also found the axle load spectra for Ontario has a smaller number of heavily overloaded axles, and peaks between loaded and unloaded axles are more distinct.
Jian et al. (2008)	The objective of this study was to provide traffic data input parameters required by the MEPDG using truck traffic information collected from WIM stations.	Researchers collaborated with the Indiana Department of Transportation (INDOT) to obtain truck traffic information from the traffic data collected by WIM stations. The truck traffic spectra and other traffic inputs were created for INDOT to implement in the MEPDG guide. Additionally, AADT data was used to analyze the spatial distributions of traffic volumes in Indiana.
Ishak et al. (2008)	The objective of this study was to address the traffic data needs of LADOTD for the implementation of the MEPDG.	Researchers conducted this study to address the traffic data needs associated with the implementation of the MEPDG. They also develop the axle load spectra from axle weight data obtained from 2003 to 2006 from portable WIM stations. And proposed recommendations to LA DOTD for the collection of traffic data.

Sayyady et al. (2011)	The objective of this study was to create regional average truck axle load distribution factors (ALDFs) using WIM data collected from North Carolina roadways using multidimensional clustering.	According to the researchers, the multidimensional clustering analysis developed representative clusters showing that ALDFs clusters have unique characteristics for primary roads, secondary roads, collectors, and local roads. In addition, this study's contributions are creating a multidimensional clustering analysis that is guided and supports MEPDG damage-based analysis, ALDF clusters that characterize specific traffic patterns in North Carolina, and an easy to use decision tree to help pavement designers to select ALDF input parameters.
Turochy et al. (2015)	The objective of this study was to examine the differences among national-level traffic inputs developed from the MEPDG, state-level traffic inputs developed from ALDOT WIM sites, and from site-specific traffic data.	Researchers divided the entire traffic input range considered in the MEPDG into 13 groups and evaluated the effects of the three levels of data independently for each group. The sensitivity of the pavement thickness required for flexible and rigid pavement of different levels of traffic data in Alabama was also developed. Ultimately, the authors provided axle load recommendations for future use by ALDOT for both rigid and flexible pavements.
Xiao and Wu (2016)	The objective of this study was to explore different approaches that provide meaningful data of the load spectra, and that relate pavement performance to traffic loading.	This study presents a systematic index approach that relates the truckload spectra directly to pavement performance and characterizes traffic loadings for volume, load, and damage. According to the authors, numerical evaluation analysis of 30 axle load spectra, 18 vehicle class distributions, 2 truck configurations, and 2 pavement types were conducted to explore the feasibility of using the summary indices. Results suggested that the systematic indices used in the study had a clear correlation with pavement performance.
Prozzi et al. (2017)	The objective of this research was to develop a methodology to quantify relative consumption of different axle loads and vehicle configuration on the transportation infrastructure.	Evaluated the effects of different axle configurations on pavements and bridges. An increase in the current GVW and axle load limits would allow reduced fuel consumption, reduced CO_2 emissions, and reduced truck congestion. A cost recovery method that can potentially fund the road repairs was proposed.
Walubita et al. (2019)	The primary objective of this research was to generate statewide traffic data for ME pavement design using clustering analysis. In addition, the authors sought to explore the use of other methods of obtain WIM traffic data and volume counts.	Using clustering analysis from 39 permanent WIM stations, 11 portable WIM stations, and 15 pneumatic stations across Texas the authors were able to generate future ME traffic data estimates. The authors also reported the portable WIM to be a cost-effective method of collecting WIM data with a 92.5% reliable if properly installed and calibrated.

2.3.4 Texas Mechanistic-Empirical (Tx-ME) Pavement Design System

The axle load spectra data for all axles single, tandem, and tridem is a required input in the MEPDG, however, it is recognized that some state highway agencies and smaller municipalities may not have the resources needed to collect detailed traffic data over time (NCHRP, 1999). Therefore, a hierarchical approach was adopted for developing the traffic inputs of new and rehabilitated pavement design to facilitate the use of the guide. This approach allows highway agencies to maximize the reliability of pavement design due to the accuracy and variability of available data. The hierarchical approach for traffic was divided into the following four levels (NCHRP, 1999).

Level 1 Inputs – Site/Project Specific Vehicle Classification and Axle Weight Data

Level 1 requires the collection and analysis of site/project-specific traffic data for the design and evaluation of high-volume highways. The traffic data collected at the site includes Automated Vehicle Classifier (AVC) data such as daily, weekly, monthly, seasonal, and annual number of specific class of vehicles, traveling over the roadway, as well as the weight measurements by WIM systems (NCHRP,1999). Level 1 is regarded as the most accurate that provides the greatest reliability due to the use of actual axle weights and vehicle classification recorder at or near the project site.

Level 2 Inputs – Site-Specific Vehicle Classification and Regional Axle Weight Data

Level 2 uses traffic data from regional or state axle weight for similar projects and roadways to develop the axle load spectra for each different type of vehicle.

Level 3 Inputs – Regional Vehicle Classification and Axle Weight Data

Level 3 does not require site/project specific AVC and WIM data other than average annual daily traffic (AADT) and truck percentage information. Level 3 uses regional and statewide vehicle classification and axle weight data to develop the axle load spectra from similar highways.

2.3.4 Texas Mechanistic-Empirical (Tx-ME) Pavement Design System

Under TxDOT Research Project 0-6622, a study was performed to establish models, tests and design procedures to mechanistically design and analyze pavements with considerations of materials and climatic condition of Texas (Hu et al., 2014). This resulted in the development of the Texas Mechanistic-Empirical Flexible Pavement Design System (TxME). This system allows TxDOT pavement designers to take advantage of the recent approaches for materials characterization and performance assessment of flexible pavements. In addition to the mechanistic-empirical models and performance-based material characterization, TxME allows the incorporation of traffic load spectrum. It also includes a reliable approach to incorporate materials variability for design purposes. The TxME has two levels of traffic inputs. Level 1 requires the user to enter the traffic load spectrum, while Level 2 pertains to the use of traditional ESALs. Table 2.11 summarizes the traffic input for each design level in the TxME. Figure 2.9(a) shows the pavement input structure and parameters pertaining to the axle load spectra. Figure 2.9 (b) shows the input window for entering the axle load distribution (in terms of the percentage of truck traffic) per vehicle class, axle group, and weight. This information can be imported and exported as comma-separated values files.

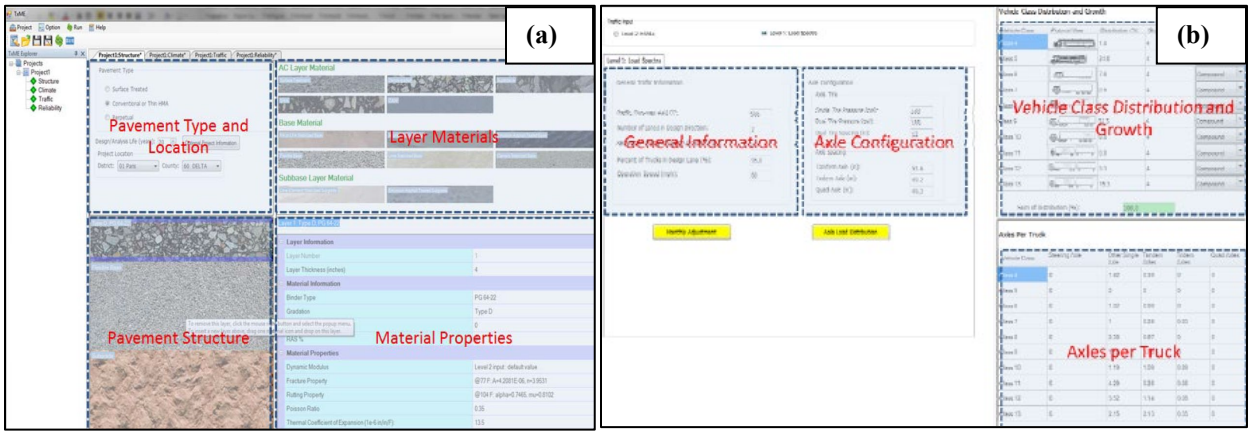

Figure 2.9 (a)TxME Pavement Structure Tab (b) TxME Traffic Input Data Tab

Table 2.11 Traffic Inputs for TxME

Level of Traffic Inputs	Approach	Inputs
Level 1	Traffic load spectrum	*General traffic information:* - Average annual daily truck traffic (AADTT), two-way - Number of lanes in design section - Percentage of trucks in design direction, % - Percentage of trucks in design lane, % - Operational speed (mph) *Axle configuration:* - Tire pressure (for single and dual tires), in psi - Dual tire spacing (in.) *Axle spacing:* - Tandem axle (in.) - Tridem axle (in.) - Quad axle (in.) *Vehicle class distribution and growth for each class (Class 4 – 13):* - Vehicle class distribution, % - Growth rate, % *Axle Distributions for each vehicle class (Class 4 – 13):* - Steering Axle (single axle, single tire) - Other Single Axle (single axle, dual tires) - Tandem Axle - Tridem Axle - Quad Axles *Traffic monthly adjustments factors per class (Class 4 – 13)* *Axle load distribution per class, season (month), and weight* - Axle factors, %
Level 2	Traffic ESALs	- 20-year ESAL (one lane and one direction), in millions - Average daily truck traffic at the beginning - Average daily truck traffic the end of 20-yr. period - Tire pressure - Operation speed (mph)

2.4 Traffic Monitoring Devices

2.4.1 Pneumatic Road Tubes

Pneumatic road tubes are one of the most commonly used sensor technologies due to their quick installation time, low maintenance, simplicity, and cost effectiveness. The pneumatic road tubes sensors send a burst of air pressure along a rubber tube when a vehicle's tire passes over the tube (Mimbela et al., 2000). This pressure pulse causes an air switch to close, producing an electrical signal that is transmitted to a traffic counter or analysis software. Pneumatic road tubes show in Figure 2.10(a) can be powered using lead-acid, gel, or other rechargeable batteries. These

road tubes are typically installed perpendicular to the traffic flow direction and can be used for single and multilane highways to count and classify vehicles illustrated in Figure 5.1(b). Moreover, they are more commonly used for short-term counting, vehicle classification, planning, or research purposes.

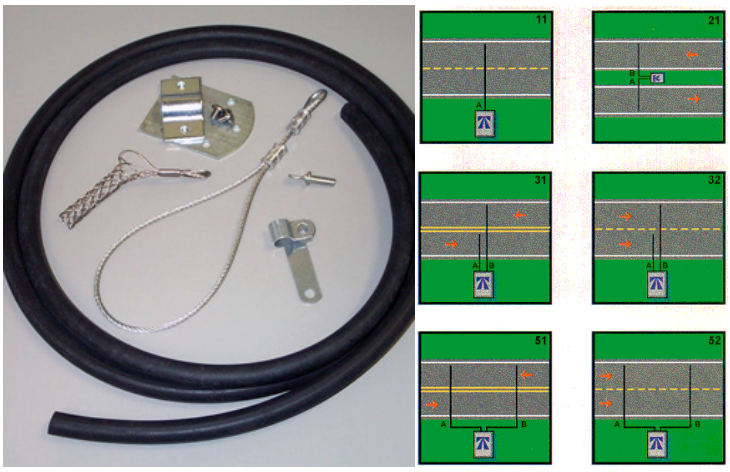

Figure 2.10 (a) Typical Road tube (b) Typical configurations for single and multilane highways (from International Road Dynamics Inc. and Mimbela et al., 2000)

2.4.2 Inductive Loop Detectors

Inductive loop detectors (ILD) are the most frequently used equipment for traffic data collection and management applications. Their size and shape vary, but the typical configuration are the 5-ft by 5-ft or 6-ft by 6-ft square loops, 6-ft diameter round loops, and rectangular configurations having a 6-ft width and variable length (Klein et al., 2006) The principal components of an inductive loop detectors are: one or more turns of insulated wire buried in a shallow saw cut in the roadway, a lead-in cable that runs from a roadside pull box to the controller cabinet, and an electronics unit located in the controller cabinet (FHWA, 2014). These wire loops are excited with signal frequencies in the range of 10 KHz to 50 KHz and function as an inductive element in conjunction with electronics unit. When vehicles pass over the loop, the inductance of the loop is decreased. This decrease causes an increase in the oscillation frequency and results in the electronics unit sending a pulse to the controller that indicates the presence of a vehicle. Table 2.12 lists all the other kinds of sensor and equipment that collect traffic related information.

Table 2.12 Strengths and Shortcomings of Different Automatic Vehicle Classifiers after (Mimbela et al, 2000)

Technology	Strengths	Shortcomings
Pneumatic Road Tubes	• Quick installation for permanent and temporary recording of data and low power usage. • Low cost and simple to maintain. • Supply software packages to assist with data analysis.	• Inaccurate axle counting when truck and bus volumes are high. • Temperature sensitivity of the air switch. • Cut tubes from vandalism and truck tire wear.
Inductive Loop	• Flexible design to satisfy large variety of applications. • Mature, well understood technology. • Provides basic traffic parameters (e.g., volume, presence, occupancy, speed, headway, and gap). • High frequency excitation models provide classification data.	• Installation requires pavement cut. • Decreases pavement life. • Installation and maintenance require lane closure. • Wire loops subject to stresses of traffic and temperature. • Multiple detectors usually required to instrument a location.
Magnetometer (Two-axis fluxgate magnetometer)	• Less susceptible than loops to stresses of traffic. • Some models transmit data over wireless RF link.	• Installation requires pavement cut. • Decreases pavement life. • Installation and maintenance require lane closure. • Some models have small detection zones
Magnetic (Induction or search coil magnetometer)	• Can be used where loops are not feasible (e.g., bridge decks). • Some models installed under roadway without need for pavement cuts. • Less susceptible than loops to stresses of traffic.	• Installation requires pavement cut or tunneling under roadway. • Cannot detect stopped vehicles.
Microwave Radar	• Generally insensitive to inclement weather. • Direct measurement of speed. • Multiple lane operation available	• Antenna beamwidth and transmitted waveform must be suitable for the application. • Doppler sensors cannot detect stopped vehicles.
Infrared	• Active sensor transmits multiple beams for accurate measurement of vehicle position, speed, and class. • Multizone passive sensors measure speed. • Multiple lane operation available.	• Operation of active sensor may be affected by fog when visibility is less than 20 ft or blowing snow is present. • Passive sensor may have reduced sensitivity to vehicles in its field of view in rain and fog.
Ultrasonic	• Multiple lane operation available.	• Some environmental conditions such as temperature change and extreme air turbulence can affect performance. Temperature compensation is built into some models. • Large pulse repetition periods may degrade occupancy measurement on freeways with vehicles traveling at moderate to high speeds.
Acoustic	• Passive detection. • Insensitive to precipitation. • Multiple lane operation available.	• Cold temperatures have been reported as affecting data accuracy. • Specific models are not recommended with slow moving vehicles in stop and go traffic.

Video Image Processor	• Monitors multiple lanes and multiple zones/lane. • Easy to add and modify detection zones. • Rich array of data available. • Provides wide-area detection when information gathered at one camera location can be linked to another.	• Inclement weather, shadows, vehicle projection into adjacent lanes, occlusion, day-to-night transition, vehicle/road contrast, and water, salt grime, icicles, and cobwebs on camera lens can affect performance. • Requires 50- to 60-ft camera mounting height (in aside-mounting configuration) for optimum presence detection and speed measurement. • Some models susceptible to camera motion caused by strong winds. • Generally cost-effective only if many detection zones are required within the field of view of the camera.

2.5 Weigh-In-Motion (WIM) Technologies

The primary purposes of weigh-in-motion (WIM) systems are (1) to record truck weights or axle loads for road analysis, (2) to screen trucks as a part of commercial vehicle weight enforcement operation and (3) to use weight information to calculate tolls on toll roads, bridges or tunnels. For research purposes, the collected data can be used for planning of roadways, road repairs, and maintenance, and to reduce traffic and its consequences (traffic congestion, accidents, etc.). A typical WIM system consists of four components: a processor and data storage unit, vehicle classification system, user communication unit, and relevant weight sensors. WIM technology allows measuring the dynamic tire forces of a moving vehicle to estimate the corresponding tire loads of the static vehicle.

Different types of WIM devices are available in the industry. The most commonly available WIM technologies are: bending plates, capacitive sensors, and strip sensors. The latter can be categorized into piezoelectric sensors (polymer or ceramic), and quartz and fiber-optic sensors (Lawrence, 2001; Malla et al., 2008). Weigh-in-motion systems can be categorized based on use and speed as described in Table 2.13. There are several factors that contribute to the accurate measurement of the traffic information using WIM devices.

Table 2.13 Classification of WIM Technology Based on Speed

WIM Category	Characteristics
High Speed Weigh-in-Motion (HS-WIM)	Data collection performed under normal traffic speed. No disturbance of traffic flow. Accuracy =15%. Overloaded vehicles diverted to the checkpoint.
Low-Speed Weigh-in-Motion (LW-WIM)	Speed restriction to minimize dynamic effects.
Bridge Weigh-in-Motion (B-WIM)	Use existing bridge to weigh vehicles via measurement of the structural response of the bridge while vehicle crossing.

WIM devices are commonly categorized based on their portability by three categories: permanent, semi-permanent, and portable systems. Permanent WIMs collect and analyze data exclusively at a single, fixed location. Semi-permanent systems have sensors built into the pavement but their data acquisition system can be disconnected and used at a different instrumented location. Portable devices can be moved as a whole for use at different locations.

2.5.1 Permanent WIM Stations

Permanent Weigh-In-Motion (WIM) stations are typically used for collecting accurate weight data and traffic volume. Axle load sensors are embedded in the pavement perpendicular to the direction of the traffic flow. Installation of WIM sensors in permanent WIM stations are divided into two groups from the installation method point of view (Burnos and Rys, 2017):

- Sensors installed in a small cut in the pavement at a depth of 1 to 4 in. (2 to 10 cm). In this case, the sensor does not have direct contact with the vehicle wheel and the axle load is transmitted to the sensor by the pavement and installation grout (which is used to fill up the groove). Polymer and piezo-ceramic sensors are mounted using this installation method.
- Sensors installed in the pavement, flush with the pavement surface. In this case, the sensor has direct contact with the vehicle tire. Bending plate, quartz, and capacitive sensors are mounted using this installation method.

Figure 2.11 illustrates different types of sensors and their corresponding installation method for instrumenting permanent and semi-permanent WIM stations.

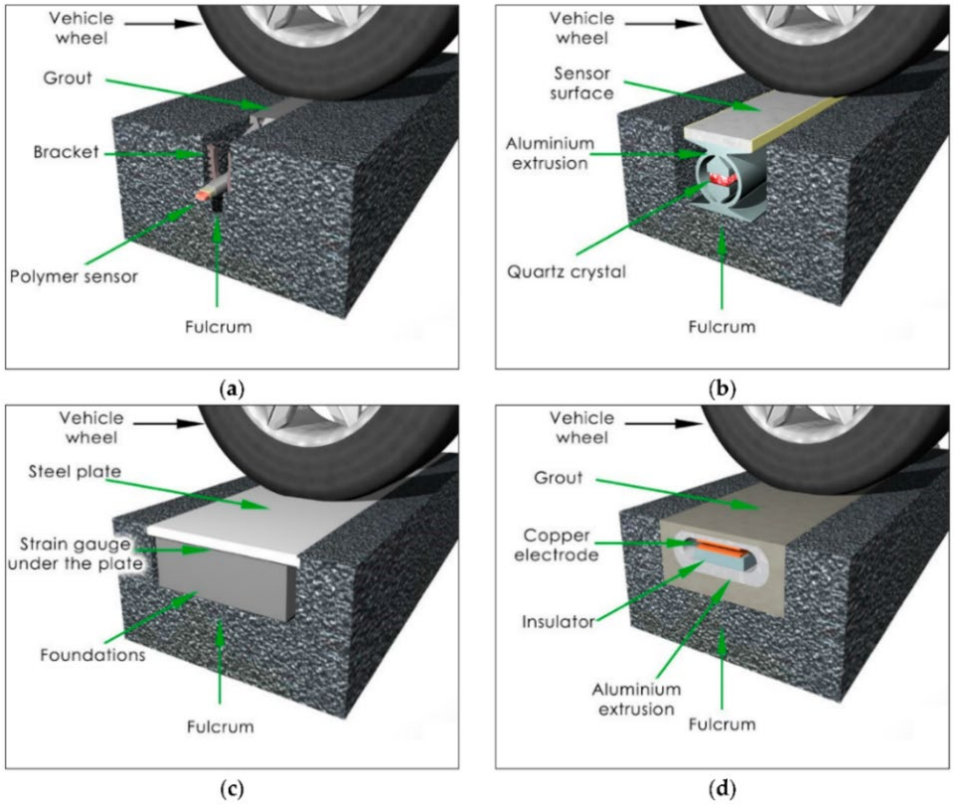

Figure 2.11 Mounting of (a) polymer sensor below the pavement surface, and (b) quartz sensor, (c) bending plate and (d) capacitive sensor installed on the level of the pavement surface (after Burnos and Rys, 2017).

As the fulcrum for the sensor is the pavement regardless of the mounting method, Burnos and Rys (2017) evaluated the effect of pavement properties on the WIM system. The researchers assumed that the pavement, by itself, is an integral part of the weighing system; as the structural integrity of the pavement and the installation grout influence the weight measurements. Despite the comprehensive data that can be extracted from the stationary WIM stations, the upfront installation funds and prohibitive maintenance costs are major challenges of such systems. According to Refai et al. (2014), permanent WIM installation could cost more than $200,000 per site, while static weight stations cost could exceed $800,000 per site. Figure 2.12 shows the active permanent WIM stations across Texas.

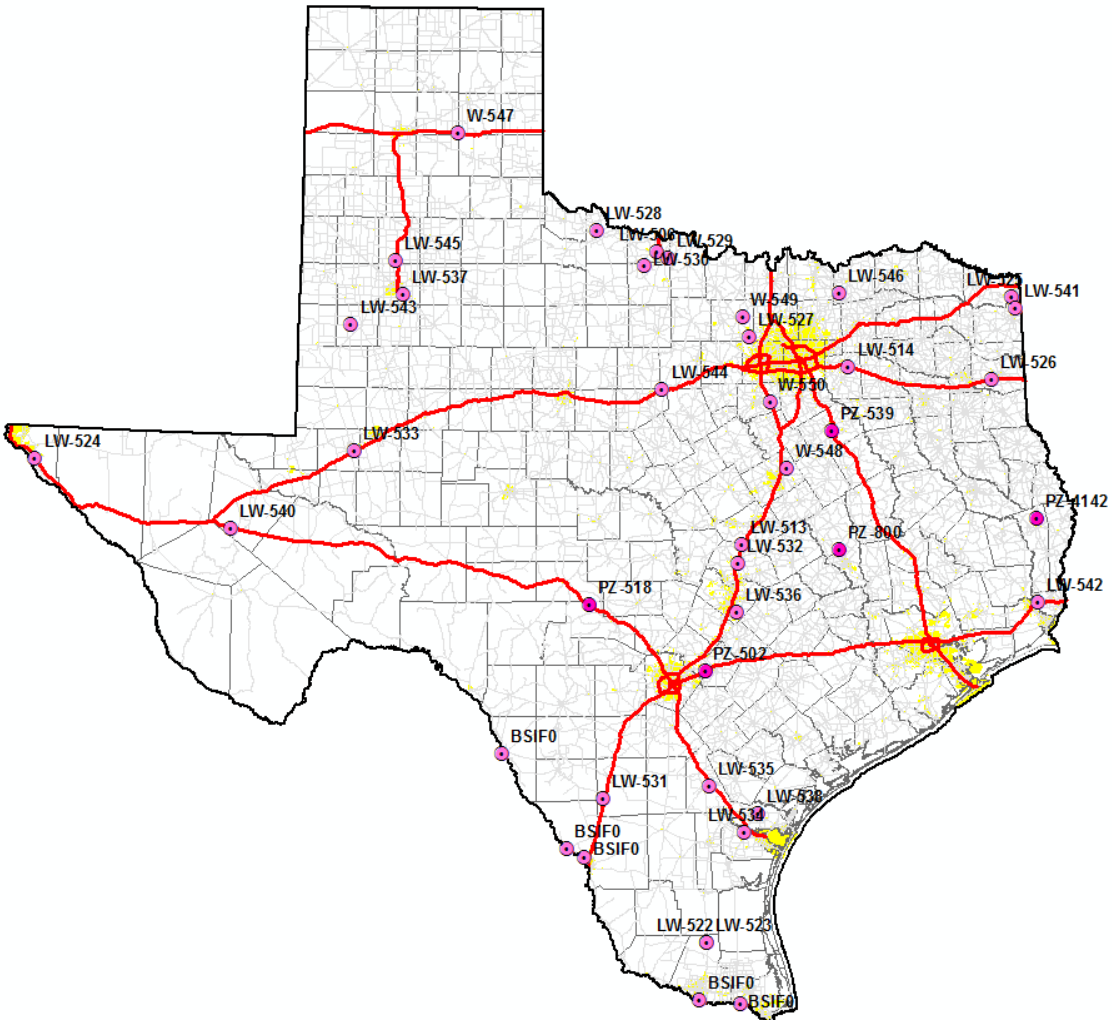

Figure 2.12 TxDOT WIM Stations (from TxDOT Truck Traffic and Loads).

2.5.2 Virtual WIM (V-WIM) stations

This system is the combination of WIM technology and Automatic Vehicle Identification (AVI) systems with a camera and Optical Character Recognition (OCR) software (Walubita et al., 2014). Similar to permanent WIM stations, the instrumentation of V-WIM stations involves axle load sensors embedded in the pavement perpendicular to the traffic flow direction. The technology for measuring axle loads is identical to the permanent WIM stations. According to Walubita et al. (2014), there are typically two setup options associated with this system as shown in Figure 2.13 (1) the system is connected with a digital warning signpost that instructs vehicles in violation to exit the highway, and (2) the system wirelessly transmits the data to an enforcement agency/agent.

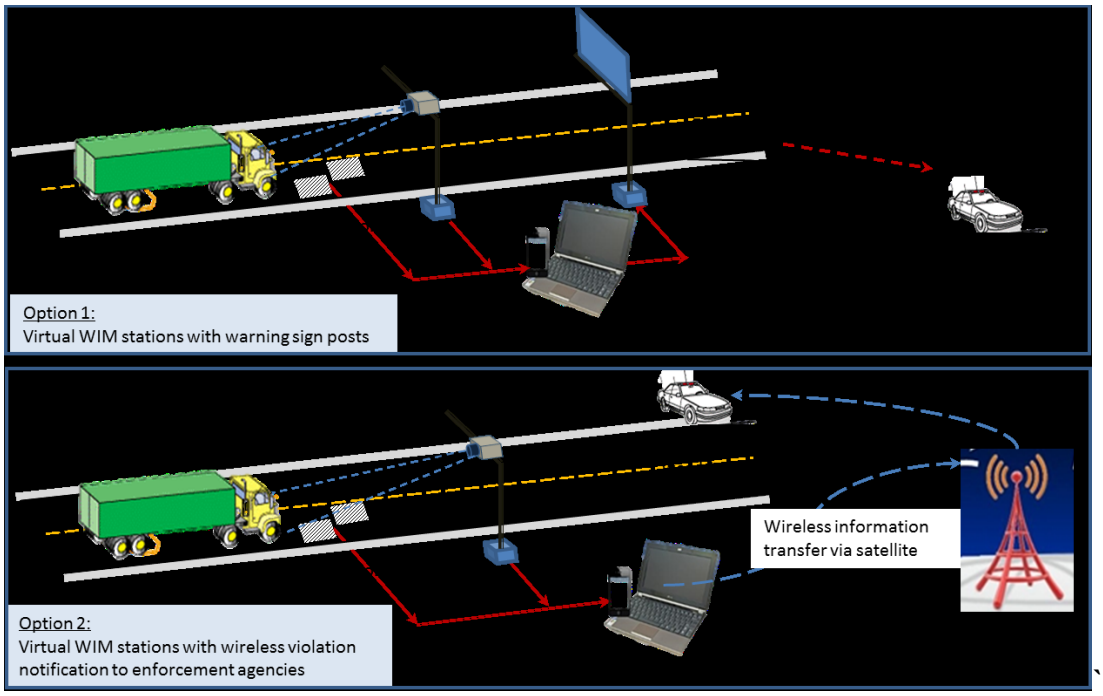

Figure 2.13 V-WIM System Installation (after Walubita et al., 2015).

2.5.3 Bridge Weigh-in-motion (BWIM)

Currently, bridge weigh-in-motion (B-WIM) systems can be divided in two different types. The first type of B-WIM systems are strain sensors coupled with separate axle-detecting sensors. These axle detecting sensors are a crucial part of the B-WIM system because they are designed to detect the presence of axles to calculate the vehicle speed, axle spacing, and classification. The second type of B-WIM system only uses strain gauge sensors that are mounted on bridge decks to detect axles and weight measurements (Al-Qadi et al.,2016). These systems could be nondestructively implemented in bridge decks by attaching a series of strain sensors beneath the bridge to record the bridge responses. The B-WIM system considers the full bridge as a weighing mechanism which can provide accurate results in terms of the axle weight, GVW, and classification of the vehicles passing over the bridges. In recent years, B-WIM systems have been deployed in several research projects to characterize the traffic loading information attributed to the site-specific conditions of the bridges (Lydon et al., 2016). Thus, the two major components that are essential for B-WIM systems are the algorithms used and the instrumentation techniques. Figure 2.14 illustrates the typical B-WIM system installed beneath the bridge deck that shows the strain peaks that would be detected.

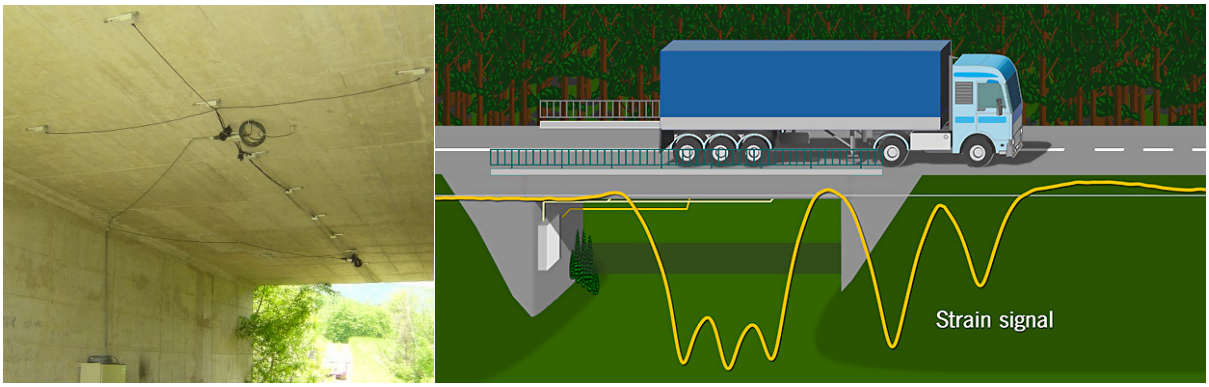

Figure 2.14 Typical B-WIM System Using Only Strain Sensors (from Labarrere, n.d.)

2.5.4 Portable Scales

Traditionally, portable scales have been used for the enforcement of load limits. These scales as shown in Figure 2.15 are designed for weighing either the wheel group or each axle to ensure the measurements comply with the regulations. Additionally, such portable scales are an integral part of the calibration process of portable and semi-portable WIM devices.

Figure 2.15 PT300™ Static Wheel Load Scales (from Intercomp, n.d.)

2.5.5 Portable Weigh-in-Motion

Portable WIM systems as shown in Figure 2.16, are often preferred over the traditional permanent WIM stations due to the convenience, and the flexibility that they provided for the characterization of the traffic information. The lower cost associated with the temporary installation and maintenance of portable WIM systems has made them a viable option for the traffic

data collection. There are several challenges for the use of portable WIM devices in the field. The most noteworthy anomaly is associated with the pavement roughness. The reliability of the collected data is greatly influenced by the vibrations generated due to the slope variance, surface cracks, rut depths, and patches on the pavement surface. Additionally, the WIM systems mounted above the surface also results in an additional dynamic motion. Such noises can potentially compromise the reliability of the static weight estimations based on dynamic measurements (Sridhar, 2008). Additionally, the flexible nature of the tire results in the adsorption horizontal force, which further adversely impact the accuracy of the results. Nonetheless, lower operating costs and ease of use makes the portable WIM systems a useful means for the collection of traffic information. Table 2.14 and 2.15 presents a comparison of different portable WIM systems.

Table 2.14 Summary of High-Speed Portable Weigh-in-motion (HS-WIM) Systems using Strip Sensors (from Walubita et al, 2015)

Category	TRS Portable WIM	ECM Portable WIM	Intercomp
Technological concept	Portable WIM with piezo-electric sensors	Portable WIM with piezo-electric sensors	Portable WIM with wireless weighing technology
Accuracy and reliability	Fairly accurate (±15%)	Fairly accurate (±10 to 15%)	Highly accurate (2 to 3%)
Simplicity of operation and user-friendliness	Simple and automatic. Data collection for vehicle speeds ≥ 20 mph	Simple and automatic. Data collection at regular highway speed	Low speed (< 3 mph)
Ease of installation	Very easy (< 2 hours)	Fairly easy	Very easy (< 15 minutes)
Maintenance and sustainability	Requires calibration at every site	No information available	Easy maintenance
Cost	$11,911	$25,000	$25,500
Data source	Vendor/supplier	Vendor/supplier	Vendor/supplier

Table 2.15 Summary of Low-Speed Portable Weigh-in-motion (LS-WIM) Systems using Portable Scales (from Walubita et al, 2015)

Category	Digiweigh DWP-80K	Intercomp LS-630	IRD DAW 300	Massload
Technological concept	Portable WIM using weighing plates	Portable WIM using weighing plates with wireless weighing technology	Portable WIM using weighing plates with Bluetooth® wireless technology	Portable WIM with ultraslim heavy-duty wheel load scales
Weight limit (dynamic)	40,000 lb per pad	44,000 lb per axle	44,000 lb per axle	40,000 lb per pad
Overload capacity	100% overload protection	150% overload protection	No information available	125% full scale safe, 150% full scale ultimate
Accuracy and reliability	Highly accurate (±3%)	Highly accurate (2 to 3%)	Highly accurate (±3%)	Highly accurate (±3% GVW at < 3 mph, ±5% GVW at 10 mph)
Speed	Low speed (< 5 mph)	Low speed (< 3 mph)	Low speed (< 6 mph)	Low speed (< 10 mph)
Ease of installation, simplicity of operation and user-friendliness	Easy setup. Simple and automatic. Operator presence required	Easy setup (< 15 min.). Simple and automatic. Operator presence required.	More complicated. Operator presence required.	Easy setup (1 < hour). Operator presence required.
Maintenance and sustainability	Easy maintenance	Easy maintenance	No information available	Easy maintenance
Cost	$6,400 and $3,500, respectively	$25,500	Ramp installation (Bluetooth) $37,841. Pit installation (wired) $25,073	$19,117
Data source	Vendor/supplier	Vendor/supplier	Vendor/supplier	Vendor/supplier

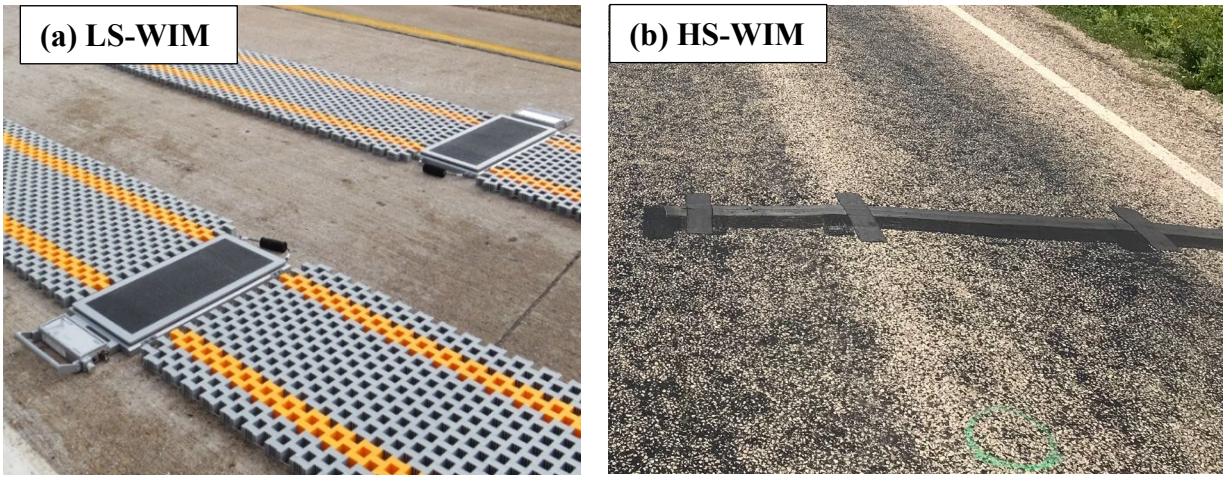

Figure 2.16 (a) Low-Speed Portable WIM and (b) High-Speed Portable WIM. (from Intercomp and Ashtiani et al, n.d.)

2.6 Sensor Technologies in WIM Systems

2.6.1 Strain Gauge Bending Plates

The bending plate device is used for traffic monitoring applications, overload detection, and data collection. It is a scale that is composed of two steel platforms that typically measured 2 ft by 6 ft and cover a 12-ft lane (Mohammad et al., 2005). These bending plates shown in Figure 2.17 use strain gages that measure tire load-induced strains that are analyzed to determine the tire load (Mohammad et al. 2005). Based on the manufacturer's information, such bending plates can weigh vehicles traveling between 5 km/h to 200 km/h and have a typical lifespan of more than 10 years.

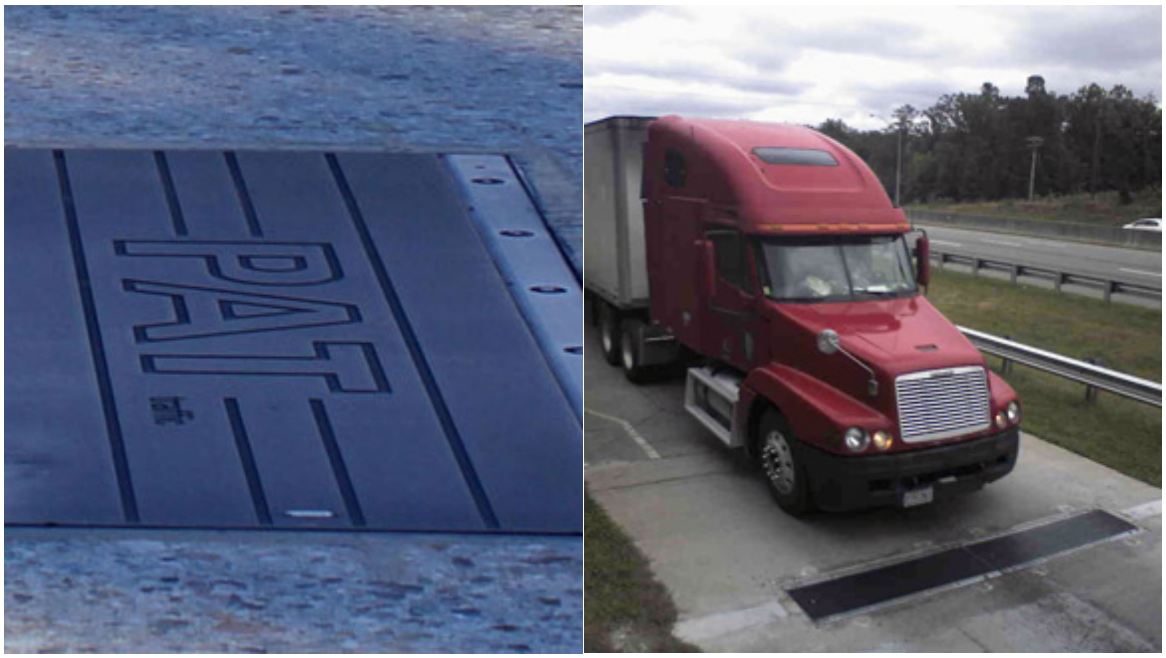

Figure 2.17 IRD-Pad Bending Plate System (from International Road Dynamics Inc., n.d)

2.6.2 Hydraulic Load Cell

These type of certified load cells shown in Figure 2.18 are essentially large scales primarily used by truckers for self-weighting. They are one of the most accurate systems for collecting weight data however, they cannot record dynamic weight, are very expensive, require high maintenance cost, and have to be overhauled every 5 to 6 years.

Figure 2.18 Hydraulic Load Cells (from Cardinal Scales. n.d.)

2.6.3 Piezoelectric Sensors

Typical piezoelectric sensors consist of a copper strand that is surrounded by piezoelectric material and that is usually covered by a copper sheath or other material. Piezoelectric sensors measure the deformation induced by tire loads on the pavement and convert it to a charge that is equivalent to the deformation. These piezoelectric sensors shown in Figure 2.19 can be affixed to the pavement surface with conveyor belts, high strength tape, or metal fixtures. However, it is more common to embed them in the pavement by making a small groove on the surface, 1 to 2 in deep by 1 to 2 in wide, and cover them with resin (Mohammad et al., 2005). The installation procedures usually take less than a day however, once installed the piezoelectric sensors are left permanently in the pavement. In addition, these piezo sensors are able to record vehicles travelling at normal highway speeds.

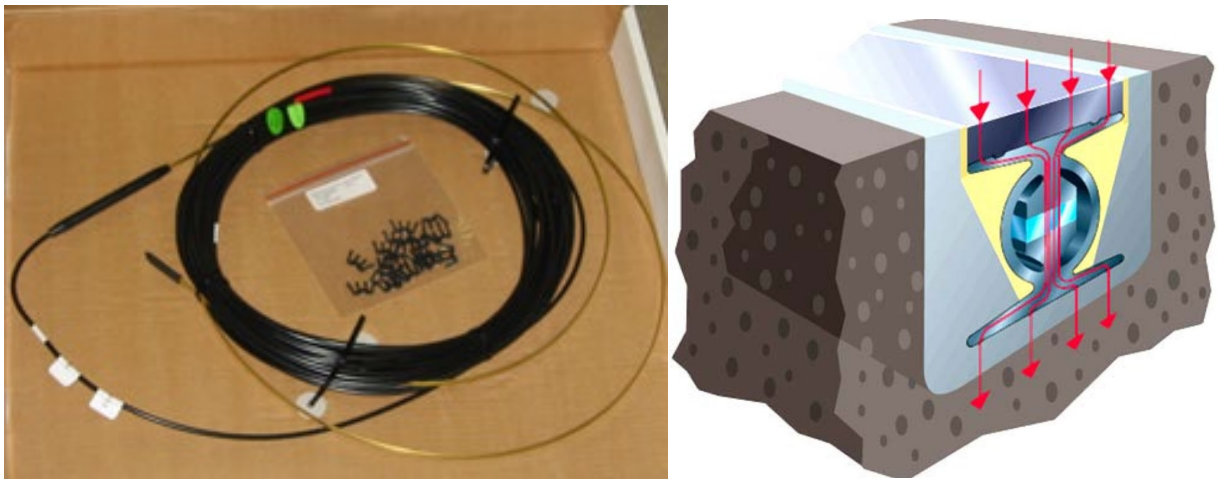

Figure 2.19 (a) RoadTrax BL Piezoelectric and (b) Kistler Lineas WIM Sensor. (from International Road Dynamics, n.d.)

Three separate studies conducted by different institutions using similar piezoelectric technologies are presented in Table 2.16. The researchers developed proprietary WIM systems using off-the-shelf components and stand-alone commercial WIM controllers. Thus, these studies propose a potential alternative to extremely expensive and labor-intensive installation of permanent WIM stations for the collection of traffic volume and weight data.

Table 2.16 Selected Research on WIM System by DOTs across the Nation

Researchers	Equipment	Components Used		Brief Description of the Study	Challenges of the Study
Faruk et al. (2016)	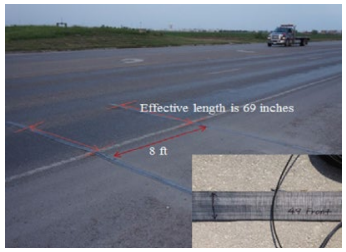	**WIM Controller**	TRS Portable WIM	The WIM system was deployed on an overweight corridor in Pharr district and provided reliable traffic data particularly for the first 7-days. The WIM system collected volume, vehicle classification, and weight distributions. Results showed that roughly 6.35% of trucks traveling in the Eastbound direction were overloaded (GVW >80kips). Sensors could be calibrated with a widely available TxDOT dump truck (Class6) and static scales.	Utilized pocket tape enclosures to affix the piezoelectric sensor to the pavement resulted in damages to the sensor, loss of operational functionalities, and accuracy. Sensors experience displacement due to continuous traffic loading, high temperatures, and housing tapes. In addition, reliability and accuracy of the collected data became questionable after 7 days, therefore seasonal data collection cannot be obtained using this WIM system.
		Sensor	Piezoelectric Roadtrax BL Sensor		
		Setup	Pocket Tape Enclosures		
		Lane Coverage	One Wheel Path (Right)		
		Sensor Length	6-feet		
Refai et al. (2014)	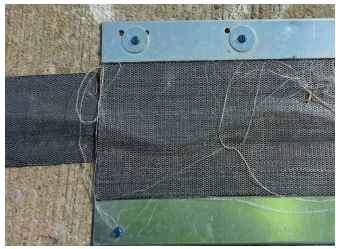	**WIM Controller**	IRD iSINC Lite	The portable WIM system was developed based on off-the-shelf components, commercially available WIM controllers, a solar powered unit with a total cost of $20,000. The portable WIM data was compared to permanent WIM data and the results indicated high correlation for both systems. In addition, the results showed that portable WIM system maintains data quality for short intervals and provides an alternative to permanent systems at about 10 percent of the cost.	Improper installation led to vibration of the sensor that resulted in the WIM controller over counting or misdetection of vehicles. In addition, using the default calibration factors for the sensors led to inaccurate vehicle classification and substantial weight error. Therefore, the portable WIM system should be calibrated at each site and every time the system is moved.
		Sensor	Piezoelectric Roadtrax BL Sensor		
		Setup	Galvanized Metal Sheets		
		Lane Coverage	One Wheel Path (Right)		
		Sensor Length	12-feet		
		Additional Monitor	REECE device		
Kwon (2012)		**WIM Controller**	Custom-Built WIM system	The data obtained from the developed WIM system was tested with data from a permanent WIM station with 97% agreement. According to the study, axle spacing and speed were almost identical with only .5% different, GVW was about 4% different, and vehicle classification was only 1.5% different. Based on the author's report, the results present an accurate account of traffic information.	The main challenge of this study was associated with the limitations of battery life for the data acquisition system. The battery for the system only lasted about 25 hours therefore, it requires daily visit from operators to exchange the battery. The weigh-pads also degraded after use causing wrinkles to form in the conveyer belt and to create errors during data collection.
		Sensor	Piezoelectric Roadtrax BL Sensor		
		Setup	Heavy Duty Conveyer Belt Pad		
		Lane Coverage	Full Lane		
		Sensor Length	12-feet		

CHAPTER 3: SURVEY OF TXDOT'S DISTRICTS

3.1 Survey Results

In order to document the extent, severity, and location of severely distressed sites affected by oversize/overweight (OS/OW) vehicles, a survey questionnaire was created and distributed to all Texas Department of Transportation (TxDOT) districts (Ashtiani et. al., 2019). Survey responses were received from the following 17 districts: Dallas, Houston, Paris, Pharr, San Angelo, Bryan, Fort Worth, Corpus Christi, Laredo, Austin, Odessa, Tyler, Abilene, El Paso, San Antonio, Yoakum, and Beaumont as noted in Figure 3.1. Furthermore, the research team was particularly interested in the survey responses from the following districts in the overload corridors of south Texas with emphasis on the Eagle Ford Shale region: 1) Laredo, 2) San Antonio, 3) Corpus Christi, 4) Yoakum, 5) Austin, 6) Bryan, and 7) Pharr district. This section summarizes the responses to the online survey and highlights the responses from districts with overweight corridors and in the Eagle Ford Shale region. The collected information was instrumental for selection of sites for deployment of the WIM devices and nondestructive field testing of representative pavements sections.

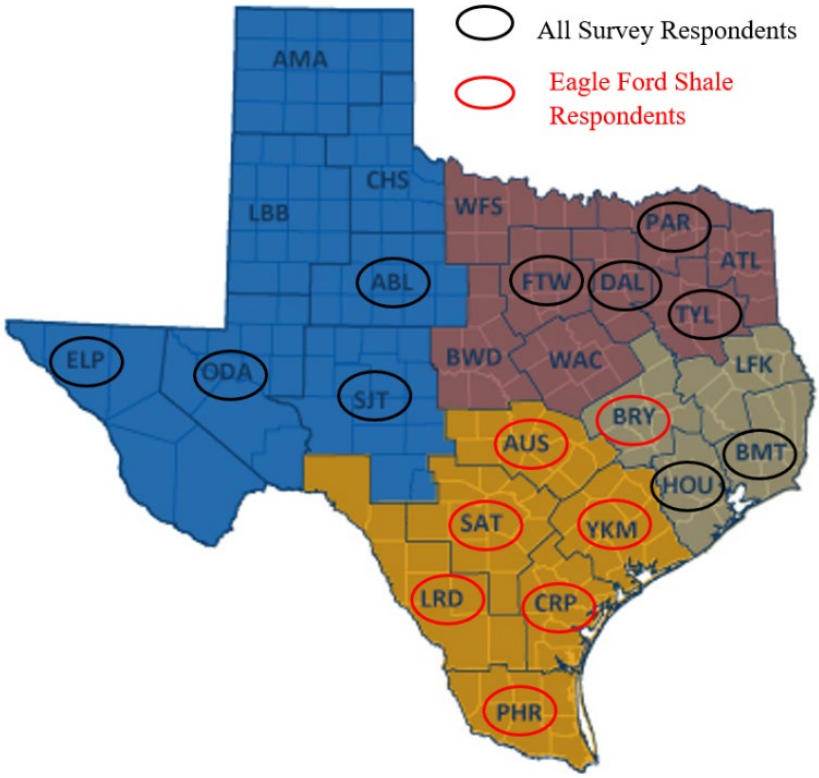

Figure 3.1 Survey Questionnaire Respondent (TxDOT Districts)

3.1.1 Is the transportation infrastructure in your district adversely affected by OW vehicles due to energy development activities?

From all the 17 districts that responded to the survey questionnaire, 94.1% indicated that their transportation infrastructure has been adversely affected by overweight vehicles due to energy development activities, as shown in Figure 3.2. The Dallas district was the only district that did not report being severely affected by overweight vehicles. As expected, all respondents in the south Texas corridors and Eagle Ford Shale answered in the affirmative.

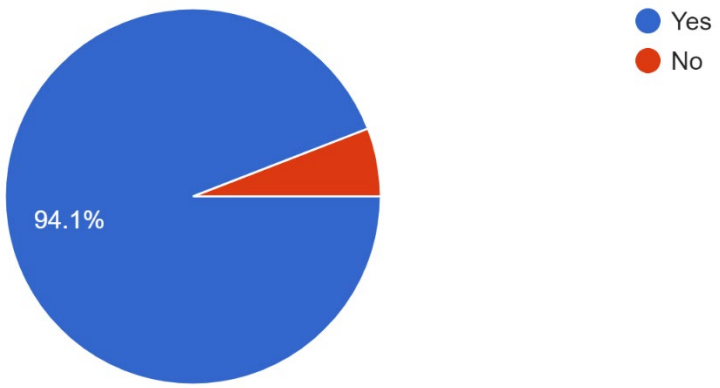

Figure 3.2 Percentage Districts Affected by Energy Development Operations

3.1.2 Severity of the damages imparted by OW vehicles associated with energy development activities

Figure 3.3 illustrates the responses to the severity of the damages imparted by overweight vehicles in each district, ranked from minimal (1) to severe (10). The Dallas district once again was the only district that did not rank the severity of the damages as high. All other respondents ranked the severity at a minimum of 5 or higher. Corpus Christi, Bryan, Abilene, Beaumont, and Tyler districts all ranked the severity at 7. While El Paso, Houston, Laredo, Yoakum, and San Antonio district ranked the severity at 8. The districts with the highest ranked severity were San Angelo, Austin, and Odessa districts at 9, 9, and 10, respectively. The results clearly indicate that the severity of the damages is more pronounced in districts with active energy development operations.

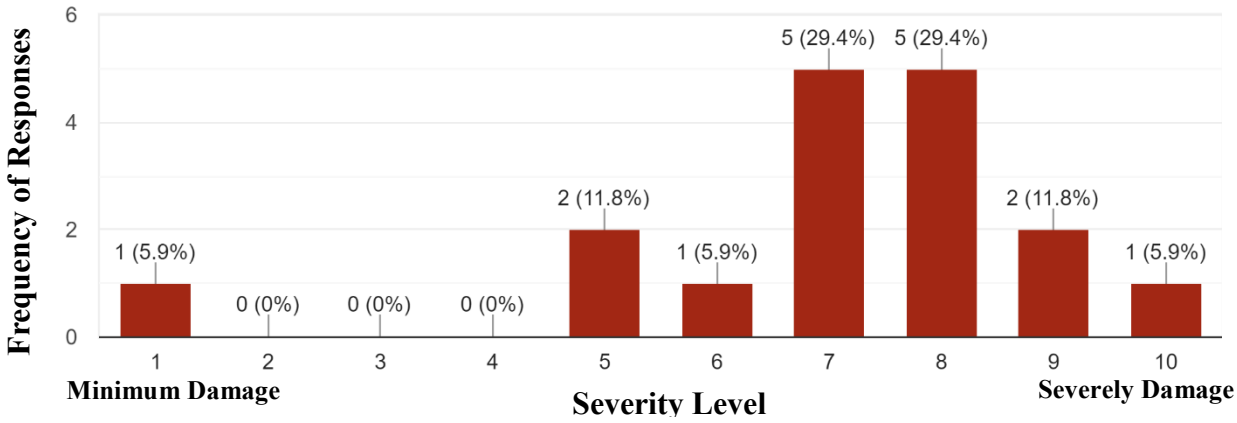

Figure 3.3 Severity of the Damages Imparted by Energy Development Operations

3.1.3 Typical Pavement Distresses/damages Due to Energy Production Activities in TxDOT's Districts:

One of the main objectives of the survey was to identify the typical pavement distresses and damages that the districts experience. As shown in Figure 3.4, the most prevalent type of distresses among all the districts are rutting (82.4%), potholes (82.4%), and fatigue cracking (76.5%). Other common distresses indicated by the respondents are slippage cracks (58.8%), edge cracks (58.8%), raveling (52.9%), and longitudinal/traverse cracking (52.9%). Tyler district indicated that the destruction of the seal coat and pavement at the entrance of well sites is also a notable distress that was not listed in our questionnaire. More importantly, for districts strictly in the Eagle Ford Shale region the top pavement distresses were rutting and pot holes, as indicated in Figure 3.5. Based on the districts responses, the results indicate that most of the distresses and damages caused by energy development operations are inflicted on flexible pavements. Figure 3.5 also illustrates that the damages associated with rigid pavements are not a significant issue with the districts in the Eagle Ford Shale. This could be attributed to few lane miles of rigid pavements as compared to the flexible pavement sections in the south Texas corridors.

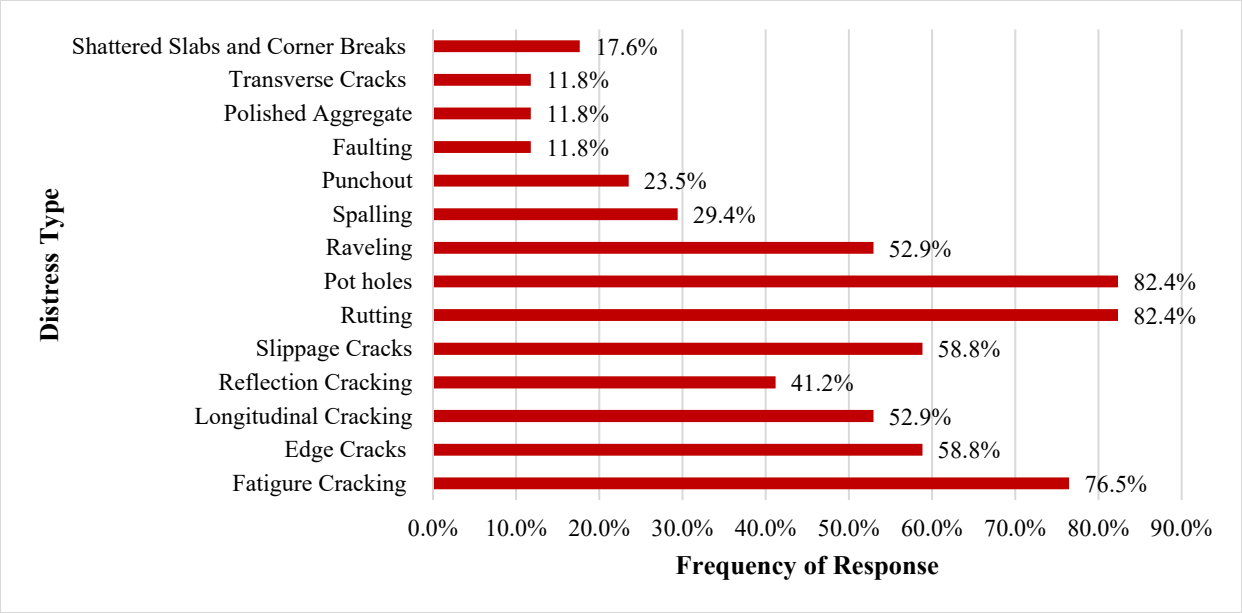

Figure 3.4 Typical Pavement Distresses and Damages Among All Responding Districts

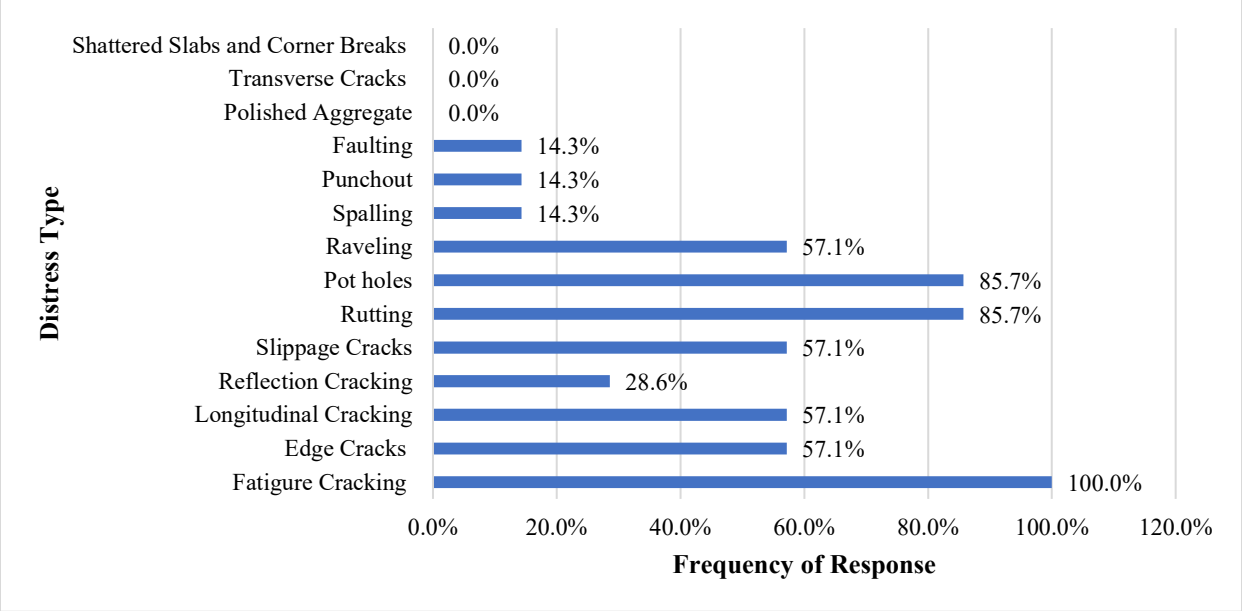

Figure 3.5 Typical Pavement Distresses and Damages Among Districts in the Eagle Ford Shale Region

3.1.4 Availability of active Weigh-In-Motion (WIM) station in each district:

The majority of the districts indicated that they do not have available active weigh-in-motion station in their district, as shown in Figure 3.6. However, Dallas, Paris, Pharr, Fort Worth, Corpus Christi, Laredo, and Odessa districts indicated that they do have operational WIM stations.

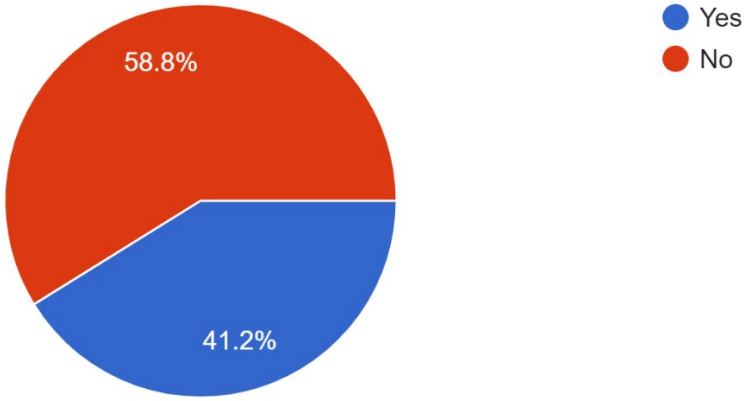

Figure 3.6 Availability of Operational Weigh-In-Motion (WIM) Stations in All Districts

3.1.5 Proximity of the Weigh-In-Motion (WIM) station from severely distressed roads:

The purpose of incorporating this question in the survey was to identify which districts had an operational weigh-in-motion (WIM) station that was closely located to severely distressed pavement sections. Having an available WIM station near to our deployed WIM device in a distressed road would aid in the cross-validation of our collected traffic data. Moreover, it would also be beneficial to see how our collected data compares to data collected from a TxDOT WIM station. However, many districts indicated that this question was not applicable to them. Pharr, Fort Worth, and Odessa districts were the only districts that indicated a specific distance from the WIM station to severely damaged roads, as summarized in Figure 3.7.

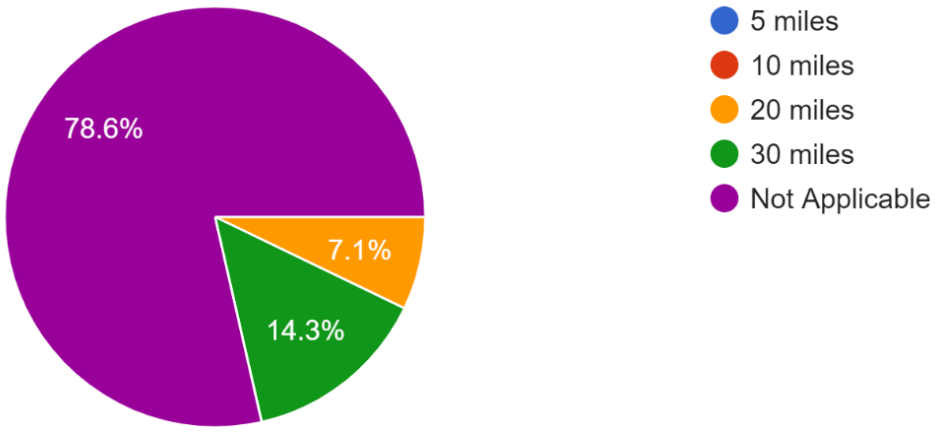

Figure 3.7 Distance Between Weigh-In-Motion (WIM) Station and Damaged Roads

3.1.6 The technologies/equipment that are used to collect traffic information

The predominate technologies and equipment used to collect traffic information in all districts are pneumatic tube counters (56.3%) and cameras (43.8%). Other technologies employed in collection of traffic data are WIM stations, inductive loops, and microwave radars, as shown in Figure 3.8. Additionally, some districts indicated that they request traffic data from the Transportation Planning and Programming Director (TP&D) division or they have permanent traffic count sites in their district.

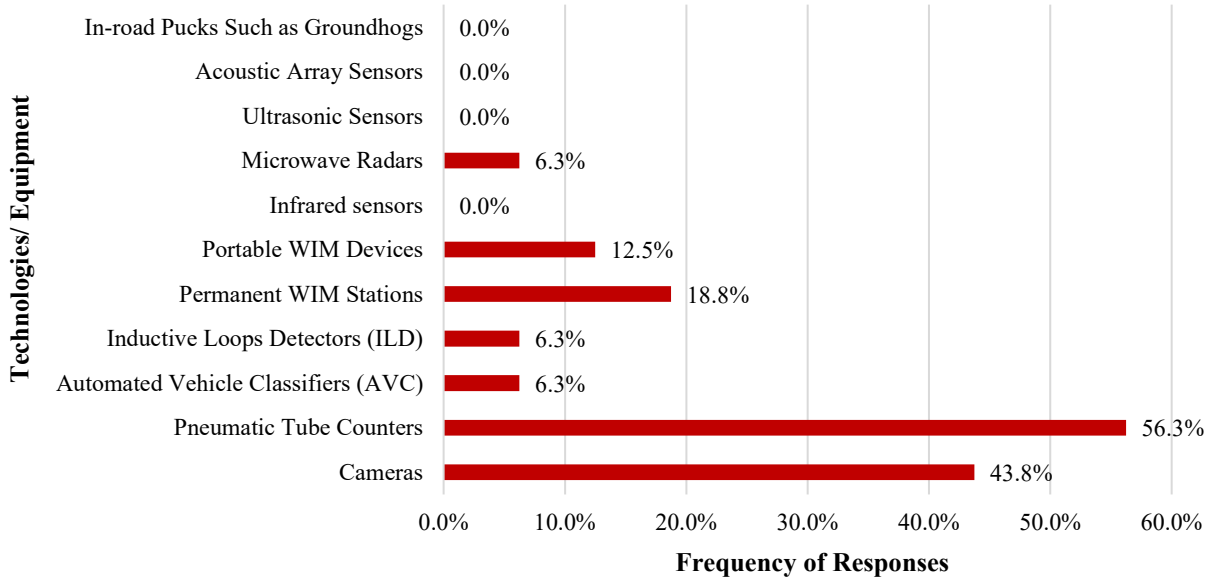

Figure 3.8 Technologies and Equipment Used to Collect Traffic Data

3.1.7 The frequency of (OS/OW) truck traffic experienced in districts highway network

Figure 3.9, summarizes the district responses to a question pertaining to the frequency of OS/OW truck traffic experienced in each district. El Paso, Abilene, and the Bryan districts were the only districts to rank the frequency of OS/OW truck traffic as relatively low. On a scale of 1 to 10, the majority of the respondents ranked the frequency of OS/OW traffic at 8 or higher in their districts. The highest ranked frequencies were indicated by Tyler, Austin, Beaumont, Yoakum, and Odessa districts, which are districts in active energy development zones.

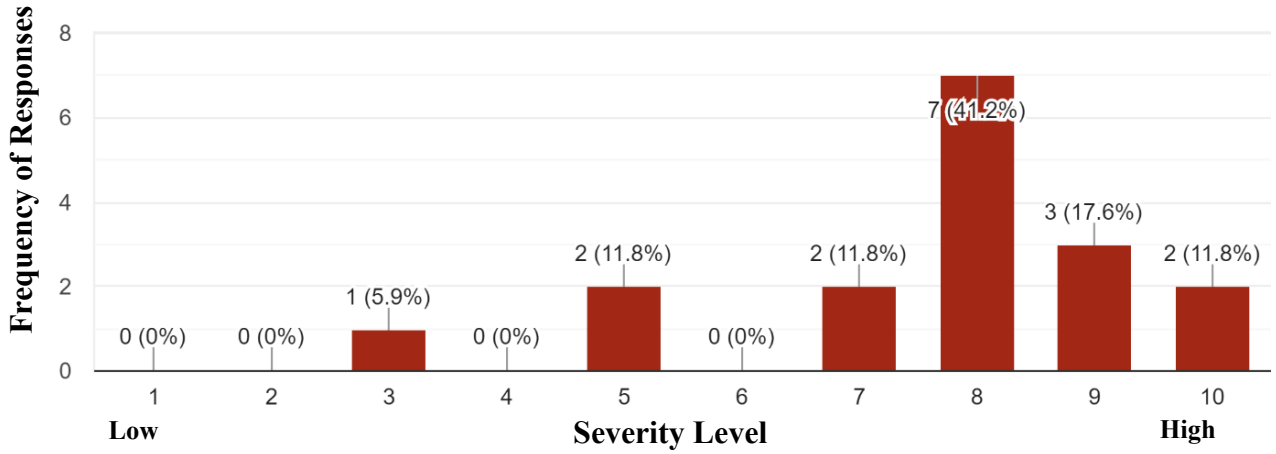

Figure 3.9 Frequency of Over-Size/Over-Weight (OS/OW) Truck Traffic

3.1.8 Growth patterns for (OS/OW) truck traffic in districts

According to the observations of the different districts throughout the state, nearly all the respondents indicated an increasing pattern in the frequency of the OS/OW truck traffic in their districts. None of the districts indicated that the traffic pattern has been similar to the pre-energy development era in Texas. Yoakum district indicated that the frequency of OS/OW has stayed the same in recent years, post energy boom. Corpus Christi district was the only district to indicate that the traffic operations of OS/OW trucks has been declining in recent years, results are illustrated in Figure 3.10.

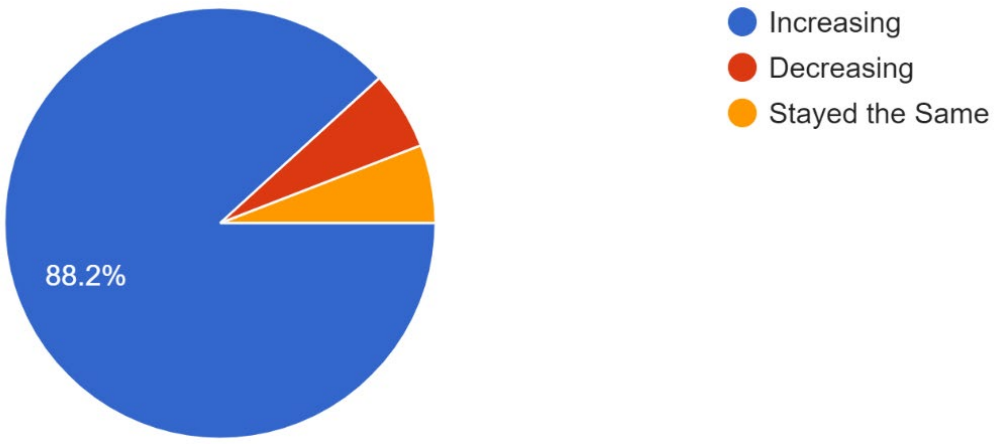

Figure 3.10 Growth trends of Over-Size/Over-Weight (OS/OW) Truck Traffic

3.1.9 Highways with high volume of OS/OW truck traffic and severely distressed roads

One of the objectives of the survey was to gather information on OS/OW corridors and information on the location of the severely damaged highways and roadways in the energy development areas with emphasis on the Eagle Ford Shale region. This information was crucial for the selection of sites for the deployment of WIM devices and non-destructive testing of representative sites. Table 3.1 illustrates the highways indicated by each district with high volume of OS/OW truck traffic. Table 3.2 illustrates specific Interstates, US Highways, State Highways, and Farm to Market roads listed by the TxDOT personnel as severely damaged. Predictably, some of the OS/OW corridors listed in Table 3.1 are the same ones that are severely damaged by the truck traffic operations and are cross-listed in Table 3.2

Table 3.1 Highways and roads with high volume of OS/OW truck traffic.

No.	District	Response
1	Dallas	No Response
2	Houston	I-10, SH3, SH 146, SH 225, SH 332, SL 8, SS 330, FM 2004
3	Paris	IH30, US75, US69, SH37, US271, SH121, US377, SH19/24, SH11, SH154
4	Pharr	UP0281, US0281, IH0002, FM1016, SH0004, FM0511, SH0048
5	San Angelo	With the exception of Real and Edwards Counties most any road in the district could be subject to OS/OW
6	Bryan	IH 45, SH 6
7	Fort Worth	US281 SH59 FM730 SH114 IH20 SH171 FM51 SH199 US67 FM2481 SH108 FM8 FM219 IH30 IH820W US377 FM1187
8	Corpus Christi	US281 and US77
9	Laredo	US 83, FM133, FM 468, SH 97, FM 469
10	Austin	All US/IH routes
11	Odessa	All of Them
12	Tyler	Gregg & Rusk Counties-SH 149, US 259, US 80, LP 281, US 79, SH 43, IH 20
13	Abilene	No Response
14	El Paso	RM 652, FM 3541, FM 2185, US 62
15	San Antonio	SH 97, SH 72, SH 16, SH 85, FM 99, FM 2924, US 87, FM 140, FM 791, FM 1344, FM 541, FM 1582, FM 624
16	Yoakum	US 90a, US 77, US 183, SH35, FM 1593, US 59
17	Beaumont	US 90, SH 146, SH 321, SH 105, IH 10, US 59
* Districts highlighted are within the Eagle Ford Shale Region		

Table 3.2 Severely distressed highways and roads that need maintenance and reparations

No.	District	Response
1	Dallas	No Response
2	Houston	US59
3	Paris	No Response
4	Pharr	FM1847, FM1732, FM0803, UP0281, US0281, IH0002, FM1016, SH0004, FM0511, SH0048, FM0507, SS0206, FM1425, SH0107, SS0115, FM0681, SH0285
5	San Angelo	SH 137, RM 33, SH 163, US 277, US 83, FM 765, US 190, US 87
6	Bryan	Various FM roadways
7	Fort Worth	SH114 US281 FM2190 FM1191 FM4 FM51 IH20 FM8 FM2491 FM219 FM 1187 RM2871
8	Corpus Christi	Most distress occurred in Karnes/Live Oak: SH 72, FM 99, SH 239, SH 123, SH 80, etc. but most have been repaired beginning 2012
9	Laredo	FM 469, US 83
10	Austin	SH 142 In Caldwell County , SH 21 in Lee County, FM 20 in Bastrop County, US 77 in Lee County
11	Odessa	Most of Them
12	Tyler	SH 149, US 259, US 79, US 80, FM 2275, FM 840, US 84, FM 2658 and FM 3231
13	Abilene	No Response
14	El Paso	RM 652, FM 3541
15	San Antonio	FM 99, FM 2924, SH 85, SH 72, FM 624, FM 1099, SH 173
16	Yoakum	FM 1593, SH 35, US 183, SH 111, FM 2656, FM 238, SH 119, FM 2542
17	Beaumont	The roadways mentioned in question 9 have all had some needed repairs over time. None of them have significant issues at the moment due to planning and identifying projects that have helped to preserve the pavement (overlays, sealcoats, etc.)
* Districts highlighted are within the Eagle Ford Shale Region		

3.1.10 The impact of energy development activities on the transportation infrastructure network, State Highways (SH), and Farm to Market (FM) roads

Based on the survey results, all respondents in the Eagle Ford Shale ranked the severity of energy development operations at a minimum of 5 or greater. Yoakum, Laredo, San Antonio, and Austin districts indicated that their transportation infrastructure has been severely impacted by the energy developments in the transportation network, as shown by Figure 3.11. The energy development impact on the districts' state highways (SH) shown in Figure 3.12, was also

significant. However, all the districts in the Eagle Ford Shale indicated that the energy development operations are more pronounced in their Farm to Market (FM) system as evidenced in Figure 3.12. The results clearly show that the existing pavement structures along the (FM) roads and some (SH) are the not sufficient to sustain the truck traffic operations by energy companies.

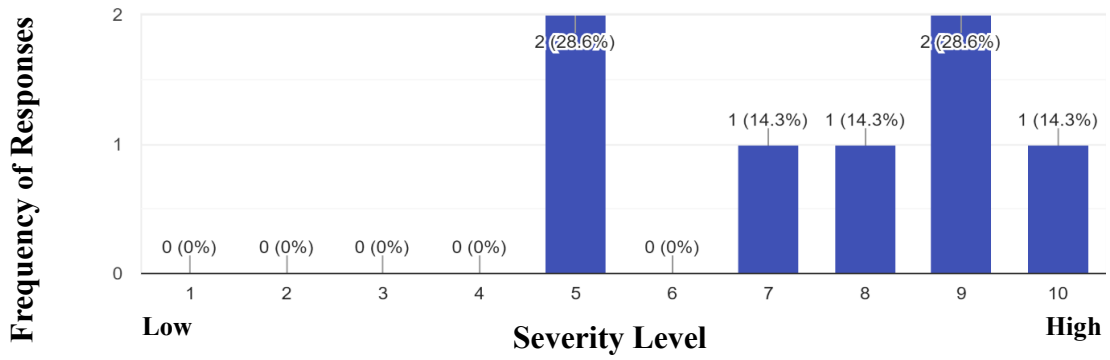

Figure 3.11 Energy development impact on the transportation infrastructure in the Eagle Ford Region

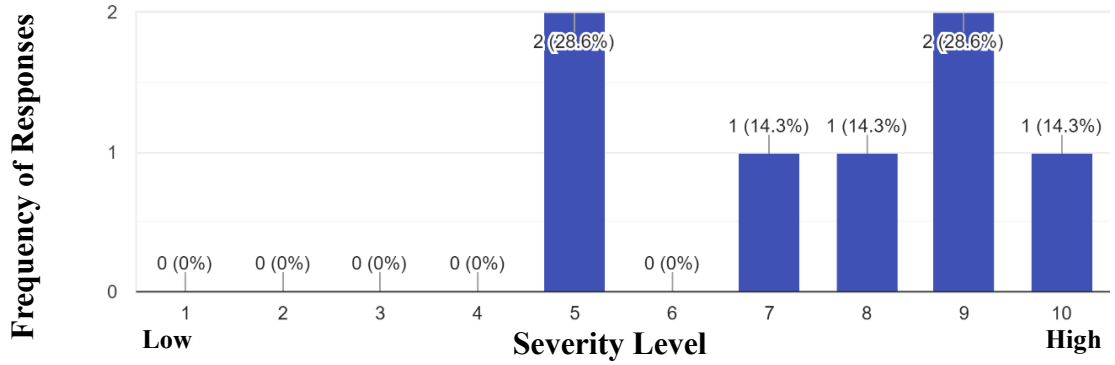

Figure 3.12 Energy development impact on State Highways (SH) in the Eagle Ford Region

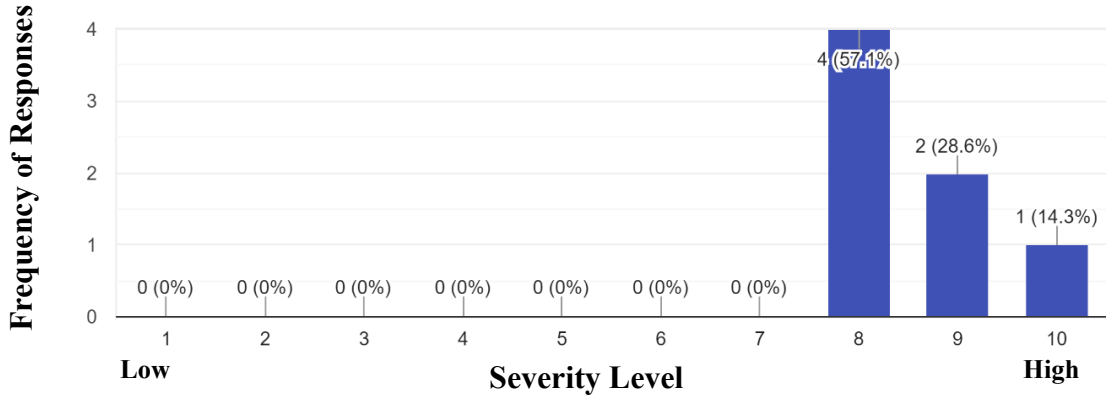

Figure 3.13 Energy development impact on Farm to Market (FM) roads in Eagle Ford Region

3.1.11 Typical pavement sections

According to the survey results, the most common pavement type for districts in the Eagle Ford Shale region is the asphalt pavement with intermediate thickness (2-1/2" to 5-1/2"), followed by a tie between thick asphaltic concrete pavement (greater than 5-1/2"), and thin surfaced flexible base pavement (less than 2-1/2"). The results suggest that flexible pavements are the most prevalent pavement sections in the Eagle Ford Shale region. Bryan, Austin, and San Antonio districts were the only respondents to report presence of rigid pavements specifically, continuously reinforced concrete pavement (CRCP), as shown in Figure 3.14.

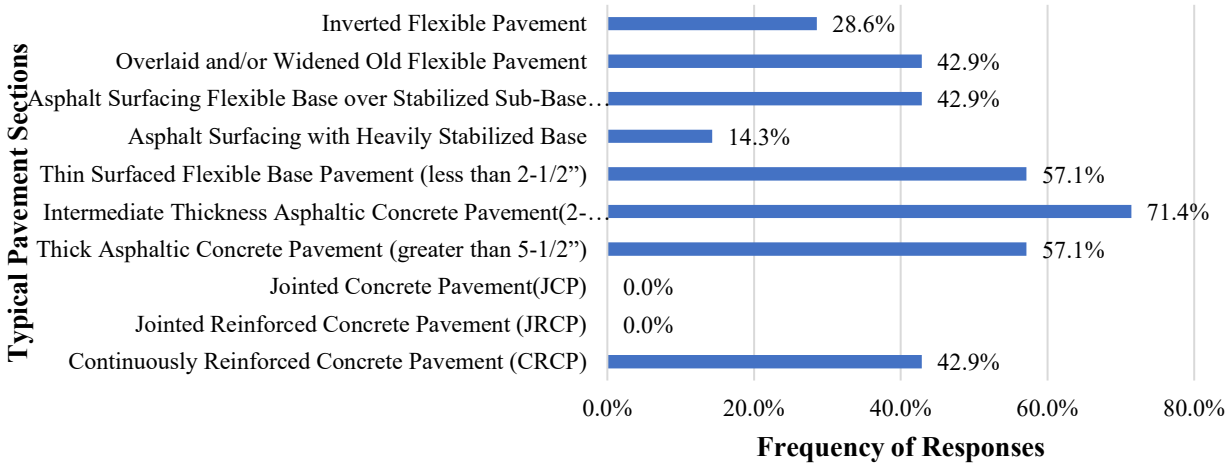

Figure 3.14 Typical pavement sections in the Eagle Ford Shale Region

CHAPTER 4: DEVELOPMENT OF THE AXLE LOAD SPECTRA

4.1 Introduction

The main objective of this chapter is to outline the rationale for the site selection and the instrumentation efforts to develop the axle load spectra database for representative sites in the energy development areas and overweight corridors of South Texas. In order to develop the axle load spectra, the research team collected necessary traffic information by deploying portable weigh-in-motion (WIM) devices to ten selected roadways. Utilizing the portable WIM devices, the research team collected information pertaining to the Gross Vehicle Weight (GVW), axle weights, vehicle classification, axle configuration, traffic volume, and vehicle speed. Additionally, the focus was on identifying the truck traffic, its distribution in the highway network, and the detrimental effect of overload traffic on the transportation infrastructure of the Laredo, San Antonio, Corpus Christi, and Yoakum districts.

4.2 Representative sites in the Eagle ford shale network

The representative sites in the Eagle Ford Shale Region were selected based on extensive communication with TxDOT personnel in districts affected by energy developing activities. The focus was on prioritizing roadways that were severely distressed and accommodate high volume of Over Size/Over Weight (OS/OW) truck traffic. In addition, the research team incorporated information such as: 1) proximity to the oil refineries, 2) neighboring oil and gas wells, 3) number of wells in the vicinity of the energy operations areas, 4) distress and conditions scores in the PMIS database, 5) current and upcoming construction/rehabilitation plans for roads in the affected highway network, and 6) previous research conducted. The study considered U.S. Highways, State Highways (SH), and Farm to Market (FM) roads to quantify the traffic operations and to further assess the detrimental effect of high volume/heavy truck traffic on the network.

Premature failure of transportation facilities which include roads and bridges in the vicinity of energy operation sites is primarily due to roads not being designed to sustain unforeseen traffic activities in the energy sector. Future armoring plans to enhance and maintain the service life of such pavements require proper traffic characterization in the network. Major Interstate highways such as, I-35 and I-37 are better suited for truck traffic operations related to energy developments, and some have operational WIM stations; therefore, these highways were not prioritized in this

study. Figure 4.1 illustrates a map of the locations of the selected sites throughout the different districts in the Eagle Ford Shale region.

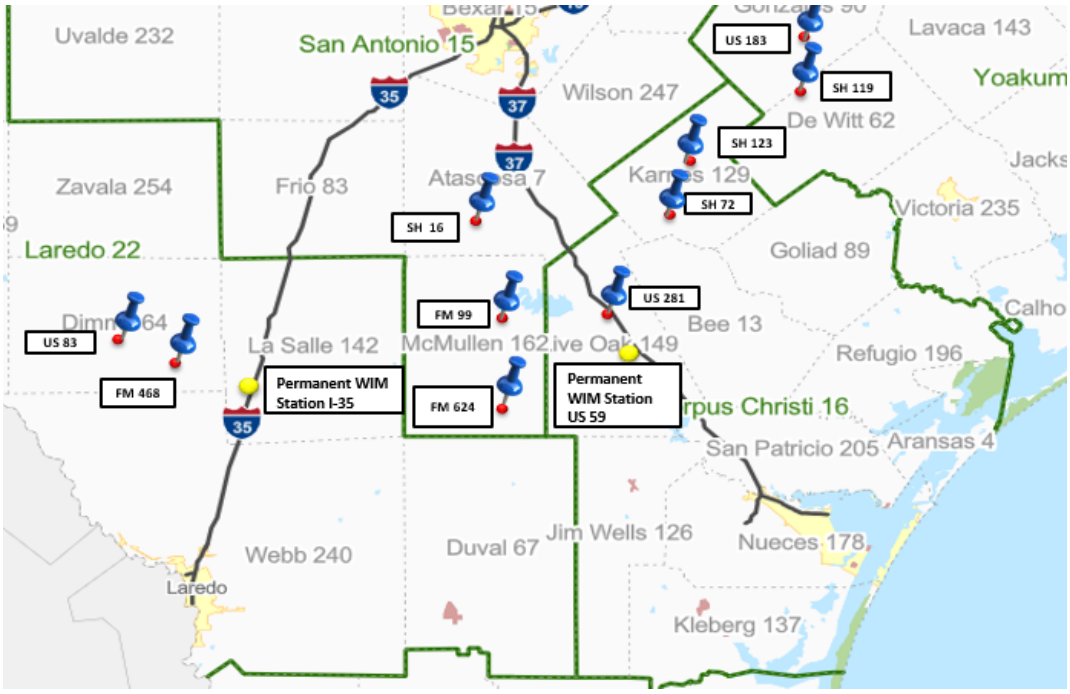

Figure 4.1 Selected Sites for Deployment of WIM Devices

4.2.1 Rationale Behind the Highway Selection

The rationale for the selection of the representative highways in the Eagle Ford Shale Region was a combination of several deciding factors as stated in the preceding section. The first step taken in identifying potential candidate highways was developing a survey questionnaire to document districts affected by energy development operations. The objective of the survey was to document the extent, severity, and location of severely distressed sites primarily affected by oversize/overweight (OS/OW) vehicles. The outcome of the survey resulted in a concise list of highways that were significantly affected by OS/OW vehicles and truck traffic due to energy development operations. The research team cross-checked the highways listed in the survey with known energy developing areas and priority corridors seen in Figure 4.2, and as expected most of them matched. The research team then referenced information from a report by Quiroga et al. (2016) report to study "well county maps" for the listed highways. These well county maps narrowed down the selection by allowing us to direct attention to areas with higher numbers of oil and gas wells. Figure 4.3 and 4.4, respectively illustrate areas with higher well densities in the Laredo District.

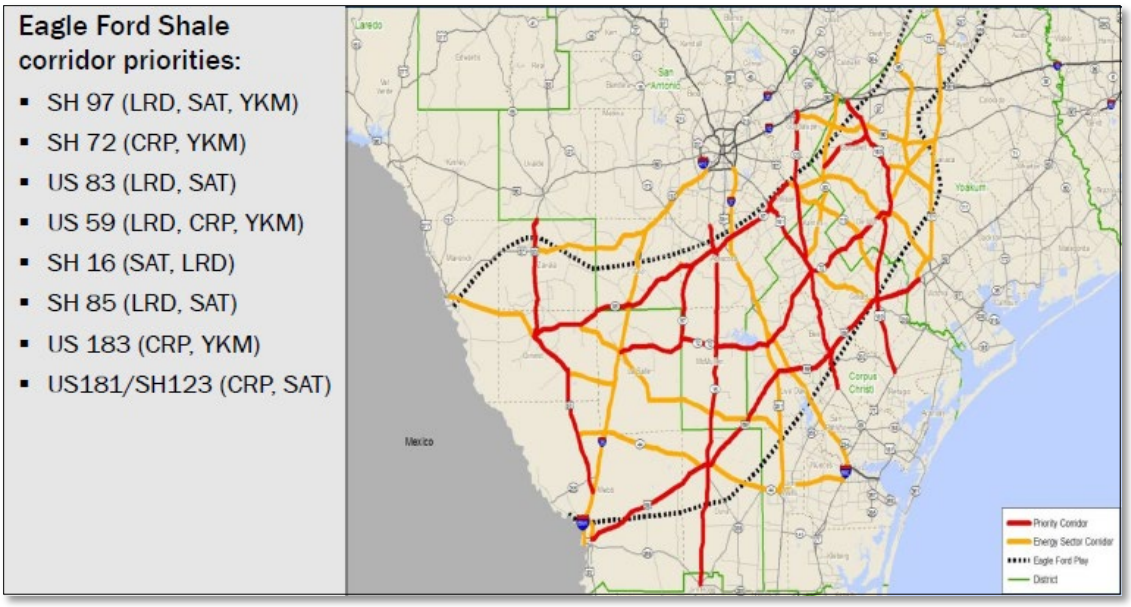

Figure 4.2 TxDOT Priority Corridors and Energy Sector Corridors (from Energy Sector Workshop, 2016)

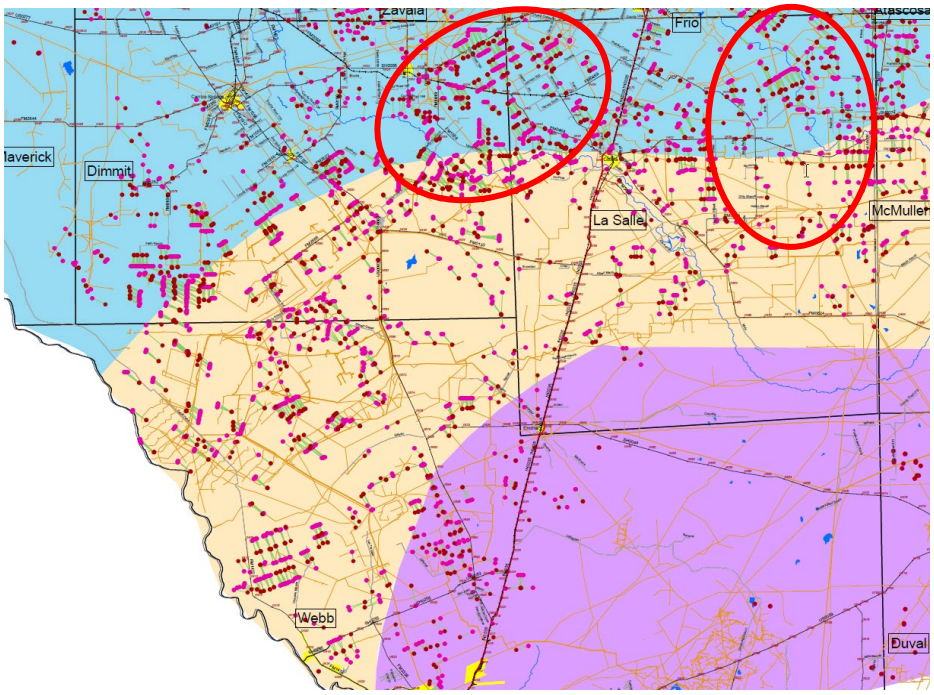

Figure 4.3 Higher Densities of Oil and Gas Well Locations in the Laredo District, Map Legend on Next Page (from Quiroga et al.,2016)

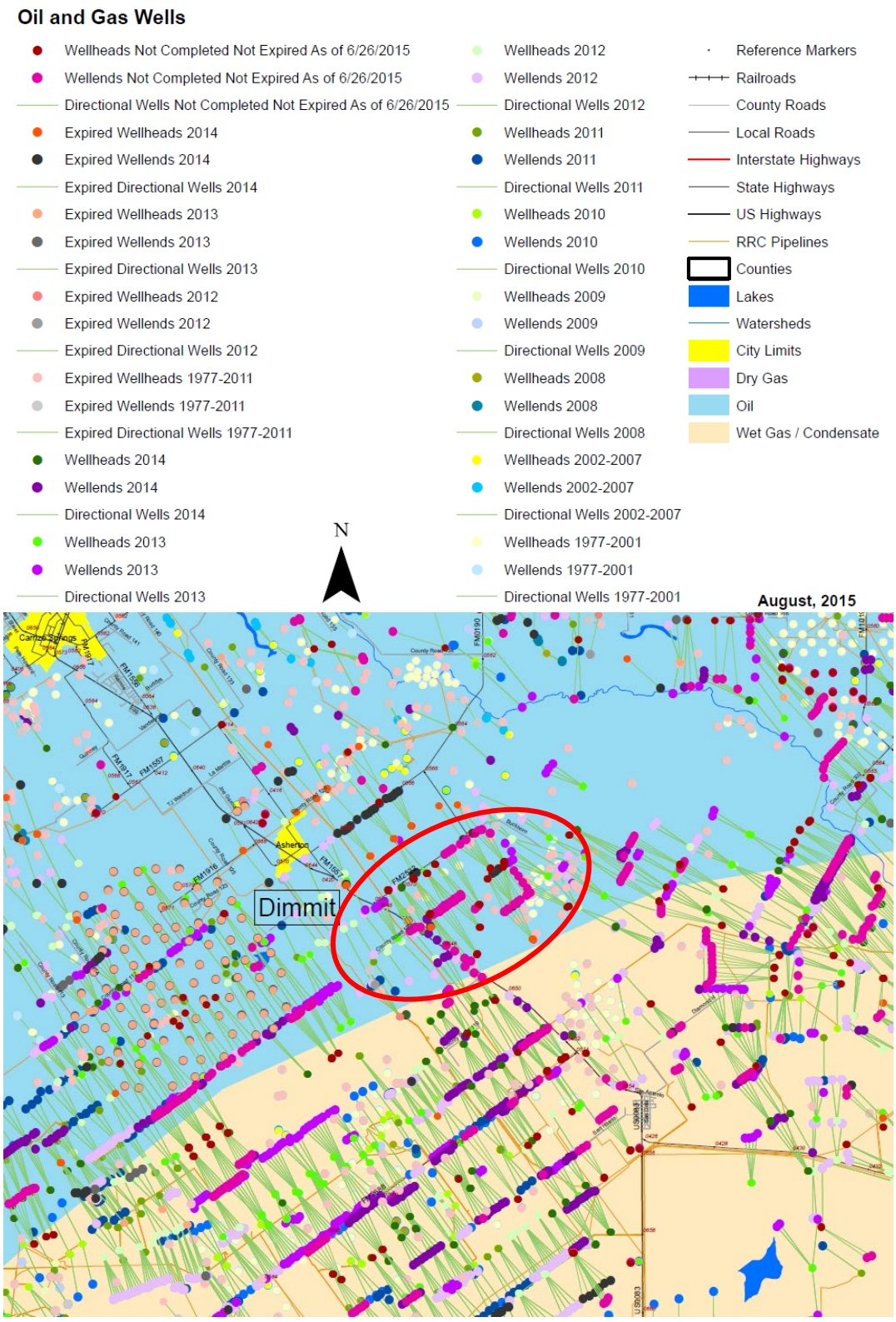

Figure 4.4 Location Oil and Gas Wells near US 83 (from Quiroga et al.,2016)

The well maps contained crucial information including historical wellheads/wellends locations, directional wells, expired wellheads/wellends, incomplete wells, and condensate areas. The dark pink and purple dots indicate the location of the most recent wells as of June 26, 2015. The yellow and salmon dots show historical wells from 1977 to 2001.

After analyzing the well maps, the location of nearby refineries and oil/gas businesses was also factored in, as these tend to generate considerable truck traffic. Figure 4.5 displays businesses related to oil and gas operations and an oil refinery, such as "Basic Energy Services" located on US 83.

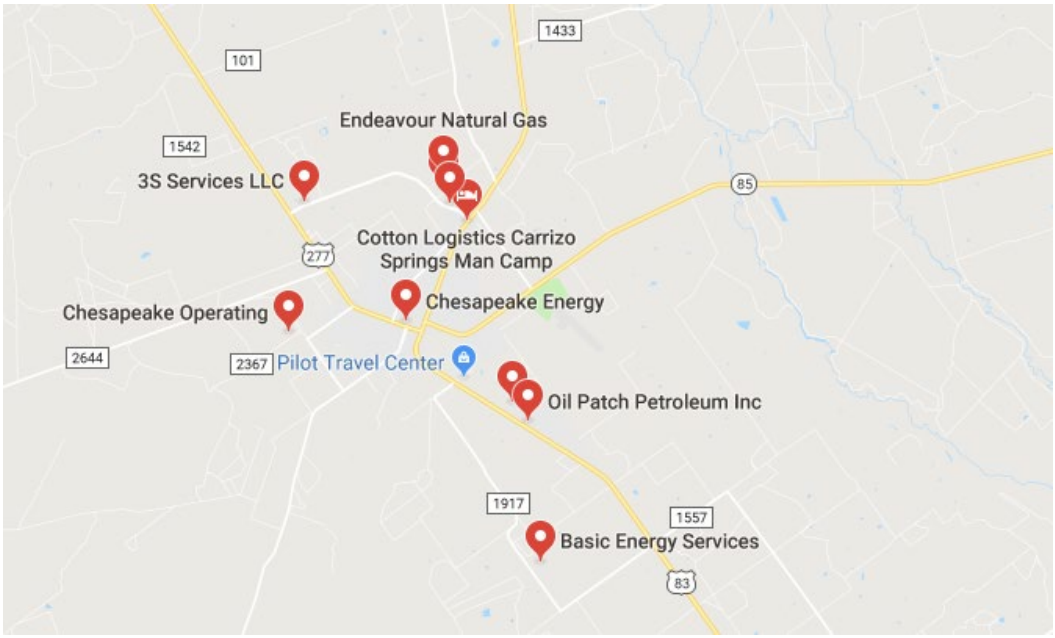

Figure 4.5 Oil Refineries and Oil & Gas Companies near US 83 in Dimmit County (from Google Maps, 2018)

Additionally, the team examined historical and recent distress and conditions scores in the PMIS database. In Figure 4.6, we observe distress and condition scores ranging from 63 to 100. Here, a condition score of 63 is fair, while a distress score of 63 is considered poor. More information on distress conditions can be found in TxDOT's 2018 PMIS Pavement Rater's Manual. The PMIS database also aided in identifying specific pavement configurations for different locations. In the case shown in Figure 4.6, the number 10 indicates a thin-surfaced flexible-base pavement.

FISC.	SIGNED_HIG	BEG_REF_M/	BEG_REI	RATING	PVMNT	DISTRESS_SC	CONDITION_
2010	US0083 K	0636	0	P	10	100	100
2010	US0083 K	0636	0.5	P	10	96	96
2010	US0083 K	0636	1	P	10	81	81
2010	US0083 K	0636	1.5	P	10	82	82
2010	US0083 K	0638	0	P	10	85	85
2010	US0083 K	0638	0.5	P	10	68	68
2010	US0083 K	0638	1	P	10	69	69
2010	US0083 K	0638	1.5	P	10	72	72
2010	US0083 K	0640	0	P	10	92	92
2010	US0083 K	0640	0.5	P	10	69	69
2010	US0083 K	0640	1	P	10	100	100
2010	US0083 K	0640	1.5	P	10	63	63
2010	US0083 K	0642	0	P	10	74	74
2010	US0083 K	0642	0.5	P	10	92	92
2010	US0083 K	0642	1	P	10	85	85

Figure 4.6 PMIS Distress and Condition Scores of US 83 in Dimmit County (from PMIS Database, 2010)

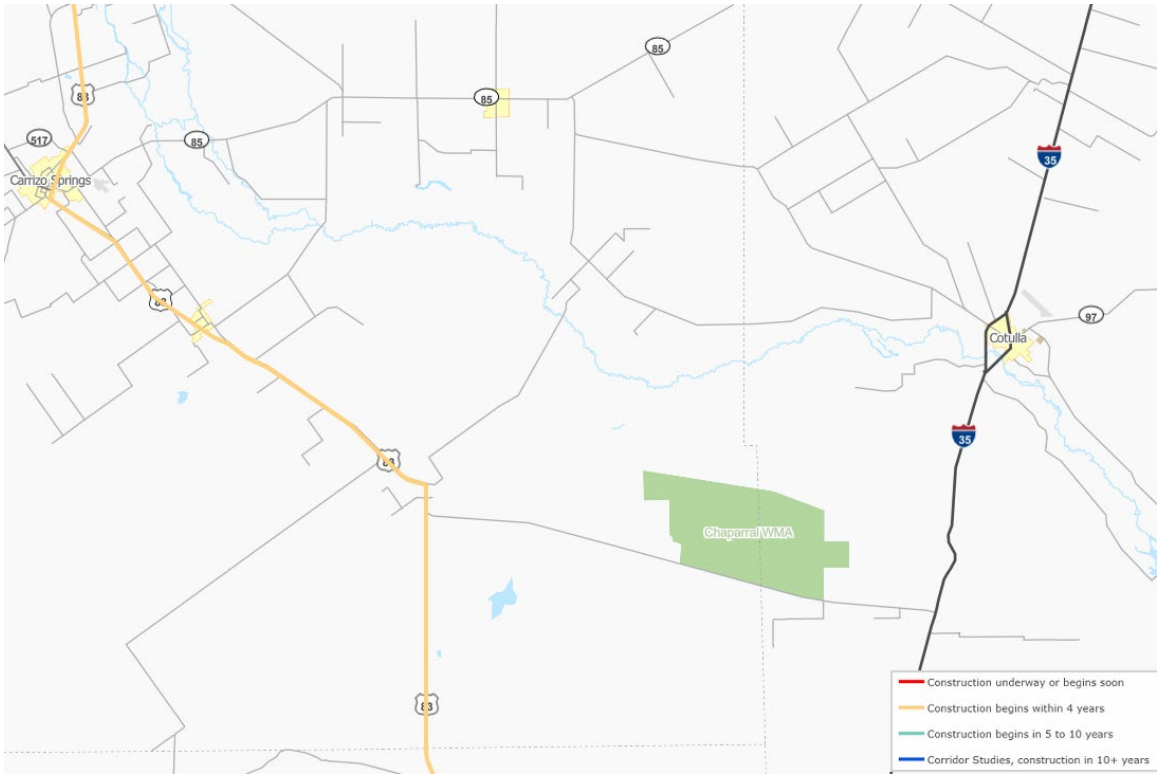

Figure 4.7 Project Tracker information of US 83 in Dimmit County (from TxDOT Project Tracker Information, 2018)

Another important factor for site selection pertains to future plans of maintenance and rehabilitation of the representative sites. Sites with no construction plans until January of 2019 were selected. This primarily serves the future tasks of the project that relate to the FWD and GPR testing of the sites for the reduction life analysis of the pavement sections. In the process of careful highway selection, highways highlighted in red were avoided, and considered highways in orange as construction for these is expected to commence in less than four years. Figure 4.7 illustrates a screenshot from the Project Tracker website that reflects the construction status of US 83.

In addition, previous research conducted on problematic highways was also factored in and 3 out of 10 highways selected were previously studied by the Texas Transportation Institute (TTI). Those included, FM 624, FM 99, and SH 72, primarily to identify the cause of premature failure of the pavement. Table 4.1 shows the details of the roadways studied by TTI. In addition to sites in Table 4.1, TTI also studied US 281 to characterize the traffic associated with energy operations.

Table 4.1 – Roadways Previously Studied by TTI (after Quiroga et al.,2016)

Roadway	County/District	Project Limits	Technical Memorandum No
FM 99	Live Oak/ Corpus Christi	US 281A to McMullen Co Line	TM-14-01
FM 443	Gonzales/ Yoakum	Curve at CR 368	TM-14-02
FM 468	La Salle/ Laredo	Cotulla	TM-14-03
SH 97	Gonzales/ Yoakum	US 80 to US 183	TM-14-04
SH 349	Martin/ Odessa	SH 176 to Dawson Co. Line	TM-14-05
SH 72	Karnes/ Corpus Christi	SH 239 to FM 792	TM-14-06
US 87	Gonzales/ Yoakum	Wilson to Dewitt Co. Line	TM-14-07
FM 624	La Salle/ Laredo	SH 16 to McMullen / LaSalle Co. Line	TM-15-01

After careful study of the network and available literature, the researchers communicated with survey respondents and TxDOT engineers in the affected districts to obtain input on the final selected highways. Table 4.2 shows the selected roadways accompanied by the rationale behind the selection of the roadways.

Table 4.2 Representative Roadways in Eagle Ford Shale Network

	District	County	Road Way	Online Survey		TxDOT Priority Corridor	Project Information	Well County Maps	Nearby Refineries & Oil/Gas Companies	PMIS Scores	Literature
1	LRD	La Salle /Dimmit	US 83	Listed as distressed road in network	Serves high volume of OS/OW traffic	TxDOT identified as priority corridor in Eagle Ford Shale Region.	1.Construction Scheduled 2. Finalizing for Construction 3. Projects Under Development	Numerous oil/gas wells in surrounding area as of 2015	1. Basic Energy Services 2. Chesapeake Energy 3. Stallion Oilfield 4.Eastern Oil Well Services 5.Sunbelt Oil& Gas Rentals	Low Distress and Condition Scores in PMIS database	N/A
2	LRD	La Salle	FM 469/ FM 468	Listed as distressed road in network	Serves high volume of OS/OW traffic	N/A	1.Construction Scheduled 2. Finalizing for Construction 3. Projects Under Development	Numerous oil/gas wells in surrounding area as of 2015	1. Chesapeake Energy on (FM 468) 2.All American Plains 3. NuStar 4. Patterson 239 5.Eog Resources 6.Noble Energy 7.NOVNational Oilwell Varco	Low Distress and Condition Scores in PMIS database	Referenced in Tech Memo TM-14-03. FM 468 in Cotulla in La Salle County. Experienced premature distress due to high volume& heavy traffic. Pavement was repaired by removing the existing surface treatment and placing 3" HMA layer.
3	SAT/ LRD	McMullen /La Salle	FM 624	Listed as distressed road in network	Serves high volume of OS/OW traffic	N/A	1.Construction Scheduled 2. Finalizing for Construction 3. Projects Under Development	Numerous oil/gas wells in surrounding area as of 2015	1. All American Plains 2. Storey Ranch	Low Distress and Condition Scores in PMIS database	Referenced in Tech Memo TM-15-01. Between SH 16 and La Salle County Line. Experienced premature distress due to high volume & heavy traffic. Used FWD, GPR, DCP, to assess the road conditions.
4	SAT/ CRP	McMullen Live Oak/ Karnes	FM 99	Listed as distressed road in network	Serves high volume of OS/OW traffic	N/A	1.Construction Scheduled 2. Finalizing for Construction 3. Projects Under Development	Numerous gas wells in surrounding area as of 2015	1.Coy City 1H on FM 99 2. Buckeye McMullen	Low Distress and Condition Scores in PMIS database	Referenced in Tech Memo TM-14-01. Construction project limits were from US 281A to the McMullen Co.Line. Researchers tested foam asphalt stabilization for 1-mile section
5	SAT/ LRD	Atascosa / McMullen	SH 16	Listed as distressed road in network	Serves high volume of OS/OW traffic	TxDOT identified as priority corridor in Eagle Ford Shale Region.	1.Construction Scheduled 2. Finalizing for Construction 3. Projects Under Development	Numerous oil/gas wells in surrounding area as of 2015	1. ETS Oilfield Services 2. Aery 1-1	Low Distress and Condition Score in PMIS database	N/A

Table 4.2 (cont.) Representative Roadways in Eagle Ford Shale Network

	District	County	Road Way	*Online Survey		**TxDOT Priority Corridor	***Project Information	†Well County Maps	††Nearby Refineries & Oil/Gas Companies	†††PMIS Scores	‡Literature
6	CRP	Karnes	US 181/ SH123	Listed as distressed road in network	Serves high volume of OS/OW traffic	TxDOT identified as priority corridor in Eagle Ford Shale Region.	1.Construction Scheduled 2. Finalizing for Construction 3.Projects Under Development	Numerous gas wells in surrounding area as of 2015	1. Total Safety	Low Distress and Condition Score in PMIS database	N/A
7	CRP/ YKM/ SAT	Live Oak/ Karnes	SH72	Listed as distressed road in network	Serves high volume of OS/OW traffic	TxDOT identified as priority corridor in Eagle Ford Shale Region.	1.Construction Scheduled 2. Finalizing for Construction 3. Projects Under Development 4. Long Term Planning	Numerous oil wells in surrounding area as of 2015	1. Energy Transfer Plant (On FM626) 2. South Sugarloaf 3. Buckeye McMullen 4. Aery1-1	Low Distress and Condition Scores in PMIS database	Referenced in Tech Memo TM-14-06. Construction project limits were from SH 239 to FM 792 in Karnes County. Investigation was performed to establish the cause of premature distress, and recommendations were provided.
8	CRP	Karnes	US 281	Listed as distressed road in network	Serves high volume of OS/OW traffic	TxDOT identified as priority corridor in Eagle Ford Shale Region.	1.Construction Scheduled 2. Finalizing for Construction 3. Projects Under Development	Numerous gas wells in surrounding area as of 2015	1. Valero Three Rivers Refinery 2. Kinder Morgan Texas Pipeline	Low Distress and Condition Score in PMIS database	Site used by Walubita and Wenting in a case study to analyze traffic data by deploying a portable WIM system. Between Reference Marker 620 - 622
9	YKM/ CRP	Gonzales	US 183	Listed as distressed road in network	Serves high volume of OS/OW traffic	TxDOT identified as priority corridor in Eagle Ford Shale Region.	1.Construction Scheduled 2. Finalizing for Construction	Numerous oil wells in surrounding area as of 2015	1. Noble Royalties Inc. 2. Original Art in Oil	Low Distress and Condition Scores in PMIS database	N/A
10	YKM	De Witt	SH 119	Listed as distressed road in network	Serves high volume of OS/OW traffic	N/A	1.Construction Scheduled 2. Finalizing for Construction 3. Projects Under Development	Numerous gas wells in surrounding area as of 2015	1. Pipeline Construction	Low Distress and Condition Score in PMIS database	N/A

* Online survey questionnaire was answered by District Engineers and Maintenance Supervisors.

**Identified Priority Corridors where obtained from the PowerPoint presentation "Energy Sector Workshop" (2016) by Randy C. Hopmann.

***Construction project information was obtained for each roadway from TxDOT Project Tracker.

†Well County maps where used from TxDOT provided documents. Referenced in Implementation Report IR-16-01 "Well County Maps"

†† Google Maps used to Identify Refineries, Oil, Gas, and other Energy related companies

†††Distress Scores and Condition Scores for each roadway where obtained from the PMIS Database for years up to 2010.

‡ Information obtained from the extensive literature that was reviewed.

4.3 Weigh-In-Motion (WIM) Data collection

4.3.1 Weight-In-Motion Equipment

For primary data collection equipment, the research team selected the portable traffic recording system (TRS) unit from International Road Dynamics (IRD) to be in compliance with previous research efforts conducted by TxDOT. The TRS unit consists of a controller, piezo input box, piezo-electric sensors, and their protective cover, as seen in Figure 4.8. The TRS unit is the main data logger that records the traffic information from the sensors placed on the road. The type of sensors used in this study are the Roadtrax BL Class I piezoelectric sensors which are installed on the road using a specialized pocket tape. This tape is used to affix the sensors to the pavement surface and allows the sensors to be easily removed and reused at another site if still serviceable.

Table 4.3 shows the equipment details and layout of the sensors. The equipment utilized was the most advantageous in this study due to its cost-effectiveness, minimum installation time, and portable convenience. In contrast, permanent WIM stations typically have higher installation cost and maintenance requirements that makes them financially challenging to operate in a continuous manner. Furthermore, they require extensive installation efforts due to the small trenches that must be cut in the pavement to permanently place the sensors, inductive loops, or weight pads on the roads. Pavement damage, traffic control requirements and user delays are additional disadvantages of such systems. Moreover, there are favorable scholarly publications by researchers in other states, such as Faruk et al. (2016) and Lubinda et al. (2019), regarding the reliability of the acquired traffic distribution and classification data using the portable TRS WIM units.

Figure 4.8 Field Equipment from Left to Right: TRS Controller, Piezo Input Box, 4in. Pocket Tape, Piezo-electric Sensors, Splice Protective Cover

Table 4.3 Portable WIM Equipment Details

WIM Equipment Used in Data Collection	
Data Logger	Portable TRS WIM Controller
Type of Sensor	Piezoelectric Roadtrax BL sensor
Sensor Placement	Pocket Tape Enclosure
Lane Coverage	One Wheel Path
Sensor Length	8-ft
Sensor Layout	2 Piezoelectric Sensors
Additional Devices Used	No Inductive Loops or Road Tubes were used

4.3.2 Field Installation

The field installation consisted of two piezoelectric sensors inserted into specialized 4 in. pocket tapes that are adhered to the pavement surface. The tapes with the inserted sensors are placed a predetermined distance which in our case, was 8 ft apart and connected to the main data acquisition system as shown in Figure 4.9. The sensors are installed to essentially register one-wheel path. Nonetheless, they nearly extend the entire length of the lane to account for wheel wander. The WIM unit automatically converts the data for 1-wheel path and translates it into the total axle weights and GVW by using an internal subroutine. For highways with multiple lanes in one direction, the piezo-sensors were installed in the outside lane of all highways, where the majority of the truck traffic travels. During summer installations, the sensors were installed with no difficulty because of the high temperature of the pavement surface. However, winter installation required heating of tapes and roads surface by means of a heat torch to allow proper adherence between the tape-pavement interfaces, as show in Figure 4.10.

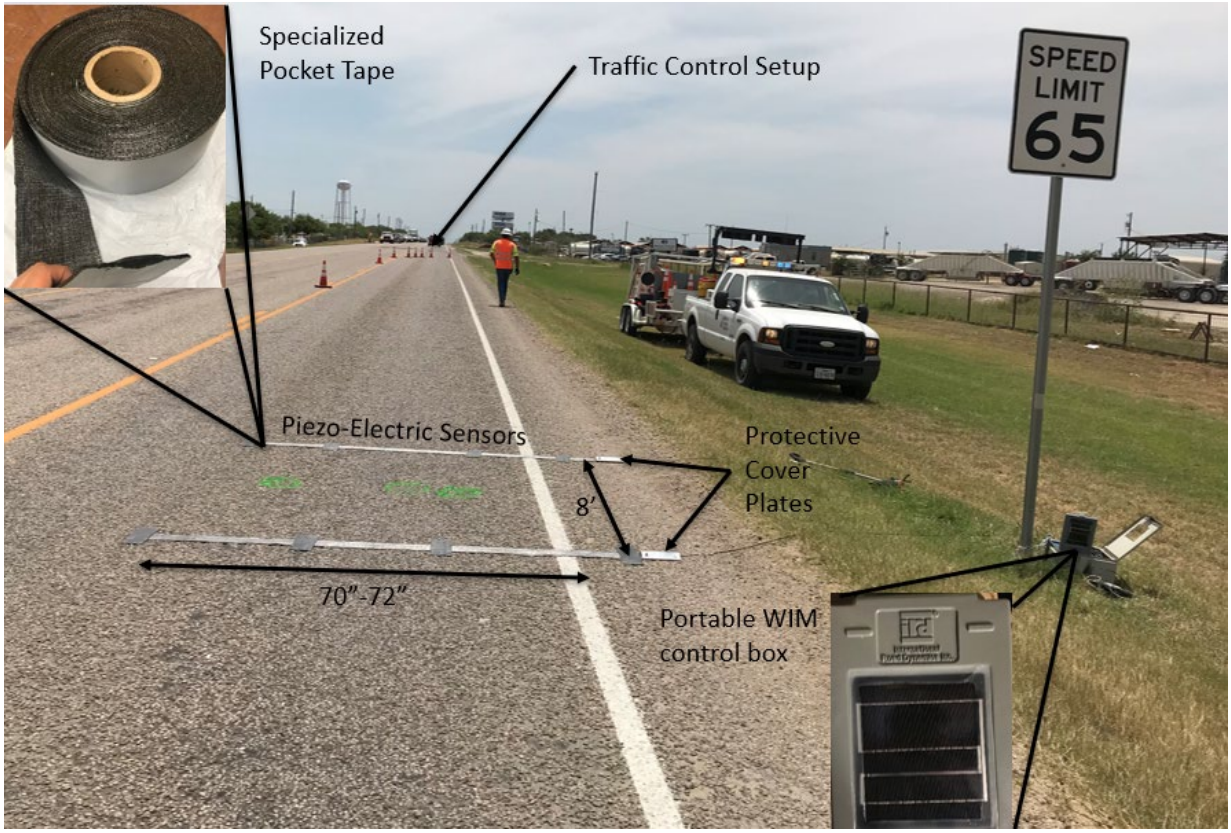

Figure 4.9 Typical Portable WIM Equipment Setup

Figure 4.10 Portable WIM Field Installation in the Winter Time

4.3.3 WIM Field Calibration

The research team successfully developed an effective method to properly calibrate the piezoelectric sensors to obtain accurate and reliable weigh-in-motion readings (Ashtiani et al., 2019). Figure 4.11 shows a flow chart of the calibration process. This process was implemented at the time of installation and removal of the WIM devices. Calibration of the WIM systems were conducted at every test site before and after the collection period to optimize the accuracy and reliability of the WIM data. For this purpose, Class 6 trucks were selected as calibration vehicles due to their accessibility across all TxDOT districts. Whereas Class 9 trucks were also selected due to their high frequency in the highway network. Therefore, both Class 6 and Class 9 trucks were used in the calibration procedure. Initially, the gross vehicle weights (GVW) and axle weights of these reference vehicles were measured using portable static axle scales and recorded as illustrated in Figure 4.12. The static weight of a fully loaded Class 6 dump truck typically ranged between 40 to 55 kips, and the loaded Class 9 truck typically ranged between 70 to 88 kips. The recorded static weights were then used as the target weight during the system calibration. The calibration runs were then conducted using with both reference vehicles while changing the vehicle speeds as shown in Figure 4.13. Finally, a calibration factor was applied to the data until the target weight was within an acceptable tolerance. In addition to the pre-calibration procedures performed, post-calibration was also conducted on the piezo-sensors to ensure sensor functionality and WIM data quality (Ashtiani et al., 2019).

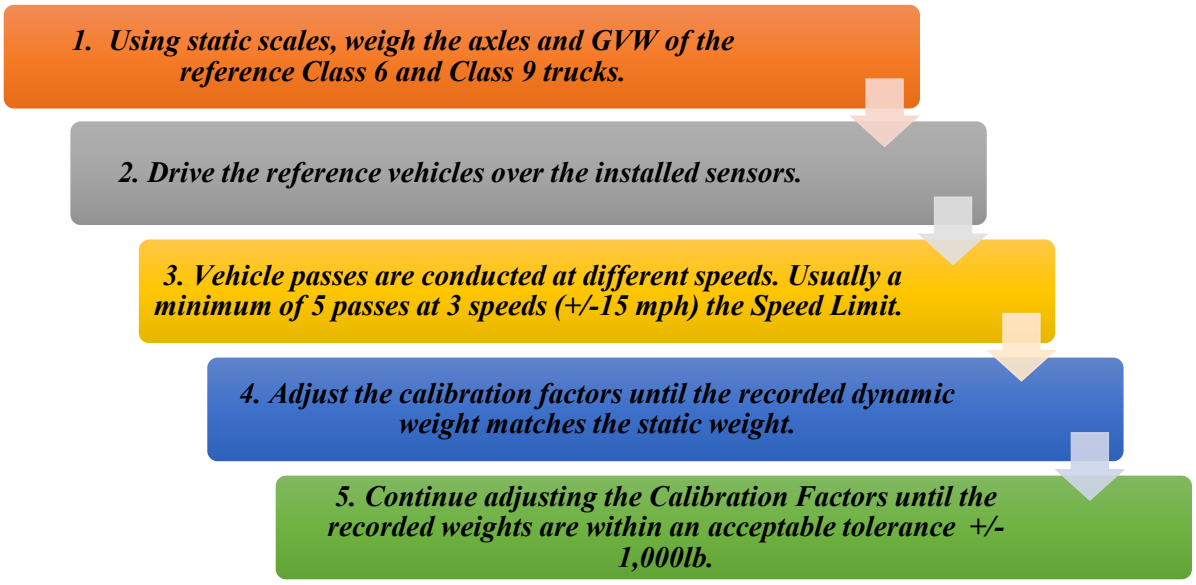

Figure 4.11 Calibration Process Implemented

Figure 4.12 Static Axle Weight Measurements: (a)Class 6 Dump Truck (b) Class 9 Water Truck (c) Class 9 Belly Dump (d) Static Axle Weight Using Portable Scales.

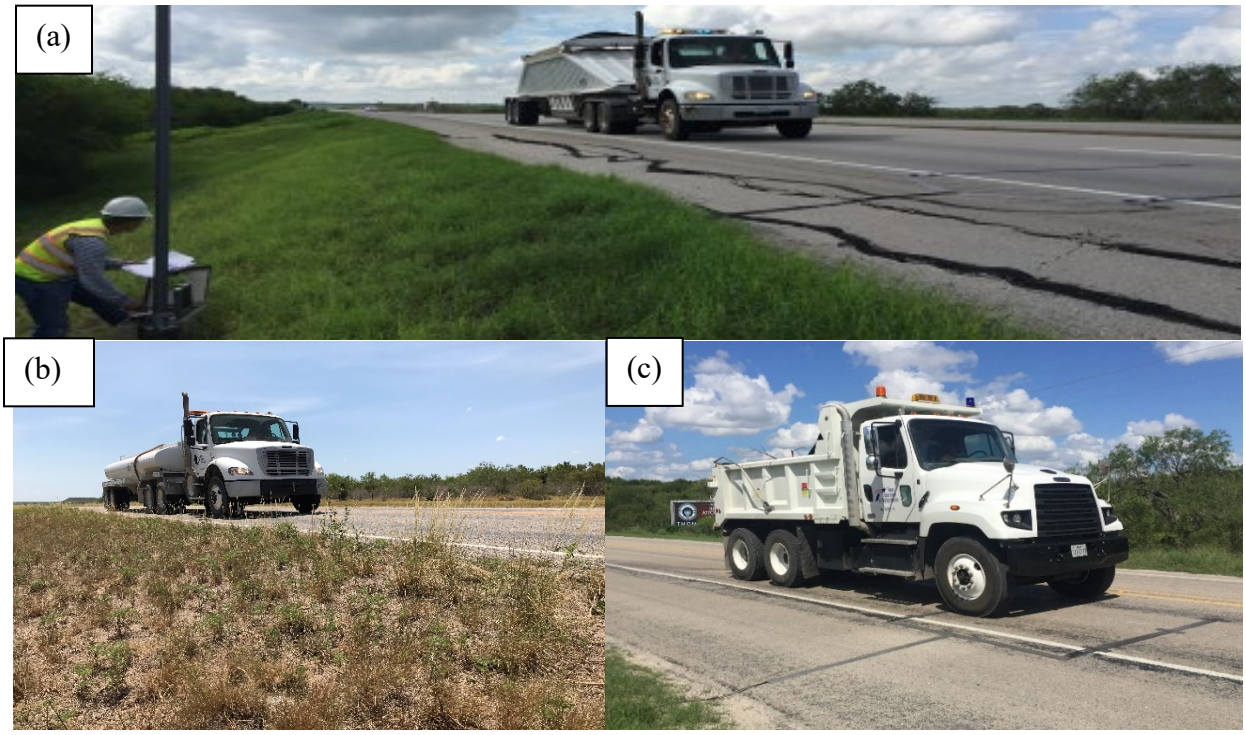

Figure 4.13 Portable WIM Calibration Runs (a)Class 9 Belly Dump (b) Class 9 Water Truck (c) Class 6 Dump Truck

4.3.4 Sensor Life

The reliability and quality of the traffic data collection is paramount to the accuracy of the predicted damages in the proposed framework. Several factors contribute to the accuracy and reliability of the WIM data collections such as pavement condition, surface distresses, surface temperature, environmental conditions, and the field calibration procedure. However, based on the research team's experience in relevant projects the operational service life of the piezo-sensors greatly influence the quality of the WIM achieved traffic data. One way to assess the performance of the sensors is by analyzing the deterioration of the calibration factors over the operational life of the installed piezo-electric sensors in the field. Figure 4.14 shows the variation of the calibration factors for several sites in San Antonio, Laredo, Corpus Christi, and Yoakum districts. The results pertaining to the sensors installed for over 50 days in the State Highway 123-80 in Corpus Christi (CRP-123-80) provides valuable insights on the longevity and service life of the piezo-electric sensors in overweight corridors of Eagle Ford Shale region.

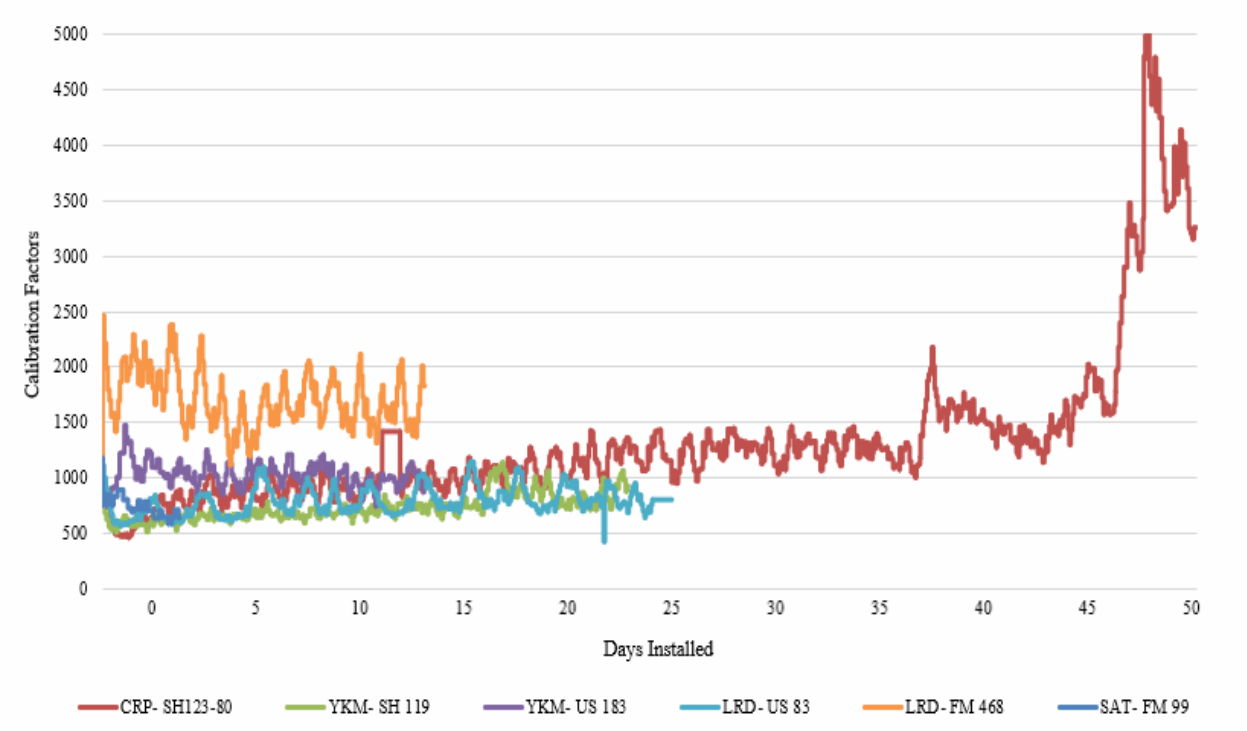

Figure 4.14 Site-Specific Calibration Factors.

4.2 Axle Load Spectra

The developed axle load spectra database was the compilation of portable WIM data collected at ten sites strategically distributed throughout the Eagle Ford Shale Region. The data collection was conducted in two-time intervals (summer and winter) to capture the effect of seasonal traffic variations, as well as the effect of environmental conditions on the damage quantification. Moreover, the WIM units were left in the field, continuously collecting data for a two-week time period per site. After sensor installation and data collection, the raw traffic data were compiled and analyzed to produce the following traffic information and traffic inputs listed in Table 4.4.

Table 4.4 Collected Traffic Data Using Portable WIM

Traffic Volume	Weight	Others
Average Daily Traffic (ADT)	Gross Vehicle Weights (GVW)	Vehicle Speed
Average Daily Truck Traffic (ADTT)	Axle Weights (Steering, Tandem, Tridem, Quad)	Speeding Vehicles
Percent Truck	Weight Distribution V.S Time	Axle Spacing
Vehicle Class Distribution	Overweight Vehicles	Wheelbase
Truck Class Distribution	Overweight Axles	Time
Hourly Distributions	Average Ten Daily Heaviest Wheel Loads (ATHWLD)	Date
Daily Distributions		

To develop the axle load spectra database, the research team first extracted raw traffic data from the TRS units and applied post-calibration factors. The data was then processed and classified by axle type (Steering, Single, Tandem, Tridem, Quad) and load intervals and then formatted as axle load distribution (ALD) input files to be compatible with the TxME and AASHTOWare software. Table 4.5 shows a sample ALD distribution for tandem axles in US 281 of the Corpus Christi District. This information not only serves for ME pavement design purposes but also aids in traffic characterization, highway planning data, overweight/oversize documentation, and pavement damage quantification. Figure 4.15 provides the stepwise flow charts for the traffic characterization in the representative test sites. The collected information was established to create a comprehensive traffic database for US highways, State highways, and Farm to Market roads of energy developing areas in the Eagle Ford Shale Region.

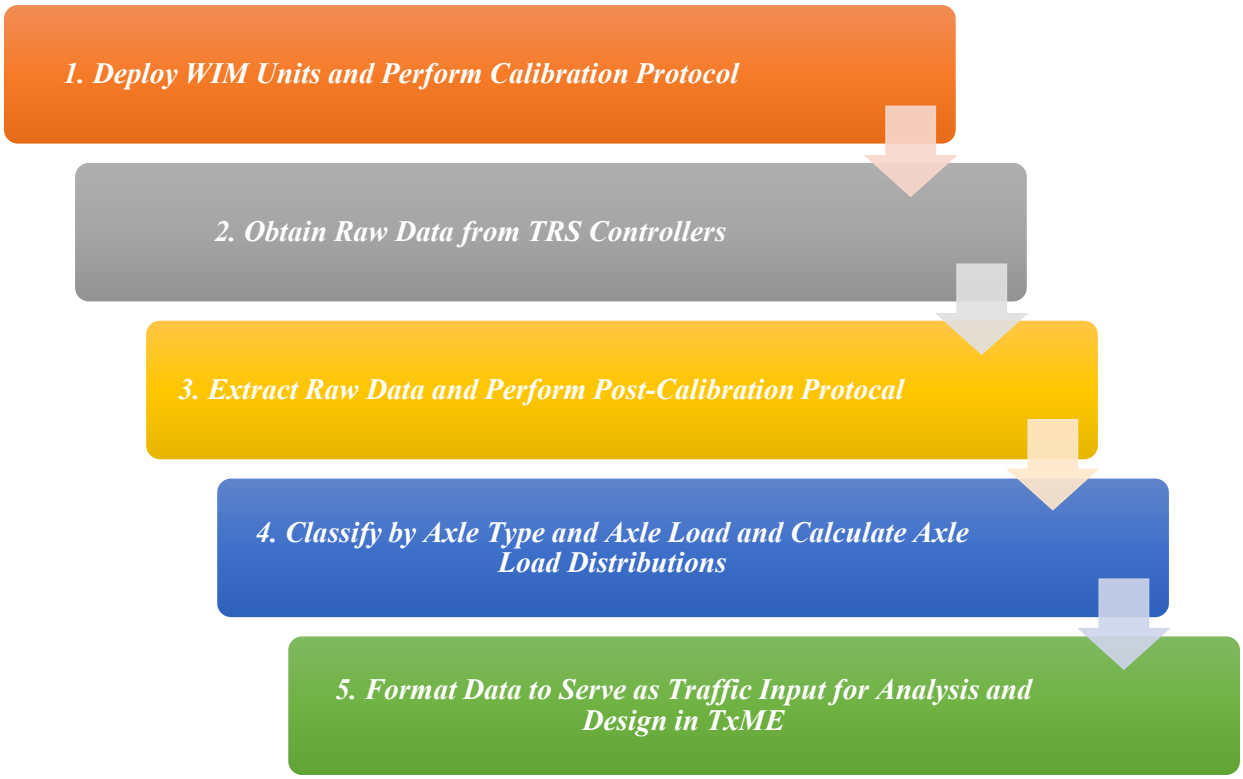

Figure 4.15 Portable WIM Data Processing Flowchart

Table 4.5 Sample Tandem Axle Distribution for TxME Traffic Inputs

Season		January	January	January	January	January	January	January	January	January	January
Vehicle Class		4	5	6	7	8	9	10	11	12	13
Axle Weights	Total	100	100	100	100	100	100	100	100	100	100
	6000	4.12	0.00	0.92	0.00	3.96	0.17	0.00	0.00	0.00	0.00
	8000	7.06	0.00	3.68	0.00	5.95	0.91	0.00	0.00	0.00	4.17
	10000	7.65	0.00	8.88	0.00	8.29	2.65	0.00	0.00	0.00	0.00
	12000	5.88	0.00	7.20	0.00	10.45	4.26	0.00	0.00	7.29	12.50
	14000	3.53	0.00	11.18	0.00	9.55	4.99	2.30	0.00	8.33	4.17
	16000	1.76	0.00	7.50	0.00	7.93	5.74	1.15	0.00	7.29	12.50
	18000	1.18	0.00	6.74	0.00	6.49	5.74	5.75	0.00	6.25	4.17
	20000	4.71	0.00	7.04	0.00	9.19	6.02	4.60	0.00	17.71	8.33
	22000	5.29	0.00	7.20	0.00	9.01	6.24	4.60	0.00	14.58	0.00
	24000	9.41	0.00	5.97	0.00	4.68	7.46	8.05	0.00	10.42	4.17
	26000	10.00	0.00	5.97	0.00	5.59	8.85	14.94	0.00	11.46	4.17
	28000	7.06	0.00	8.12	0.00	4.68	9.19	14.94	0.00	9.38	4.17
	30000	12.94	0.00	3.83	0.00	3.60	7.71	6.90	0.00	2.08	4.17
	32000	6.47	0.00	4.59	0.00	2.34	6.37	11.49	0.00	1.04	0.00
	34000	5.88	0.00	2.30	0.00	1.98	5.29	9.20	0.00	1.04	8.33
	36000	2.94	0.00	2.14	0.00	2.16	4.71	2.30	0.00	1.04	0.00
	38000	0.59	0.00	1.99	0.00	0.54	3.52	1.15	0.00	2.08	4.17
	40000	0.59	0.00	1.38	0.00	1.26	3.16	3.45	0.00	0.00	8.33
	42000	1.76	0.00	0.77	0.00	0.90	2.51	2.30	0.00	0.00	8.33
	44000	0.59	0.00	0.77	0.00	0.18	1.84	4.60	0.00	0.00	4.17
	46000	0.00	0.00	0.61	0.00	0.54	1.24	0.00	0.00	0.00	0.00
	48000	0.00	0.00	0.31	0.00	0.18	0.69	1.15	0.00	0.00	0.00
	50000	0.00	0.00	0.00	0.00	0.18	0.34	1.15	0.00	0.00	0.00
	52000	0.59	0.00	0.15	0.00	0.36	0.22	0.00	0.00	0.00	0.00
	54000	0.00	0.00	0.15	0.00	0.00	0.12	0.00	0.00	0.00	4.17
	56000	0.00	0.00	0.31	0.00	0.00	0.03	0.00	0.00	0.00	0.00
	58000	0.00	0.00	0.15	0.00	0.00	0.01	0.00	0.00	0.00	0.00
	60000	0.00	0.00	0.15	0.00	0.00	0.02	0.00	0.00	0.00	0.00
	62000	0.00	0.00	0.00	0.00	0.00	0.00	0.00	0.00	0.00	0.00
	64000	0.00	0.00	0.00	0.00	0.00	0.00	0.00	0.00	0.00	0.00
	66000	0.00	0.00	0.00	0.00	0.00	0.00	0.00	0.00	0.00	0.00
	68000	0.00	0.00	0.00	0.00	0.00	0.00	0.00	0.00	0.00	0.00
	70000	0.00	0.00	0.00	0.00	0.00	0.00	0.00	0.00	0.00	0.00
	72000	0.00	0.00	0.00	0.00	0.00	0.00	0.00	0.00	0.00	0.00
	74000	0.00	0.00	0.00	0.00	0.00	0.00	0.00	0.00	0.00	0.00
	76000	0.00	0.00	0.00	0.00	0.00	0.00	0.00	0.00	0.00	0.00
	78000	0.00	0.00	0.00	0.00	0.00	0.00	0.00	0.00	0.00	0.00
	80000	0.00	0.00	0.00	0.00	0.00	0.00	0.00	0.00	0.00	0.00
	82000	0.00	0.00	0.00	0.00	0.00	0.00	0.00	0.00	0.00	0.00

4.2.1 Truck Class Distribution

The vehicle class distribution function was one of the most essential pieces of traffic information collected by the portable WIM units. This information is a direct input to the Texas Mechanistic pavement design software (TxME), and has a significant influence on the final result. From the collected traffic data, prevalent truck classes identified in all ten highways were Class 5 and Class 9 trucks as circled in Figure 4.16. Class 5 trucks have a steering axle and rear axle with dual tires and are typically associated as small delivery trucks such as Penske and U-Haul trucks. Class 9 trucks have a single steering axle and two tandem axles in the back. The types of Class 9 trucks can range significantly as they are used to transport finished goods, oil, gasoline, equipment and much more.

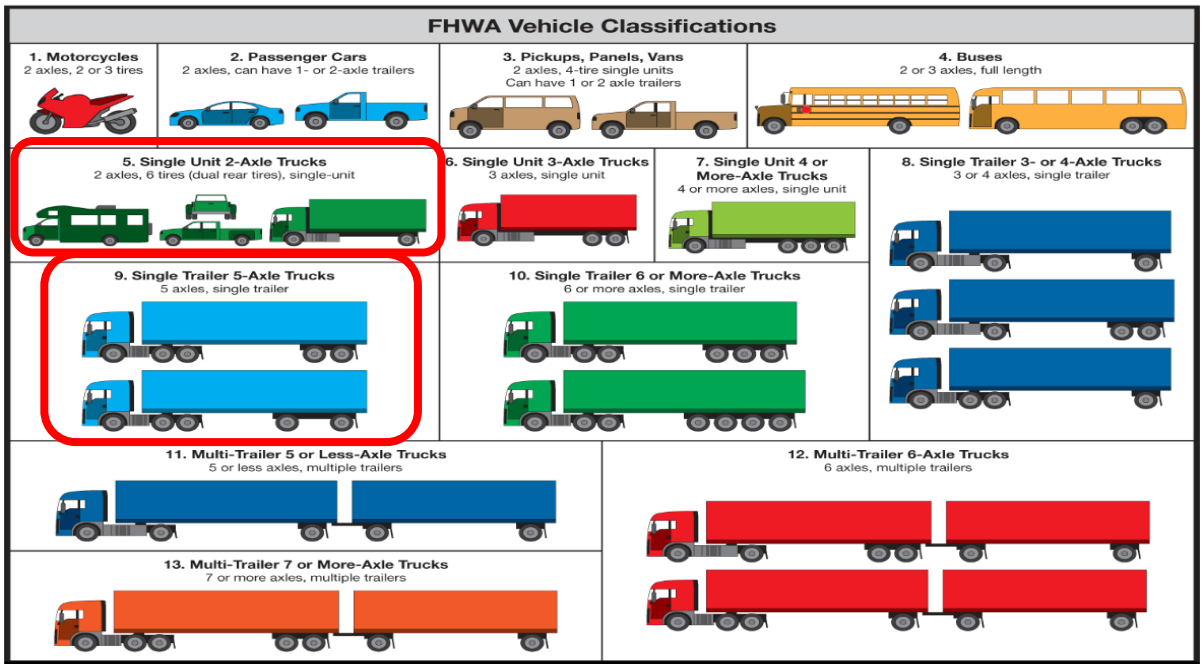

Figure 4.16 FHWA Vehicle Classifications

Figure 4.17 illustrates the truck class distributions comparisons versus percent trucks for different highway types (FM, SH, US). From different highway structures, Class 9 was the most common truck followed by Class 5. Farm-to-Market (FM) roads generally tend to have a higher number of Class 5 delivery trucks compared to the state highways (SH) and US highways. In contrast, US highways had the highest Class 9 and fewest Class 5 trucks. Moreover, Figure 4.18 illustrates the truck class distributions among all portable WIM sites in the Eagle Ford. These results are in agreement with the trends found in the literature.

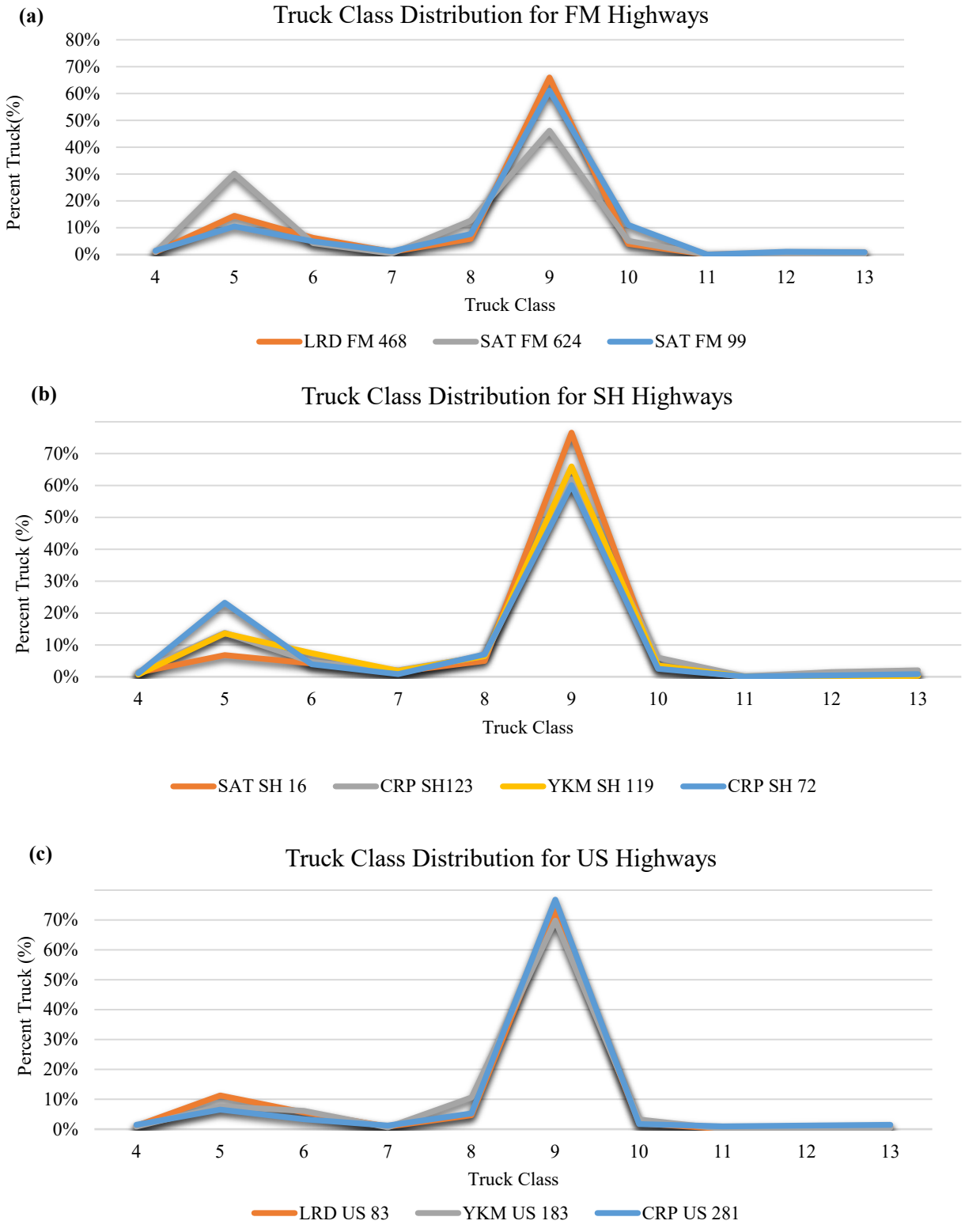

Figure 4.17 Truck Class Distributions: (a) FM Highways (b) SH Highways (c) US Highways in the Eagle Ford Shale

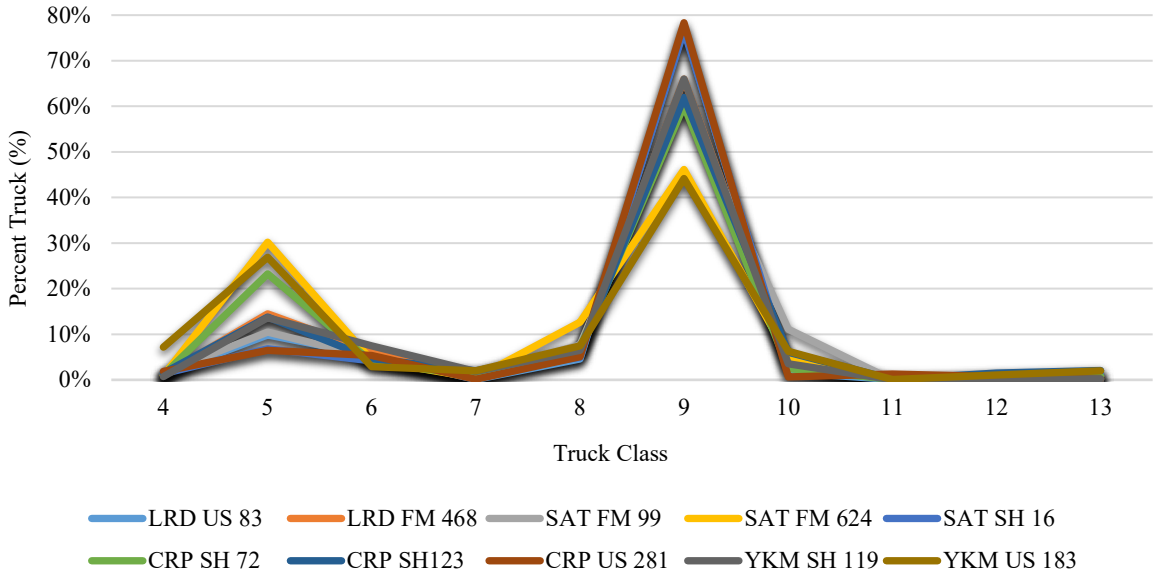

Figure 4.18 Truck Class Distributions of All Portable WIM Sites in the Eagle Ford Shale

4.2.2 Truck Misclassifications

Portable WIM units are characteristically reliable at collecting and classifying vehicular traffic. Figure 4.19 illustrates the typical error classifications associated with each type of truck class. As illustrated, these misclassifications errors tend to be low. The classes of trucks with the highest error percentage are Class 4 and Class 7. Class 4 is a predominant characterized by buses, and therefore, new bus configurations could be the source of that error. While Class 7 trucks are typically characterized by dump trucks with multiple rear axles that can be deployed when needed; they often have a lift axle that could mislead the algorithm the WIM unit uses. Other sources of errors can be attributed to pavement surface imperfections, traffic driving over the sensor splice, damaged sensors, or unconventional truck configurations. Figure 4.20 illustrates the truck class distribution of US 83 in the Laredo District. This plot shows the truck class distribution of the summer and winter collection period and the differences are imperceptible. Despite two different data collection times, the portable WIM unit classified the incoming traffic appropriately thus validating the results.

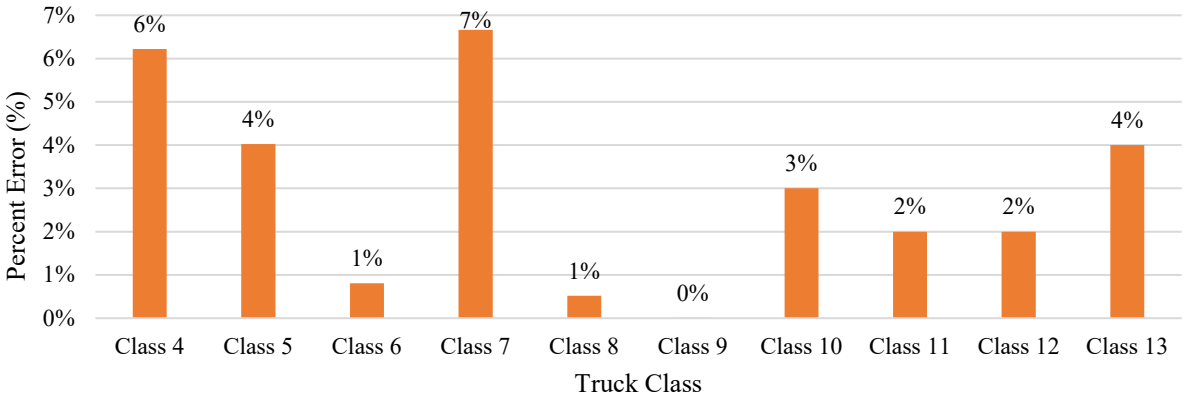

Figure 4.19 Truck Class Distributions Misclassification Error

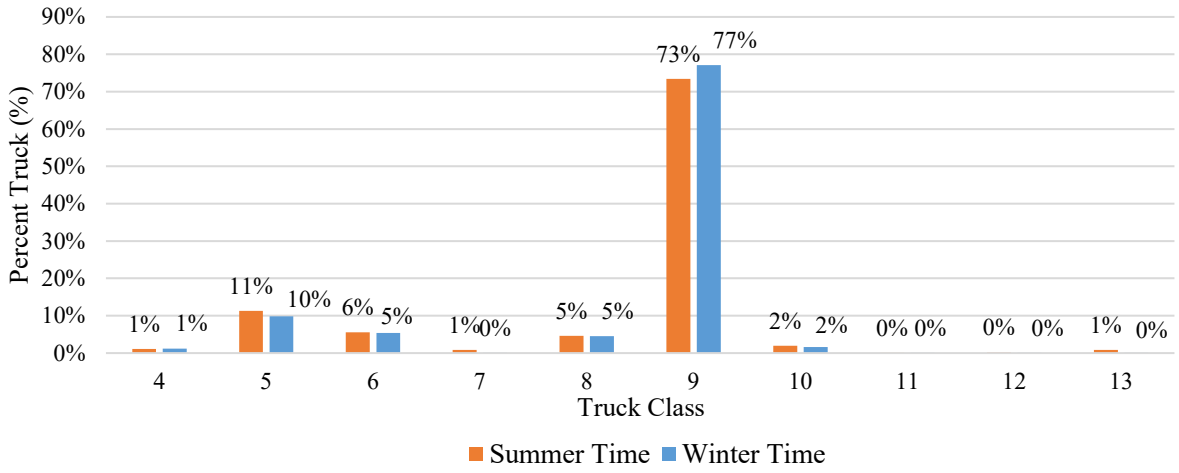

Figure 4.20 Seasonal Variation of Truck Class Distributions

4.2.3 Data Validation-Steering Axle Analysis

Contracting institutions and state agencies primarily favor portable WIM devices due to their minimal traffic interruption, cost effectiveness, and ease of operation in remote areas compared to stationary WIM stations. Validating WIM data can be cumbersome at times because researchers often don't have the means to justify the weight readings; thus, the reliability of the data becomes questionable. However, there are a few metrics that can give an indication of the accuracy and reliability of the WIM data being collected, such as using the steering axle weight of typical Class 9 trucks. According to truck manufacturers, typical steering axle weights of Class 9 trucks range between 8,000 to 12,000 lb. The steering axle weight that was used as the reference axle weight during calibration of the portable WIM units was 10,500 lb. Figure 4.21 illustrates the

typical steering axle weight of Class 9 trucks in SH 16 of the San Antonio Districts. As shown in the figure, the bulk majority of the weight distributions fall within the expected 8,000 to 12,000 lb. range. As a matter of fact, 93% of the weight distributions fell in this range and 36% of weight distributions fell in the 10,500 lb. interval. This proved that the WIM units are collecting accurate WIM data that is suitable for the development of the axle load spectra.

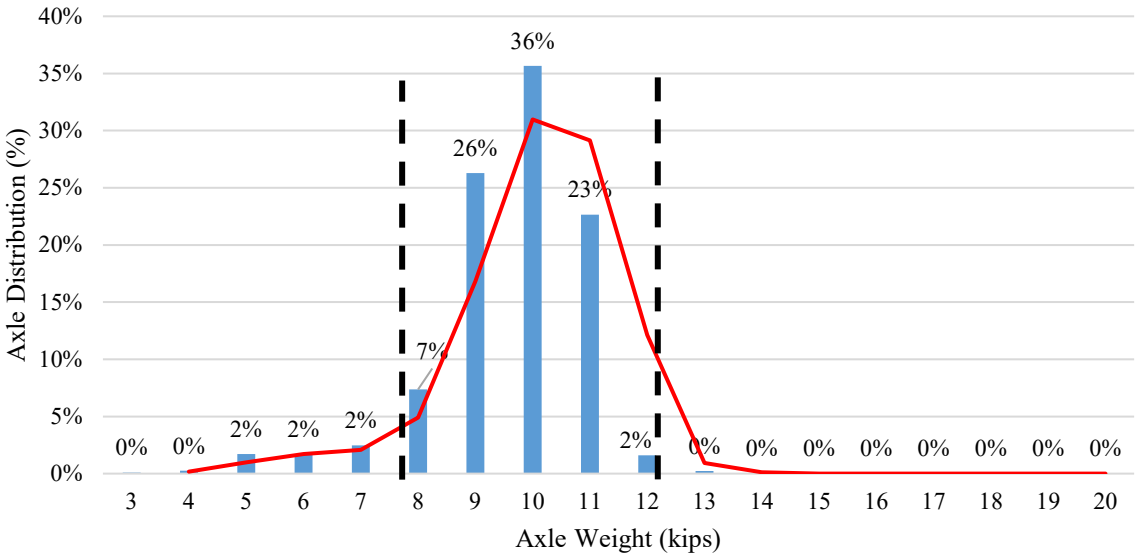

Figure 4.21 Steering Axle Weight Distribution of Class 9 Trucks in SH 16

Figure 4.22 and Figure 4.23 similarly illustrate steering axle plots of other WIM sites with one major distinction. The plot of Figure 4.22 was selected to show that the steering axle weight was still within the expected range. However, the most common axle weight (37%) was in the lower spectrum at 9,000 lb. The researchers attributed the lower steering axle weights to the low GVW distributions collected at this site. In contrast, Figure 4.23(a) illustrates the steering axle weight of FM 468 in the Laredo District. This figure shows the steering axle weights in the higher spectrum with the most common axle weight (23%) at the 12,000 lb. interval. The reason behind these results is attributed to the WIM data collected at FM 468, which contained some of the heaviest GVW distributions in the entire Eagle Ford Shale Region. Reference plots for the GVW Distributions for SH 119 and FM 468 are illustrated in Figure 4.23(b) and Figure 4.23(c).

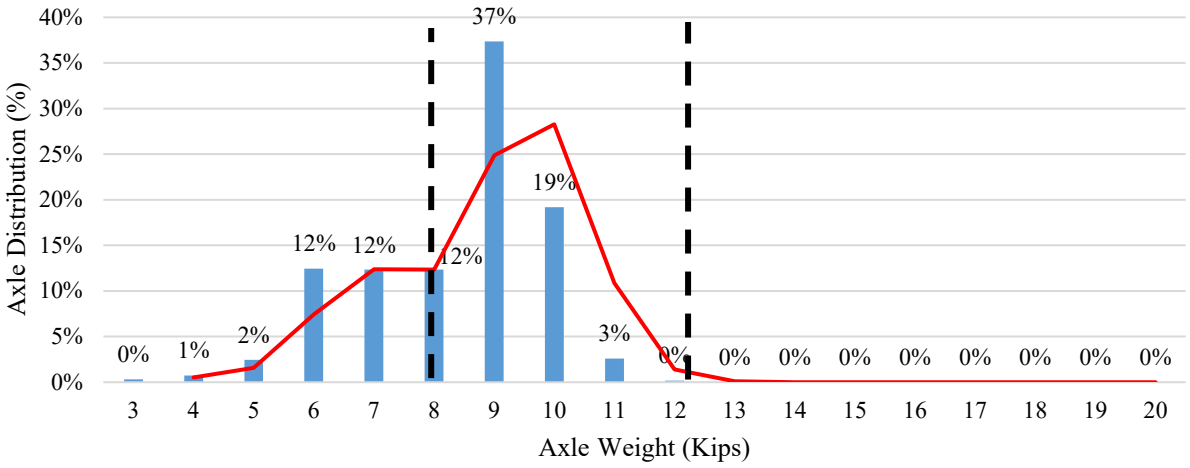

Figure 4.22 Steering Axle Weight Distribution of Class 9 Trucks in SH 119

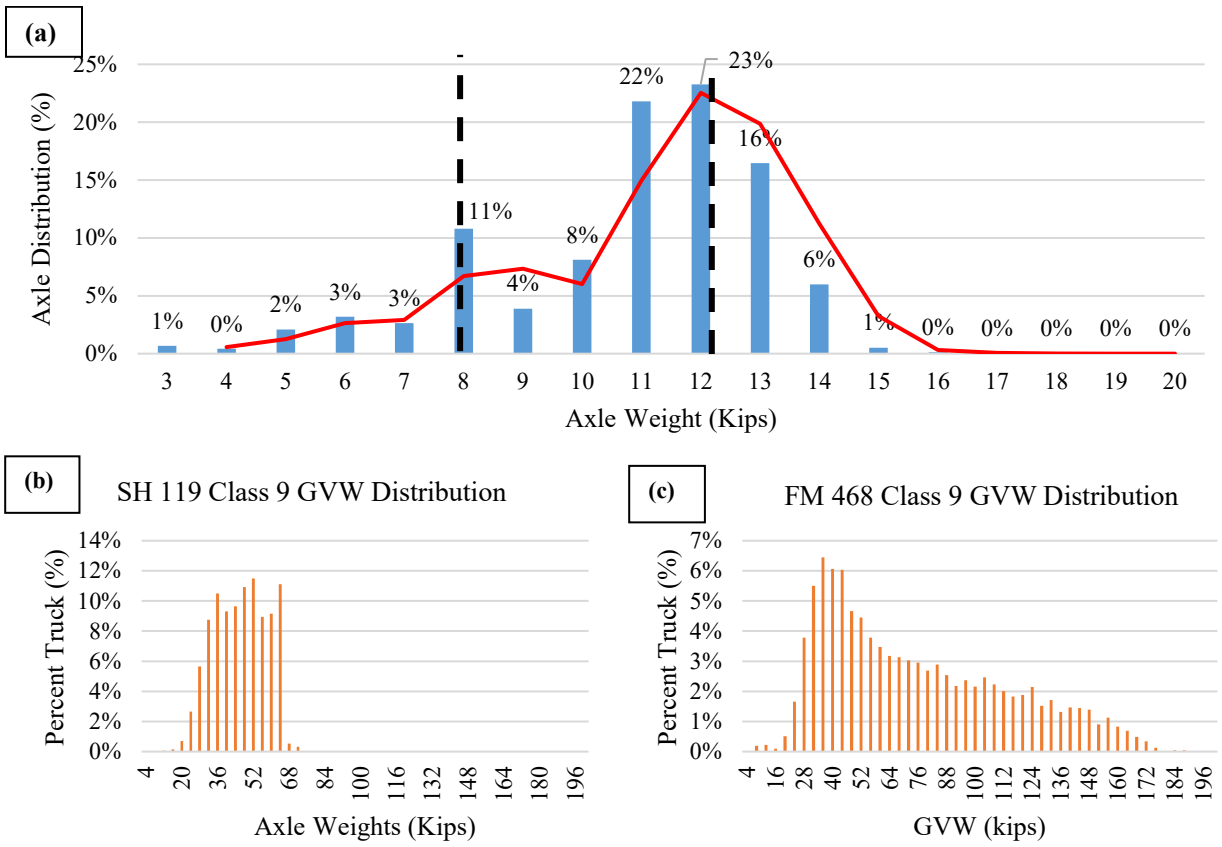

Figure 4.23 (a) Steering Axle Weight Distribution of Class 9 Trucks in FM 468 (b) Reference GVW Distribution SH 119 (c) Reference GVW Distribution FM 468

Figure 4.24 illustrates the average steering axle weight of Class 9 trucks for all portable WIM sites collected in the Eagle Ford Shale. A small spread of steering axle weights can be seen in the plot which can be attributed to a number of different reasons. Nonetheless, the vast majority of the steering axle weights are within the desired range. In addition, Figure 4.25 illustrates plots of steering axle weights collected for SH 16 and US 183 highways with their respective typical Coefficient of Variance (COV). These plots show a COV less than 15%, which is congruent with the error percentage ±15% indicated by the equipment manufacturer. Similar trends are true for the rest of the WIM test sites.

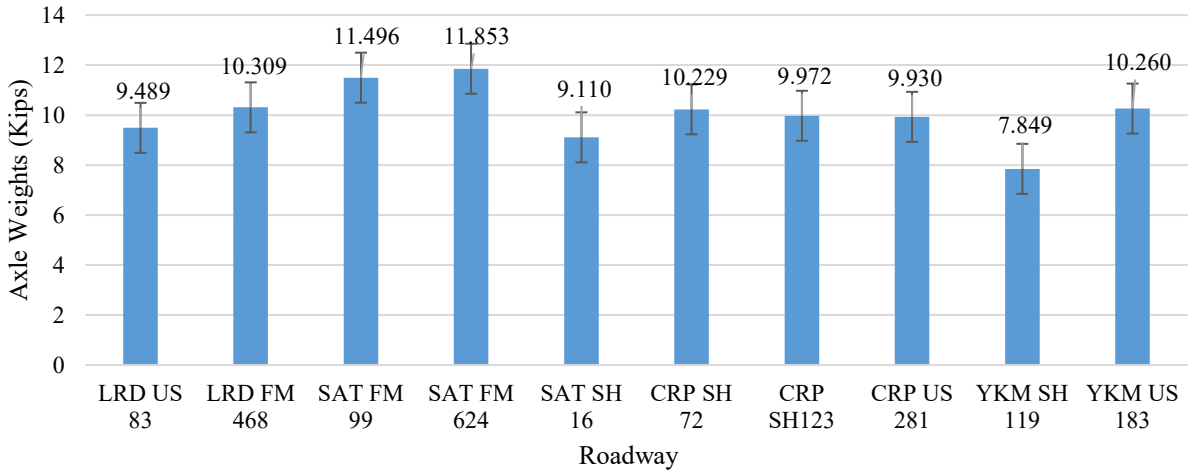

Figure 4.24 Steering Axle Weight Distributions of Class 9 Trucks in All Sites

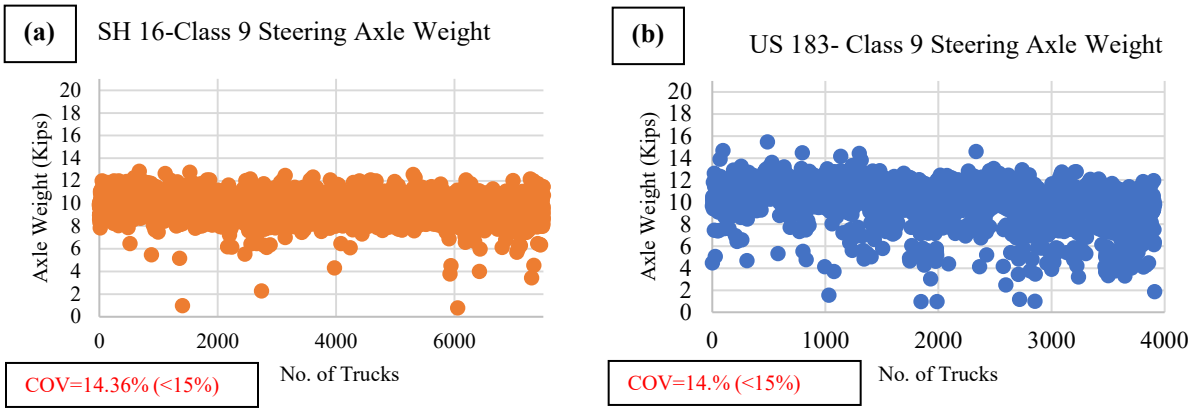

Figure 4.25(a) Class 9 Steering Axle Weight Coefficient of Variance (COV) for SH 119 (b) Class 9 Steering Axle Weight Coefficient of Variance (COV) for US 183

4.2.4 Gross Vehicle Weight (GVW) Analysis

Two types of GVW distributions were primarily observed throughout all WIM sites. The first type of distribution is illustrated by Figure 4.26, which shows the gross vehicle weight distributions with respect to truck percentage for all classes of trucks in US 281 of the Corpus Christi District. This plot can be characterized by a bimodal distribution that is attributed to unloaded trucks in the 20,000 lb. to 44,000 lb. range and loaded trucks in the 76,000 lb. to 100,000 lb. range. These GVWs coincide with historical WIM data throughout Texas and the current LTPP data. However, it must be noted that GVW distributions are shifted past the 80,000 lb. weight limit due to the large number of overloaded trucks this highway supports. Another metric that is often employed is the minimal gross vehicle weight analysis, in this check little to no trucks should be present at the 10,000 lb. or less weight interval. Figure 4.26 shows only 4% of the data in that range. Nonetheless, truck percentages in this range are acceptable because it is known that Class 5 trucks tend to be light vehicles that peak at that the 10,000 lb. to 12,000 lb. weight interval.

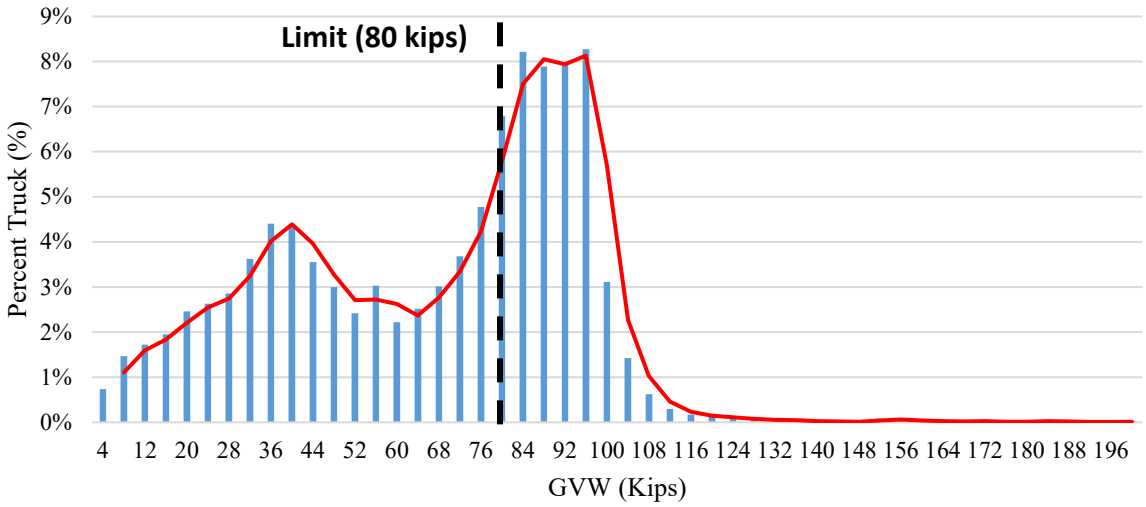

Figure 4.26 GVW Distributions of All Trucks in US 281

The second type of GVW distribution that was observed was located in areas with heavy traffic operations and overweight traffic. Usually, the bimodal distribution is significantly less pronounced as illustrated by Figure 4.27. Where a small peak is visible at the 12,000 lb. interval, due to the high number of Class 5 trucks and second peak is visible at the 36,000 lb. interval that is linked unloaded trucks. Despite the weight distributions peaking at a lower weight range, the plot also shows the GVW distribution extending to the 180,000 lb. weight interval. The typical

trucks that are most prevalent in the energy development highway network can be seen in Figure 4.28.

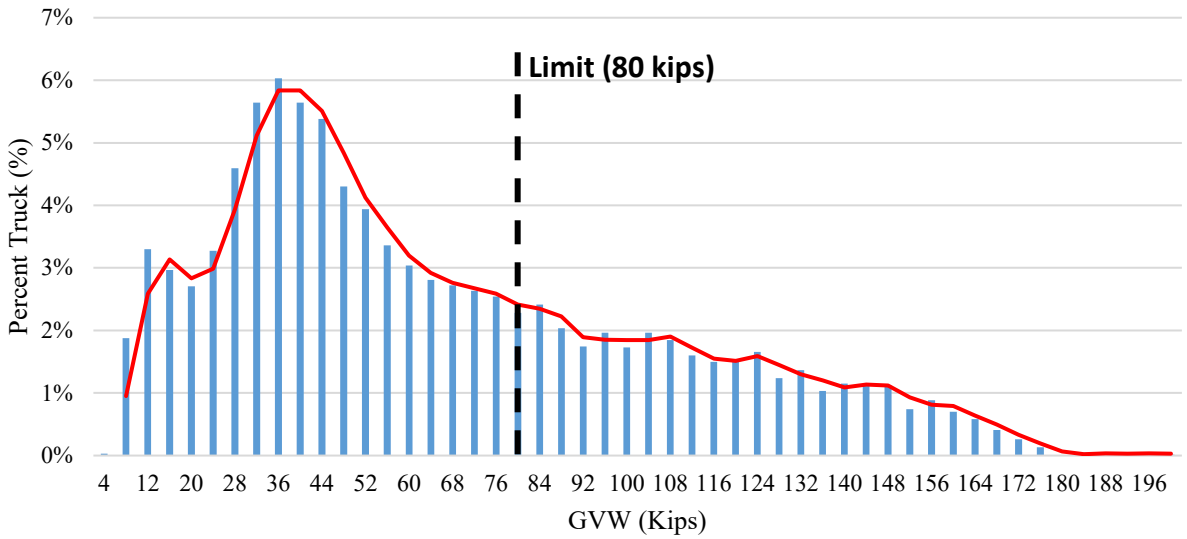

Figure 4.27 GVW Weight Distributions of All Trucks in FM 468

Figure 4.28 Class 9 Oil Tanker and Class 9 Sand Box Truck

4.2.5 Overweight (OW) Axle Analysis

One of the primary objectives of this study was to capture GVW and axle weight distributions of heavy vehicles operating in the overloaded corridors and energy sector zones of South Texas. In the process, the researchers captured surprising results. Eight out of the ten selected highways experienced a significantly high number overweight truck traffic (10%<). The Districts with the heaviest truck traffic operations were the Corpus Christi District and the Laredo District. However, despite having numerous oil/gas wells in the surrounding areas, pipeline

construction, and equipment movement, the highways in the Yoakum District were not significantly affected. Figure 4.29 illustrates the overweight (OW) truck distributions of US 281 for both the summer and the winter seasons. The plot shows an overweight distribution of 17% in the winter time and an astounding 45% overweight distribution in the summer. That is nearly half of all trucks travelling on this highway were overweight, a significant number that detrimentally impacts the pavement structure especially in the summer when the stiffness properties of the asphalt layer are the weakest. Heavy truck traffic operations in this area may be due to a nearby oil refinery in Three Rivers, Texas and transportation of heavy equipment as illustrated in Figure 4.30.

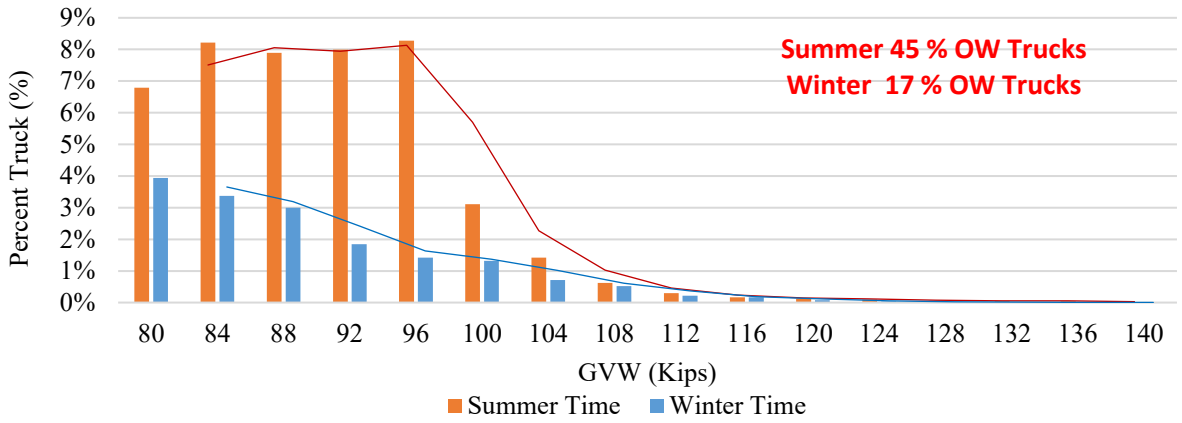

Figure 4.29 GVW Weight Distributions of All Trucks in FM 468

Figure 4.30 Heavy Traffic Operations in US 281 near Three Rivers Texas.

Meanwhile, Figure 4.31 also illustrates the OW truck distributions for FM 468 for both summer and winter time. Similarly, this plot shows a smaller OW truck distribution for the winter at 12% compared to a 32% distribution for the summer. The main distinction is that the summer distributions extend to the 180,000 lb weight interval which is alarming for any roads, especially FM roads that are not designed to sustain such heavy truck weights. FM 468 also had some of the heaviest truck traffic in terms of GVW. The portable WIM unit deployed at this site captured trucks weighting in excess of 250,000 lbs. Unsurprisingly, this site was the most damaged and distressed site showing multiple distress types such as rutting, fatigue cracking, flushing, and pot holes among others.

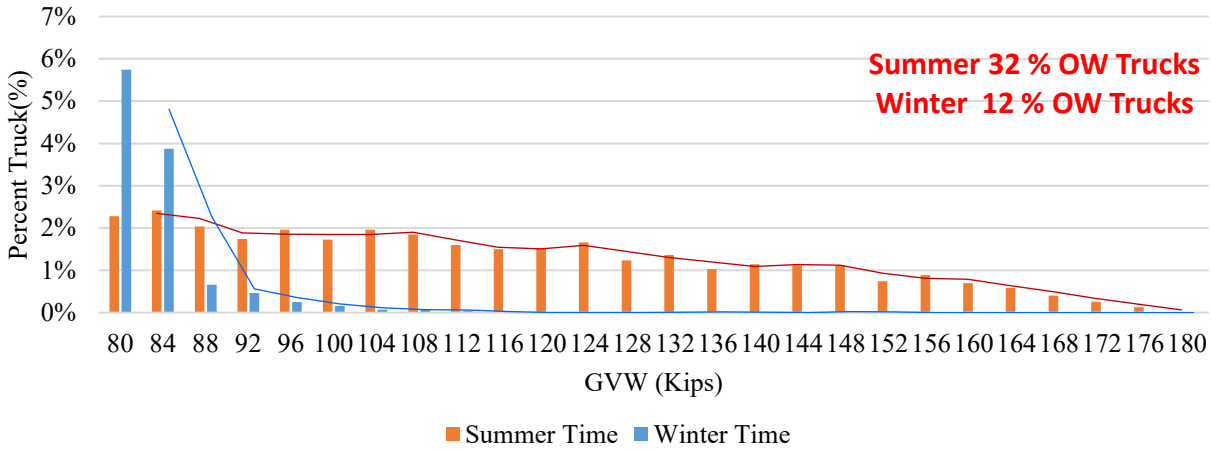

Figure 4.31 GVW Weight Distributions of All Trucks in FM 468

FM 99 is a small load zoned road with a weight limit set at 58,420lbs. However, as shown in Figure 4.32 that limit does not prevent the oil and gas industry from driving over this road. Figure 4.33 illustrates the OW vehicle distributions plot of FM 99 in the San Antonio District for both the summer and winter collection time. The portable WIM unit deployed at this site captured data that characterized the overweight truck distributions as high as 56% for the summer time. While in the winter time, as much as 63% of the truck traffic was overweight. These incredibly high percentages of overweight truck traffic detrimentally impact the pavement structures and bridges. The impacts of these heavy truck traffic operations are furthered discussed in the following sections.

Figure 4.32 Oversize/Overweight Loads travelling on FM 99 of the San Antonio District.

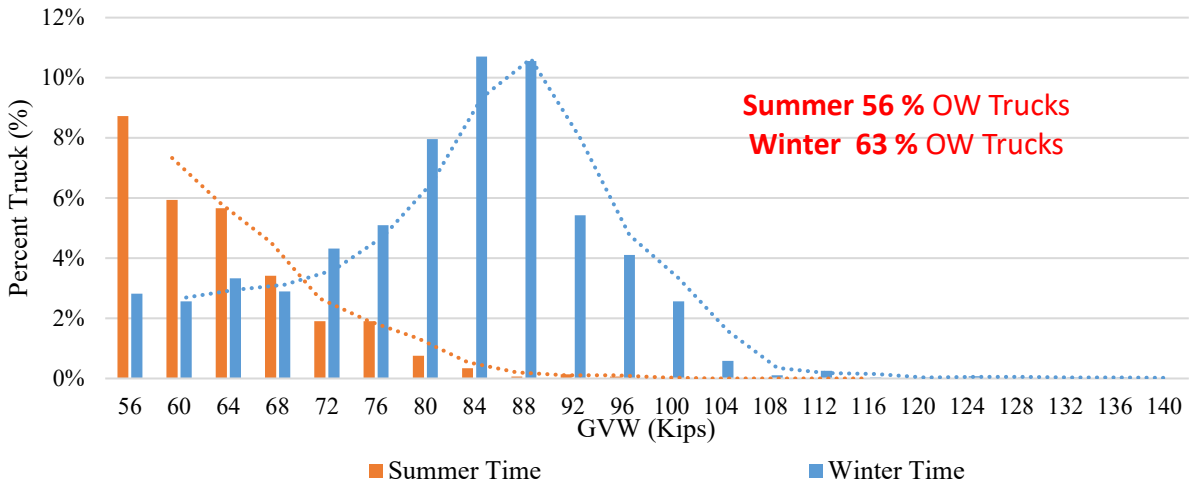

Figure 4.33 OW Weight Distributions of All Trucks in FM 99

Figure 4.34 illustrates OW truck distributions in SH 123/ BU 181 of the Corpus Christi District for both the summer and the winter time. The portable WIM data collected was consistent throughout both time intervals, characterizing the OW distribution for the winter time at 35% and 36% for the summer. These results indicate that a third of all truck traffic in this highway is overweight at any given season. In addition, GVW in excess of 360,000lbs have been recorded in

this highway during the summer time. To verify the validity of the collected information, the research team contacted the local TxDOT office and it was confirmed that they had issued permits for trucks weighting in excess of 300,000lbs. In terms of damage quantification, a single passage of this load can be enough to impart significant damage to the pavement structure, culverts, and nearby bridges.

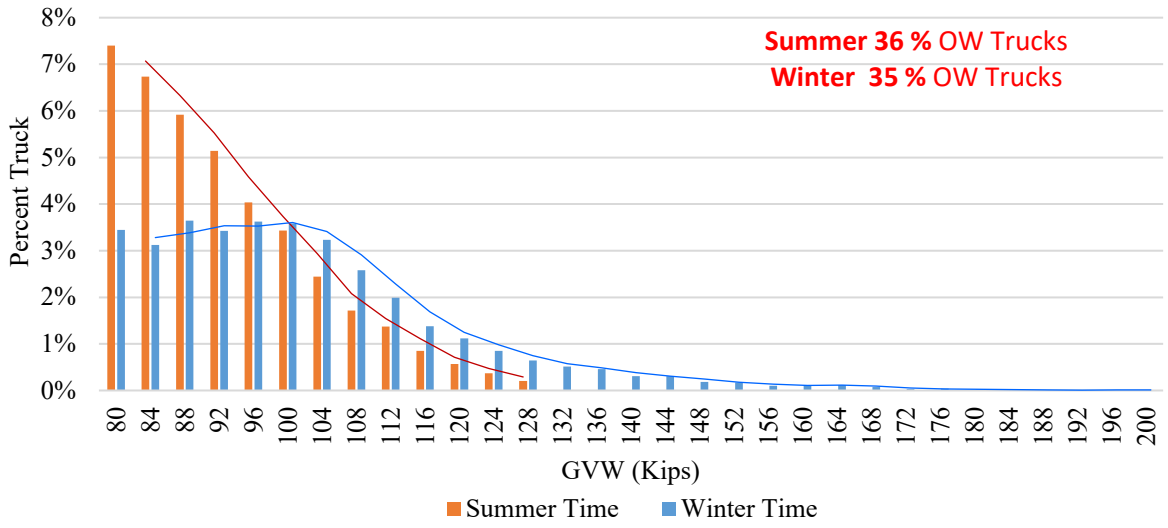

Figure 4.34 GVW Weight Distributions of All Trucks in SH 123/ BU181

Figure 4.35 illustrates the OW truck distributions among all FM, SH, and US highways in the Eagle Ford Shale. The trend observed shows that OW truck distributions are highest in the summer time with the exception of US 83 and FM 99. This trend can be attributed to a number of different reasons including, seasonal variation of crude oil price per barrel. The price of oil generally tends to be more expensive in the summer time therefore, energy companies are more enticed to produce more barrels of oil since they have a higher return on their investment. As a result, there are more wells being drilled that generate a plethora of truck traffic even for just one drilling site. In addition, the results show that Farm-to-Market roads can have overweight distributions up to 64%, state highways of up to 36%, and US highways up to 45% for highways in the surrounding network.

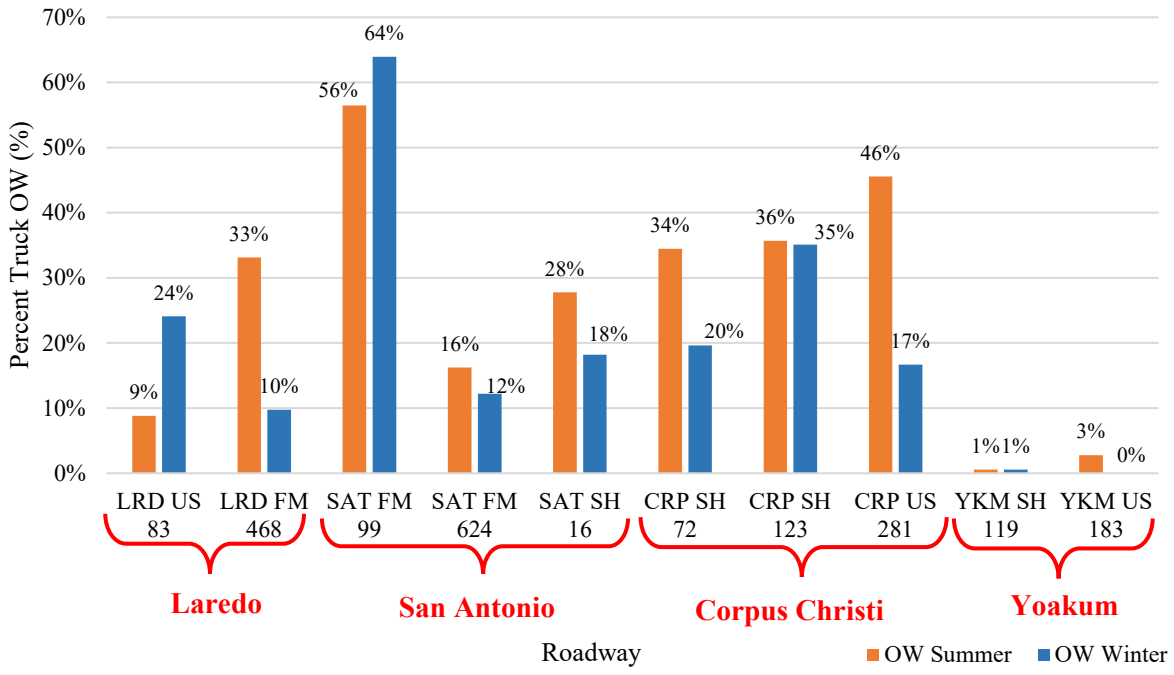

Figure 4.35 Seasonal Variation of OW Truck Traffic for All Ten Test Sites

4.2.6 Other Axle Analysis

Tandem axles typically follow similar weight distributions to that of Class 9 GVW trucks. This information coincides, since Class 9 trucks are the most common truck in almost every highway network, and composed of two tandem axles. In most highways, tandem axles are also typically characterized by a bimodal distribution that is attributed the unloaded and loaded tandem axles. Figure 4.36 illustrates this bimodal distribution of unloaded tandem axles in the range of 14,000 lb. to 26,000 lb., while the loaded tandem axles in the 32,000lb. to 42,000lb. range for SH 72. Figure 4.37 illustrates the tridem axle weight distributions for SH 16 which show the distributions substantially shifted to the loaded and overloaded side. In addition, for heavy loaded highways such as the one illustrated in Figure 4.38, the quad axle distributions increase and then peaks in the 70,000 lb. range, essentially showing significantly overloaded quad axles (79%).

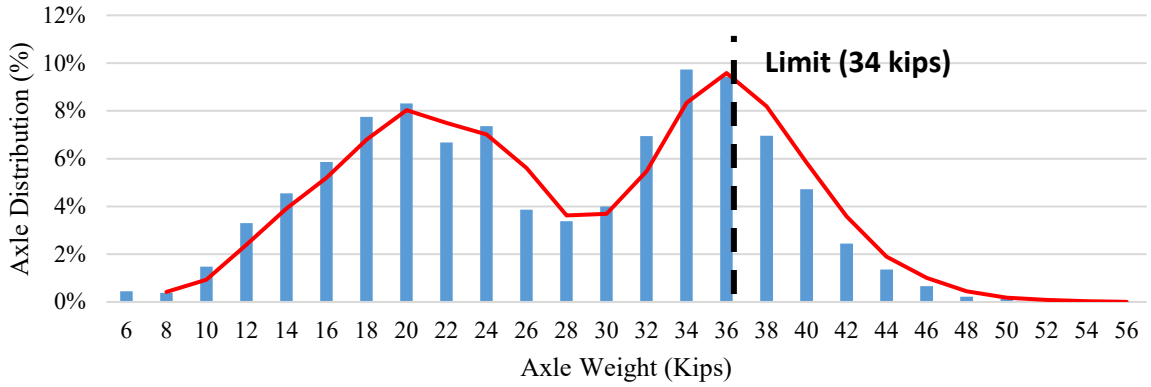

Figure 4.36 Tandem Axle Weight Distributions for All Trucks in SH 72

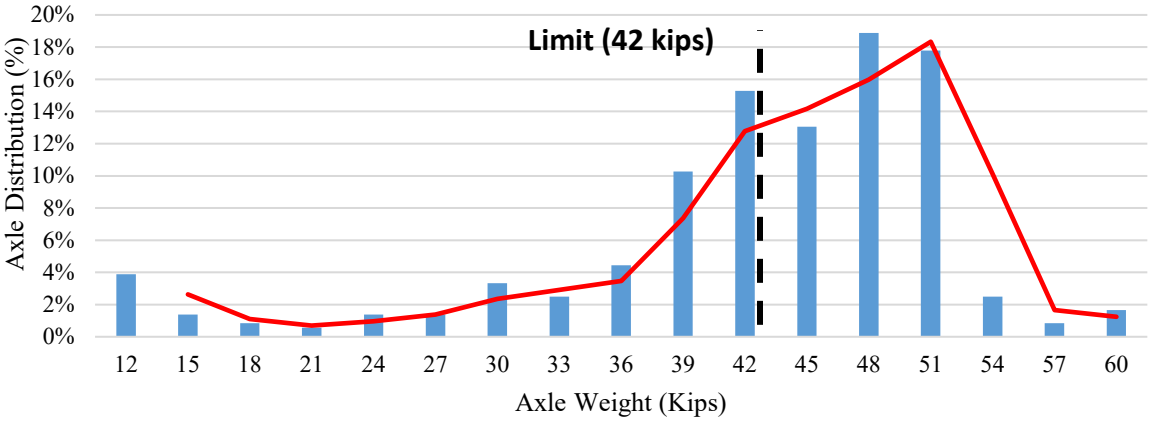

Figure 4.37 Tridem Axle Weight Distributions for All Trucks in SH 16

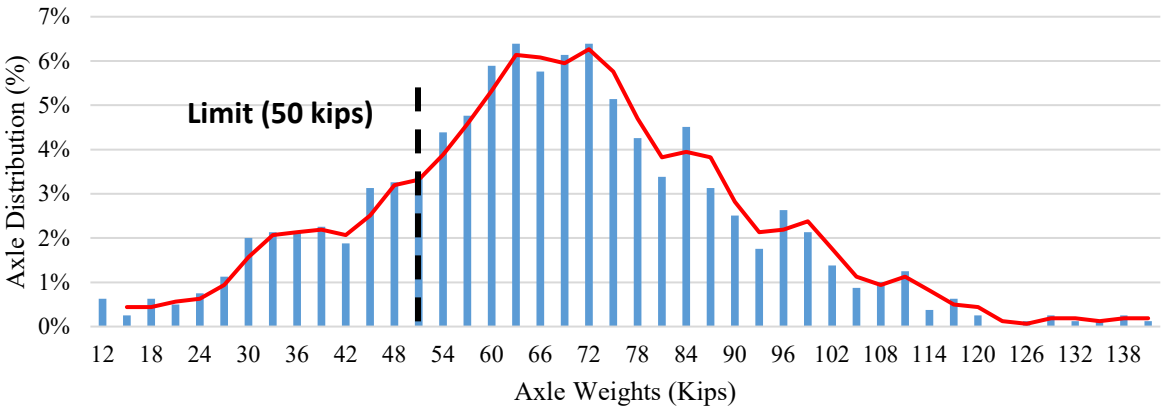

Figure 4.38 Quad Axle Weight Distributions for All Trucks in SH 123 / BU 181

CHAPTER 5: NONDESTRUCTIVE TESTING (NDT) OF REPRESENTATIVE PAVEMENT SECTIONS

This section documents the results of pavement condition surveys and Non-Destructive Testing (NDT) testing conducted at the ten selected sites in the Eagle Ford Shale network. For the forensic studies portion, Falling Weight Deflectometer (FWD) and Ground Penetrating Radar (GPR) were deployed to the field for the determination of the layer profile and back-calculation of layer moduli of the sites in the surveyed network. The collected information was utilized for damage quantification purposes of the representative pavement sections.

5.1 Visual Inspection of Selected Sites

Proper evaluation of the pavement conditions was a primary concern to accurately quantify the pavement damages imparted by the overweight truck traffic. In order to properly assess the pavement conditions, it was necessary to identify the type and severity of the distress-related damages. To achieve this objective, visual inspections of pavement sections were conducted under lane closure by examining 100 ft. before and 100 ft after the portable WIM station (Ashtiani et al., 2019). We documented and reported the different distress types present in each of the inspected sections per TxDOT's 2018 PMIS Pavement Rater's Manual. Figure 5.1 shows an illustration of the visual inspection plan the research team incorporated. Table 5.1 indicates the selected roadways, the roadbed type, the data collection lane, the reference markers, and their exact GPS location.

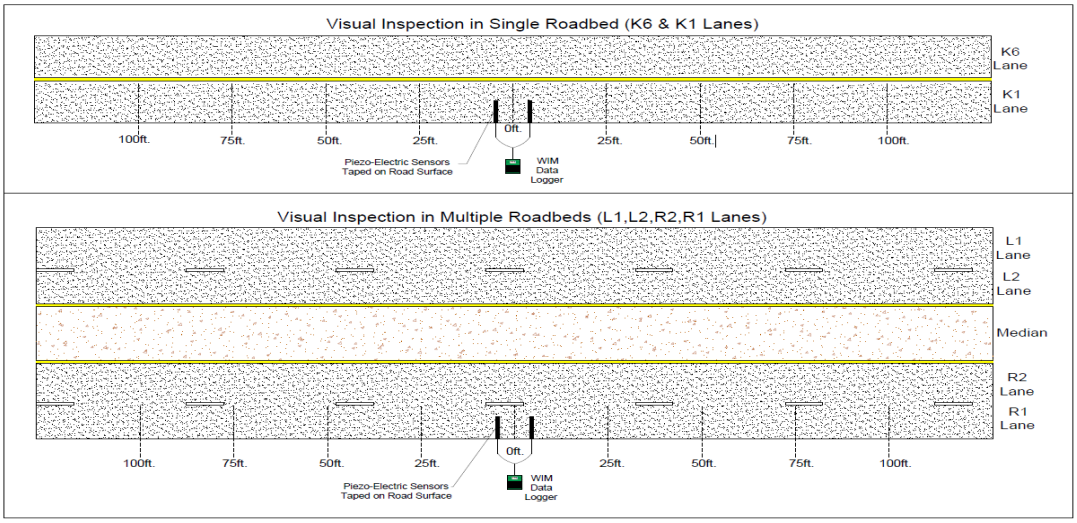

Figure 5.1 Visual Inspection Survey Illustration.

Table 5.1 Location of Selected Roadways in Eagle Ford Shale Network

District	County	Roadway	Road Bed	Lane	Texas Reference Marker (TRM)	GPS Coordinate
Laredo	Dimmit	**US 83** (SB Lane)	Single	K1	638	(28.504907, -99.838659)
	La Salle	**FM 468** (WB Lane)	Single	K6	440	(28.531170, -99.398022)
San Antonio	McMullen	**FM 624** (WB Lane)	Single	K6	500	(28.125868, -98.525511)
	McMullen	**FM 99** (SB Lane)	Single	K1	588	(28.465600, -98.440487)
	Atascosa	**SH 16** (SB Lane)	Single	K1	642	(28.784422, -98.540370)
Corpus Christi	Live Oak	**US 281** (NB Lane)	Multiple	L1	622	(28.452511, -98.183444)
	Karnes	**SH 72** (WB Lane)	Single	K1	536	(28.739827, -97.940206)
	Karnes	**SH 123** (SB Lane)	Single	K1	552	(28.878125, -97.893333)
Yoakum	Gonzales	**US 183** (SB Lane)	Single	K6	580	(29.459768, -97.435360)
	Dewitt	**SH 119** (WB Lane)	Single	K1	544	(29.036632, -97.572325)

The initial visual inspection survey was conducted on Farm-to-Market (FM) 468 in LaSalle County of the Laredo District. Upon initial inspection, FM 468 appeared to be in a severely distressed state exhibiting multiple distress types. The first distress present on both K1 and K6 lanes was severe flushing on both right and left wheel paths throughout the entire section, as shown in Figure 5.2. The flushing rated 3, according to TxDOT's 2018 PMIS Pavement Rater's Manual, begins in the intersection with FM 469 and continues past the Dimmit County line. The second documented distress was shallow to severe rutting throughout most of the inspected section. The rutting illustrated in Figure 5.3, ranged from .25 in to .50 in in both wheel paths and covered approximately 70% of the wheel paths area. Moreover, an area with a large patch appearing to be milled out and replaced, as shown in Figure 5.4, was also reported. However, the patch already seems to be disintegrating. Alligator cracking is also developing in the wheel paths covering an area of approximately 30%. In addition, raveling and potholes were also spotted in certain places of the inspected area. Heavily loaded vehicles coupled with a thin asphalt layer are believed to be the reasons for the many distresses present and the poor ride quality of FM 468.

Figure 5.2 Severe Flushing in FM 468 - La Salle County

Figure 5.3 Shallow Rutting in FM 468 - La Salle County

Figure 5.4 Patches in FM 468 - La Salle County

Table 5.2 lists a summary of the different pavement distresses associated with each of the ten inspected highways. As indicated in Table 5.2, rutting and flushing are the predominant pavement distresses related to highways in the Eagle Ford Shale. However, these distresses are expected as these highways service high volumes of heavily loaded truck traffic and overweight vehicles related to the oil-gas industry and heavy equipment transportation. Moreover, it was also found that the severe rutting and flushing were more pronounced in FM and SH roads because in addition to the heavy traffic, these highways also have less robust structural layers due to their nature of initial design. The safety of such pavement sections during wet seasons can become a concern as segments with severe rutting coupled with flushing can become extremely slippery due to accumulation of rainwater in the wheel path. Detailed information pertaining to the visual inspection conducted on the selected sites are provided in Appendix A.

Table 5.2 Pavement Distresses in Representative Roadways in Eagle Ford Shale Network

District		Laredo		San Antonio			Corpus Christi			Yoakum	
County		La Salle	Dimmit	Atascosa	McMullen	McMullen	Live Oak	Karnes	Karnes	Dewitt	Gonzales
Roadway		FM 468	US 83	SH 16	FM 99	FM 624	US 281	SH 72	BU 181	SH 119	US 183
Pavement Distresses	Rutting	X	X	X	X	X	X	X	X		X
	Patching	X			X						
	Block Cracking	X									
	Alligator Cracking	X	X		X		X				
	Longitudinal Cracking						X				X
	Transverse Cracking										
	Raveling		X	X					X		
	Flushing	X	X	X	X	X	X	X	X		X
	Failures										
	Potholes	X			X						

5.2 Ground Penetrating Radar (GPR)

GPR testing was conducted on the selected pavement sections in Table 5.1 of the overload corridors of the Eagle Ford Shale region (Morovatdar et al., 2019) An air-coupled GPR unit equipped with a 2 GHz antenna was deployed to properly evaluate the pavement layer configuration, as shown in Figure 5.5. This air-coupled GPR is normally operated at highway speed and does not require traffic control.

Figure 5.5 GPR Testing in Laredo District

The collected GPR data was analyzed and interpreted using the computer software RADAN. It should be noted that GPR surveys were collected at two times in each roadway under similar conditions in order to ensure the accuracy of the collected data. Therefore, the reported pavement layer thicknesses are based on the average values between the two operated tests. Moreover, in order to properly evaluate the pavement layer thicknesses, validation of the GPR data was conducted by comparing the collected results with other available TxDOT databases and with communication with TxDOT engineers.

5.2.1 Validation of the GPR Data Collected in the Network

Data mining from available databases, pavement design plans, and communication with TxDOT personnel was conducted to confirm the pavement profiles of the studied sections. To

further explain this process, the GPR measurements from SH 72 are used as an example of measurements where post-processing required further verification. Figure 5.6 shows the GPR collected data for the specified location. Analysis of the GPR image showed a shallow interface corresponding to a 1.5 in. overlay on top of a hot mix asphalt (HMA) layer with a thickness that varies between 4 in. to 6 in., with an average of 5.1 in. However, from such image, the base-subgrade interface was not discernible. To verify the available and complement the missing information, the research team proceeded to contact the Districts to request pavement design plans and conducted an extensive search within the available databases.

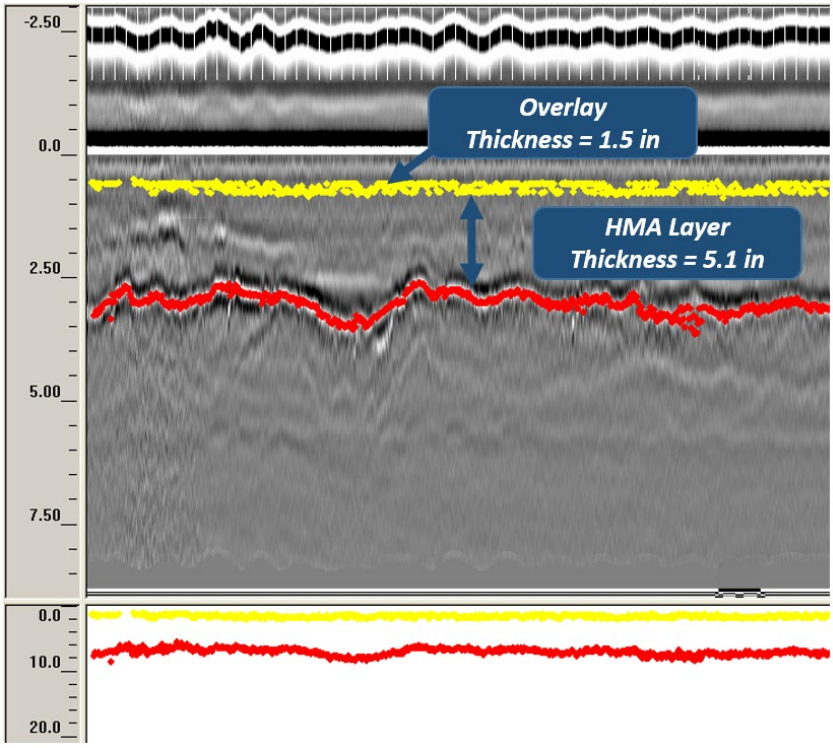

Figure 5.6 GPR Data from SH 72, Corpus Christi

- ***Pavement Design Plans***

  For the described case, the research team thoroughly reviewed the pavement design plans, corresponding to Reference Marker 536 of SH 72, located in Karnes County. Figure 5.7 shows the proposed design plans and specifications as of November 2017. From the design plans, State Highway 72 was designed to have a 1.5 in. asphalt overlay, 5 in. of HMA, 16 in. of 1% cement treated base (CTB) constructed over 8 in. of 3% cement treated subgrade (CTS). Thus, the overlay and HMA layer thicknesses obtained from post-processed GPR

data were found to be in agreement with the pavement design. In this case, the design plan further supplemented the base thickness missing from the GPR measurements.

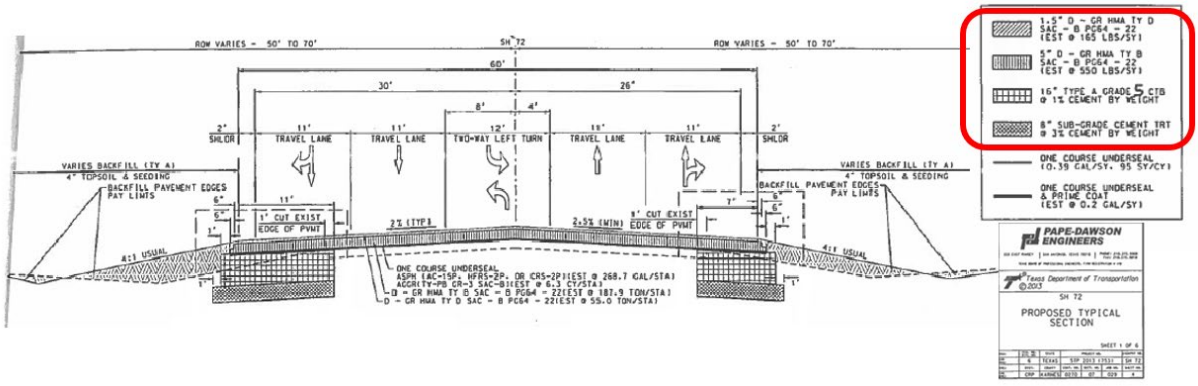

Figure 5.7 Pavement Design Plan for SH 72 in Karnes County (Corpus Christi)

- ***TxDOT's Personnel Interview and Intranet Resources***

  We also communicated with TxDOT's District personnel to verify and/or supplement layer configuration information. For the case explained here, a shallow layer as seen by the GPR could be attributed either to an overlay or to the presence of moisture underneath the pavement surface. TxDOT's maintenance supervisor confirmed the presence of an asphalt overlay in the SH 72 pavement structure. It was determined in Technical Memorandum 14-06 (Sebesta, 2014) that a section along SH 72 in Karnes County was redesigned in 2014 to address the severe distresses it experienced due to the energy development traffic.

Ultimately, Table 5.3 illustrates the validated pavement layer thicknesses from the GPR results.

Table 5.3 Pavement Layer Configurations attributed to the Representative Roadways in Eagle Ford Shale Network

Roadway Information				Pavement Design Plans	PMIS Database		TxDOT's Personnel Interview	TxDOT's Intranet Resources	GPR Results (in)		
District	County	Roadway	TRM	Information	Pavement Type	PMIS Definition			**Overlay**	**AC**	**Base**
Laredo	Dimmit	**US 83** (SB Lane)	Near 638	1.5 in. Overlay	10	Surface Treatment Pavement	-	-	**1.5**	**4.8**	**6.2**
	La Salle	**FM 468** (WB Lane)	440	2.5 in. HMA, 6 in. Base	10	Surface Treatment Pavement	-	3 in. HMA	**-**	**2.1**	**9.8**
San Antonio	McMullen	**FM 624** (WB Lane)	500	7.5 in. Base layer	6	Thin Asphaltic Concrete (Under 2.5")	GPR results are verified (Gil Romo)	6 in. Base layer	**-**	**1.3**	**8.9**
	McMullen	**FM 99** (SB Lane)	588	-	10	Surface Treatment Pavement	GPR results are verified (Gil Romo)	6 in. Base layer	**-**	**1.5**	**8.3**
	Atascosa	**SH 16** (SB Lane)	642	-	10	Surface Treatment Pavement	GPR results are verified (Gil Romo)	-	**-**	**3.5**	**7.4**
Corpus Christi	Live Oak	**US 281** (NB Lane)	622	2 in. Overlay 4-6 in. HMA 18 in. Base	5	Medium Thickness AC (2.5"-5.5")	-	At least 8 in. of Base layer	**1.5**	**5.5**	**18**
	Karnes	**SH 72** (WB Lane)	536	1.5 in Overlay 5 in. HMA 16 in. CTB 8 in. Subgrade Cement Treated	5	Medium Thickness AC (2.5"-5.5")	This roadway has Overlay (Kevin Butler)	At least 5 in. of AC, Cement Treated Base (CTB)	**1.5**	**5.1**	**16[a] +8[b]**
	Karnes	**SH 123** (SB Lane)	Near 552	5.5 in. HMA 15 in. Base	5	Medium Thickness AC (2.5"-5.5")	-	At least 8 in. of Base layer	**-**	**5.5**	**15**
Yoakum	Gonzales	**US 183** (SB Lane)	Near 580	6 in. HMA 8 in. Base	5	Medium Thickness AC (2.5"-5.5")	-	At least 6 in. of Base layer	**-**	**5.5**	**8**
	Dewitt	**SH 119** (EB Lane)	Near 544	4 in. HMA 12 in. Base	5	Medium Thickness AC (2.5"-5.5")	-	At least 6 in. of Base layer	**-**	**3.5**	**10.5**

[a]Cement Treated Base (CTB) layer

[b]Cement Treated Subgrade

5.3 Falling Weight Deflectometer (FWD)

Falling Weight Deflectometer (FWD) data was also collected for the studied pavement sections mentioned before to identify the layer moduli, as shown in the Figure 5.8. The deflections obtained from the seven geophones were inputted into a back-calculation program to determine the layer moduli of the pavement structure.

Figure 5.8 (a) TxDOT's Falling Weight Deflectometer Testing on FM 88

Figure 5.9 shows the FWD setup that was arranged for data collection. It essentially, consisted of 3 drops per test spots, 3 spots spaced (25 ft distance) in the right wheel path to consider the load-induced damage on back calculated material properties (Ashtiani et al.,2019) The same testing pattern followed in between both wheel-paths to mitigate the effect of possible systematic errors incurred in the back-calculation procedure.

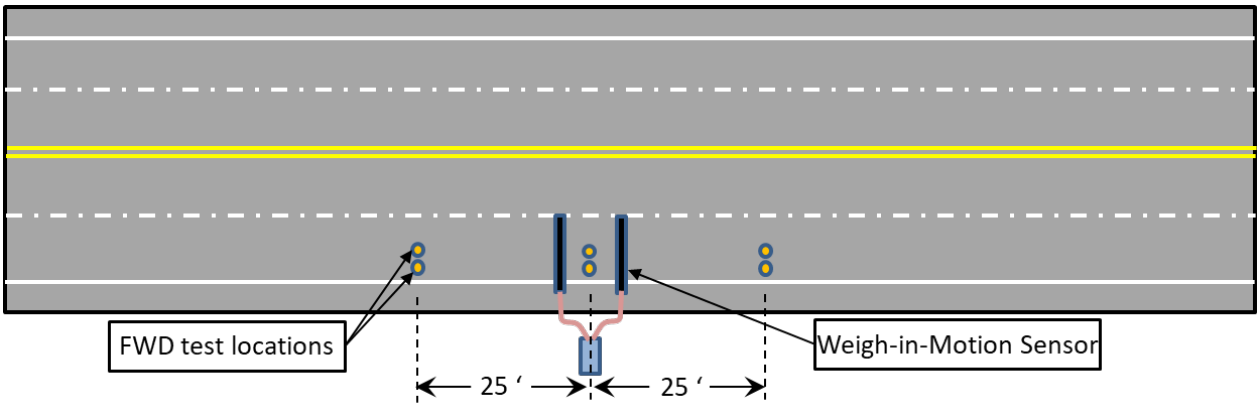

Figure 5.9 FWD Testing Setup

To back-calculate the layer modulus, an iterative pattern was used to calculate theoretical deflections. Using MODULUS 7, the users vary the material properties until an acceptable match of measured deflection is obtained. Moreover, it should be noted that the accuracy of the back calculated layer modulus are highly dependent on the following input parameters: pavement layer thickness, seed modulus, subgrade modulus, and depth to bedrock.

The FWD measurements from FM 624 roadway, are used as an example to explain the back-calculation procedure. Figure 5.10 shows the deflection basins diagram attributed to FM 624 roadway (for different loads) obtained from the seven FWD geophones.

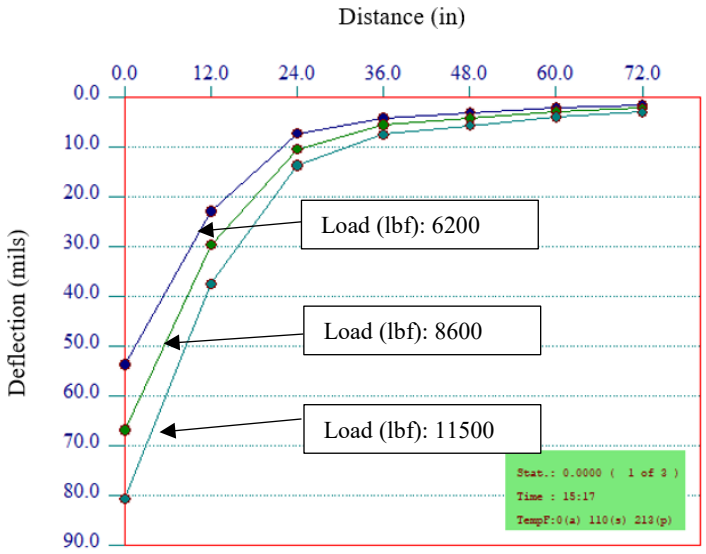

Figure 5.10 Deflection Basins from FM 624, San Antonio

Figure 5.11 illustrates the back-calculation program environment used to analyze the FWD deflection data. Analysis of the GPR data indicates that the Farm to Market 624 consisted of 1.3 in. of seal coat as the surface layer and 8.9 in. of granular-based layer. Using engineering judgment considering the roadway type, visual inspection of the sites, and reviewing quoted typical range of moduli in the literature, the seed modulus range in the program.

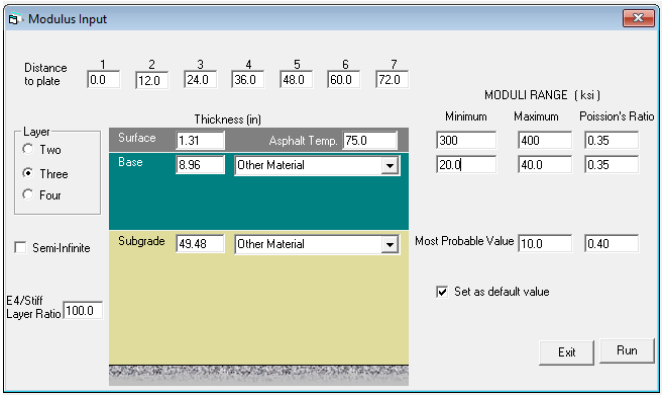

Figure 5.11 Backcalculation Layer Moduli for FM 624 in San Antonio

Based on results, the 8.9 in. granular base layer in FM 624 is relatively weak as the stiffness modulus values for this layer hit the lower allowed threshold of 20 ksi in the back-calculation procedure. It was also observed that the FM 624 consisted of subgrade layer with low structural capacity (6 ksi) and surface layer with 358 ksi.

5.3.1 Seasonal Climate Variation Effect on Modulus Value

In addition, it should be noted that in order to properly evaluate the effect of seasonal variation and the climatic conditions on pavement stiffness properties, the research team conducted FWD test in both summer and winter seasons for selected corridors in the network. Surface temperature and moisture in the system are the prominent factors that affect the stiffness and strength properties of multi-layer pavement systems. Considering that the HMA is viscoelastic in nature, its strength is greatly dependent on the temperature, which increases significantly with decrease in the pavement temperature. For granular base and subgrade layers the stiffness properties are highly connected with the moisture condition. The change in stiffness is related to the state of moisture tension in unsaturated soils, also known as soil suction (Chandra et al., 1989). Soil suction is made up of two components: 1) Osmotic suction due to salts dissolved in the pore water 2) matric suction due to the attraction of water for the surfaces of the soil particles.

In addition, Figure 5.12(a) illustrates the annual average temperature in San Antonio located in the Eagle Ford Shale region. As evidenced by this plot, the average temperature in winter season is 38% less than in summer. Moreover, as shown in Figure 12(b), the average monthly precipitation is connected with potential moisture infiltration into the pavement layers. As a result of the substantial differences in precipitation and temperature in both summer and winter seasons, the materials properties were also significantly different. For this reason, a plan was devised to perform FWD testing in both summer and winter times to capture the variation of the damage factors in different seasons of the year.

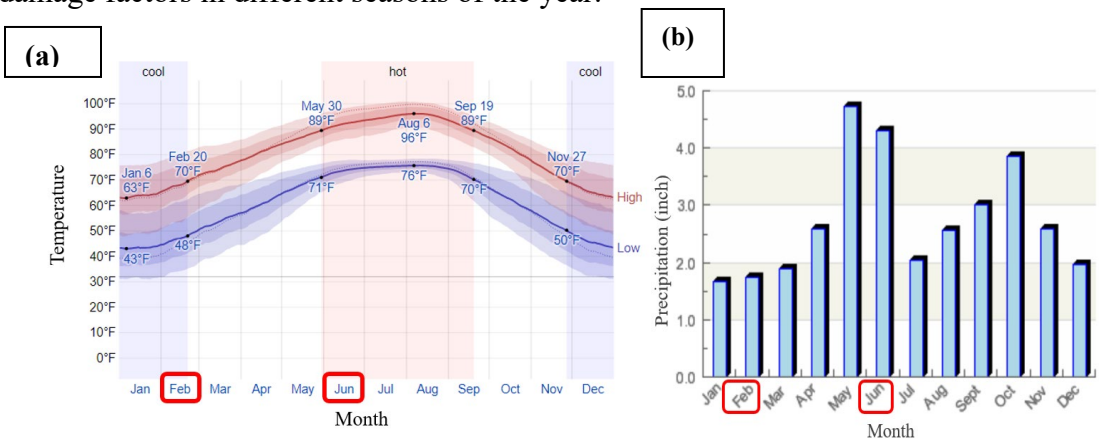

Figure 5.12 (a) Annual Average Temperature (b) Average Monthly Precipidation in San Antonio, Texas

The analysis of summer and winter FWD results indicated that for FM highways the obtained winter-based layer modulus were 26%, 12%, and 27% higher than the summer values for surface, base, and subgrade layers, respectively. Similar trends in the seasonal effect of the modulus values were found for SH and US highways, Table 5.4 illustrates those results. In addition, the site-specific back-calculated pavement layer modulus of all ten selected sites are presented in Table 5.5.

Table 5.4 Seasonal Effect on Back-calculated Layer Modulus Values

Roadway	Season						Percent Difference (%)		
	Winter			Summer					
	AC	Base	Subgrade	AC	Base	Subgrade	AC	Base	Subgrade
FM	565	24	9	419	21	6	26	12	27
SH	718	45	12	522	42	10	27	7	14
US	895	57	12	550	50	8	39	12	33

Table 5.5 Pavement Layer Modulus of the Selected Highways in the Eagle Ford Shale Network

Selected Roadways in Eagle Ford Shale Network				***Pavement Layer Modulus in Summer Season (ksi)***				***Pavement Layer Modulus in Winter Season (ksi)***			
District	County	Roadway	TRM	***Overlay***	***AC***	***Base***	***Subgrade***	***Overlay***	***AC***	***Base***	***Subgrade***
Laredo	Dimmit	**US 83** (SB Lane)	Near 638	***550***	***550***	***50***	***8***	***880***	***880***	***60***	***11.4***
	La Salle	**FM 468** (WB Lane)	440	**-**	***450***	***22***	***6***	-	***628***	***25***	***9.4***
San Antonio	McMullen	**FM 624** (WB Lane)	500	**-**	***358***	***20***	***6***	-	***416***	***22***	***7.1***
	McMullen	**FM 99** (SB Lane)	588	**-**	***450***	***22***	***7***	-	***650***	***26***	***9.7***
	Atascosa	**SH 16** (SB Lane)	642	**-**	***567***	***47***	***14***	-	***760***	***50***	***15.2***
Corpus Christi	Live Oak	**US 281** (NB Lane)	622	***550***	***550***	***50***	***8***	***956***	***956***	***55***	***12.5***
	Karnes	**SH 72** (WB Lane)	536	***429***	***429***	***234[a]***	***22[b]*** ***8[c]***	***688***	***688***	***201[a]***	***27[b]*** ***10[c]***
	Karnes	**SH 123** (SB Lane)	Near 552	**-**	***550***	***40***	***7***	-	***705***	***45***	***8.2***
Yoakum	Gonzales	**US 183** (SB Lane)	Near 580	**-**	***550***	***50***	***8***	-	***850***	***55***	***12***
	Dewitt	**SH 119** (EB Lane)	Near 544	**-**	***540***	***38***	***7***	-	***717***	***40***	***8***

a: Cement Treated Base, **b:** Cement Treated Subgrade, and **c:** Subgrade Soil

CHAPTER 6: NUMERICAL ANALYSIS METHODOLOGY

This chapter focuses on explaining the methodology to mechanistically predict the service life of the selected roadways by using different pavement design parameters and approaches. The primary objective of this study was to utilize the collected WIM information from the deployed units to mechanistically quantify the damages imparted by heavy truck traffic operations in the energy development areas of South Texas. In addition, this study also highlights the differences in service life for the developed axle load spectra (ALS) versus the traditional ESAL concept.

6.1 Equivalent Single Axle Load (ESAL) Concept

Previous pavement design software such as AASHTO's Guide for Design of Pavement Structures or Texas Flexible Pavement Design System (FPS) traditionally revolved around the Equivalent Single Axle Loads (ESAL's) concept derived from the AASHTO Road Test. In this method, an ESAL is essentially a cumulative traffic statistic that represents a mixed traffic stream of different axle loads and axle configuration predicted over an analysis period and converted into an equivalent number (TxDOT, 2005). This equivalent number is expressed as an 18,000 lb. or 18 kips axle load and its reference axle is a single axle with dual tires. This concept was developed to establish a damaged relationship for comparing the effects of axles carrying different weight.

The primary purpose of utilizing ESALs is not the actual load of the axle but more importantly the damage inflicted to the pavement caused by the wheel load. Therefore, to quantify the pavement damage induced by energy-related operations, Equivalent Axle Load Factors (EALFs) are used. These EALF values for each axle type (Single, Tandem, Tridem, Quad) multiplied by the projected number of load repetitions result in the projected Equivalent Single Axle Load (ESAL) for design of pavement sections as indicated in Equation 6.1:

$$ESAL = \sum_{i=1}^{m} (EALF)_i n_i \,, \tag{6.1}$$

where n_i is the number of passes of i^{th}-axle load group, and $(EALF)_i$ is the axle load equivalency for the i^{th}-axle load group. The EALF values are primarily dependent on the pavement types, pavement layers, thicknesses, and structural integrity of the pavement layers in the network. Due the fact that each network has its own specific characteristics, using the traditional Asphalt Institute EALFs can be problematic and render inaccurate results.

6.1.1 Asphalt Institute Equivalent Axle Load Factors (EALFs)

Current EALFs are based on the AASHTO formulations with several simplifying assumptions for generalization across the nation. Equations 6.2 through 6.4 present the basis for the calculations of EALF developed over 40 years ago in the 1970s by AASHTO.

$$log\left(\frac{W_{tx}}{W_{t18}}\right) = 4.79\log(18+1) - 4.79\log(L_x + L_2) + logL_2 + \frac{G_t}{\beta_x} - \frac{G_t}{\beta_{18}} \quad (6.2)$$

$$G_t = log\left(\frac{4.2-p_t}{4.2-1.5}\right) \quad (6.3)$$

$$\beta_x = 0.4 + \frac{0.081(L_x+L_2)^{3.23}}{(SN+1)^{5.19}{L_2}^{3.23}} \quad (6.4)$$

where:

W_{tx} = Number of x-axle load repetitions after time *t*,

W_{t18} = Number of 18 kip axle load repetitions after time *t*,

L_x = Load in kips on one single axle, one set on tandem axles and one set of tridem axles,

L_2 = Axle code, 1 for single axle, 2 for tandem axle, and 3 for tridem axle,

SN = Structural number,

p_t = Terminal Serviceability,

G_t = Function of terminal serviceability, and

β_{18} = Value of β_x when L_x is equal to 18 kips and L_2 is one.

Using the series of the equations presented above, the equivalent axle load factor can be calculated as the inverse of Equation 2:

$$EALF = \frac{W_{t18}}{W_{tx}} \quad (6.5)$$

As illustrated in Equation 6.2, the EALF for each axle load group is a function of the structural number (SN), which in turn is related to other parameters such as layer stiffness, drainage conditions, and pavement layer thickness. Generally, the Asphalt Institute (AI) assumes structural number (SN) of 5 and terminal serviceability (p_t) of 2.5 to develop tables of EALFs that are widely used by the pavement design industry to characterize the damage imparted by i^{th}-axle load group

relative to standard axle on the pavements (Huang, 1993). However, there are several sources of inaccuracy and systematic errors present in such assumptions. The major shortcomings of using the Asphalt Institute load equivalency factors to quantify damage are as follows:

- The EALF tables developed are for specified structural number (SN) and terminal serviceability (p_t) based on equations developed and later modified in the AASHTO road test conducted in the 1950s.
- Utilizing the assumption of SN = 5 substantially underestimates the pavement damage. Especially considering that the pavements in these energy development zones have been subjected to years of heavy loading and already show signs of severe distress.
- The structural number (SN) is a function of the layer thicknesses, drainage conditions and the stiffness properties of the layers. Basically, indicating that EALFs should not be a single value and should be different based on the features of the pavement systems in the network.

6.1.2 Modified Equivalent Axle Load Factors (EALFs)

As a result of the weaknesses with the Asphalt Institute (EALFs) discussed in the previous section, modified EALFs developed by Ashtiani et. al (2019) were also incorporated in this study. The new modified EALF values were developed based on extensive field data that realistically characterized the traffic in the overweight corridors and the energy developing areas of the Eagle Ford Shale Region. Information such as traffic distributions, vehicle classifications, GVW's, axle weights, and axle configurations were obtained from the collected WIM data and incorporated into the damage quantification algorithms. In addition, information on loading conditions like tire footprint, tire pressure, and layer moduli were also incorporated into the finite element model to obtain critical pavement responses. The critical pavement responses that were of particular interest were the tensile strain at the bottom of Asphalt Concrete (AC) layer, the compressive strain at the top of the subgrade layer, and the cumulative surface deflection. The researchers developed three classifications of EALFs derived from different measures of failure criteria based on fatigue cracking, rutting, and surface deflection failure criteria (Morovatdar et al., 2020):. The highest EALF value for each failure criteria was ultimately selected as the final modified EALF value, as shown in Equation 6.6. The three different classifications of EALFs are explain in further detail below.

$$Modified\ EALF = Max\ (EALF_{fatigue}, EALF_{rutting}, EALF_{deflection}) \quad (6.6)$$

Fatigue Cracking EALF

In the Asphalt Institute approach, the most critical pavement response that controls the fatigue performance of flexible pavements is the tensile strain at the bottom of the asphalt layer, as shown in Equation 6.7:

$$N_f = 7.96 \times 10^{-2}(\varepsilon_t)^{3.29}(E_{AC})^{0.85} \quad (6.7)$$

where the N_f is the allowable number of load applications to fatigue failure, ε_t is the tensile strain at the bottom of the asphalt layer, E_{AC} is the modulus of the asphalt layer. The equivalent axle load factor for axle load group x compared to standard 18-kip axle based on the fatigue criteria can be calculated from Equation 6.8 as:

$$EALF_{fatigue} = \left(\frac{W_{t18}}{W_{tx}}\right) = \left(\frac{\varepsilon_{t\,x}}{\varepsilon_{t\,18}}\right)^{3.29} \quad (6.8)$$

Permanent Deformation (Rutting) EALF

The rutting model in the Asphalt Institute method assumes the asphalt layer and the base layer does not experience any permanent deformation, that all rutting is experienced by the subgrade layer. Therefore, the critical pavement response that controls the rutting performance of flexible pavements is the compressive strain εc at the top of the subgrade illustrated by Equation 6.9.

$$EALF_{rutting} = \left(\frac{W_{t18}}{W_{tx}}\right) = \left(\frac{\varepsilon_{c\,x}}{\varepsilon_{c\,18}}\right)^{4.47} \quad (6.9)$$

Here N_f is the allowable number of load applications to rutting failure. The axle load factor based on the rutting criterion can be calculated from Equation 6.10 as:

$$EALF_{rutting} = \left(\frac{W_{t18}}{W_{tx}}\right) = \left(\frac{\varepsilon_{c\,x}}{\varepsilon_{c\,18}}\right)^{4.47} \quad (6.10)$$

Cumulative Surface Deflection EALF

Contrary to the Asphalt Institute assumption that no permanent deformation occurs in the asphalt and base layer, an additional failure criterion was considered that uses the cumulative surface deflection. This measure was also incorporated because it is known that rutting will in deed develop in the asphalt and base layer of flexible pavements. The cumulative plastic deformation

was used to develop the new measure of EALF based on surface deflection as shown in Equations 6.11 through 6.13:

$$N = \left(\frac{1}{D}\right)^{3.8} \tag{6.11}$$

Single Axles: $$EALF_{deflection} = \left(\frac{W_{t18}}{W_{tx}}\right) = \left(\frac{D}{D_b}\right)^{3.8}, \tag{6.12}$$

Multiple Axles: $$EALF_{deflection} = \left(\frac{W_{t18}}{W_{tx}}\right) = \left(\frac{D}{D_b}\right)^{3.8} + \sum\left(\frac{\Delta_i}{D_b}\right)^{3.8} \tag{6.13}$$

In these equations, D is the surface deflection, $\frac{D}{D_b}$ is the ratio of pavement surface deflections caused by a single axle load to those calculated under the standard 18-kip axle (D_b). The difference in magnitude between the maximum deflection calculated under each succeeding axle and the intermediate deflection between axles is shown by Δ_i. (Kawa et al., 1998). In addition, the main benefits of using these modified EALFs are summarized below (Morovatdar et al., 2020):

- Pavement responses subjected to site specific loading conditions were accurately simulated through the incorporation of the WIM, FWD, and GPR data that were collected at each site.
- The numerical simulations confirmed that the modified EALF values were considerably higher than the traditional Asphalt Institute. Hence indicating that the Asphalt Institute factors that are commonly used pavement design engineers underestimate the damage.
- The numerical simulations also revealed that both the rutting and surface deflection criteria had the highest damages factors between the three proposed criteria's.

6.2 Methodology Used to Perform Service Life Analysis

In order to perform the service life analysis of the representative highway sections, the procedure illustrated in Figure 6.1 was implemented. First, the pavement layer configurations had to be determined to be input into the structural module of the TxME. Information pertaining to the layer configurations and layer thicknesses was obtained from the GPR results collected at these pavement sections. The layer modulus values were also obtained from the collected FWD tests mentioned in the preceding sections of this thesis. The back-calculated layer modulus obtained from the FWD tests from both the summer and winter time were averaged and incorporated into the software. Other information pertaining to the material properties such as facture and rutting

properties were derived from the pavement design plans or from extensive review of the literature. Figure 6.2 illustrates the typical structure tab in the current TxME software.

Figure 6.1 Flow Chart for Performing Service Life Analysis

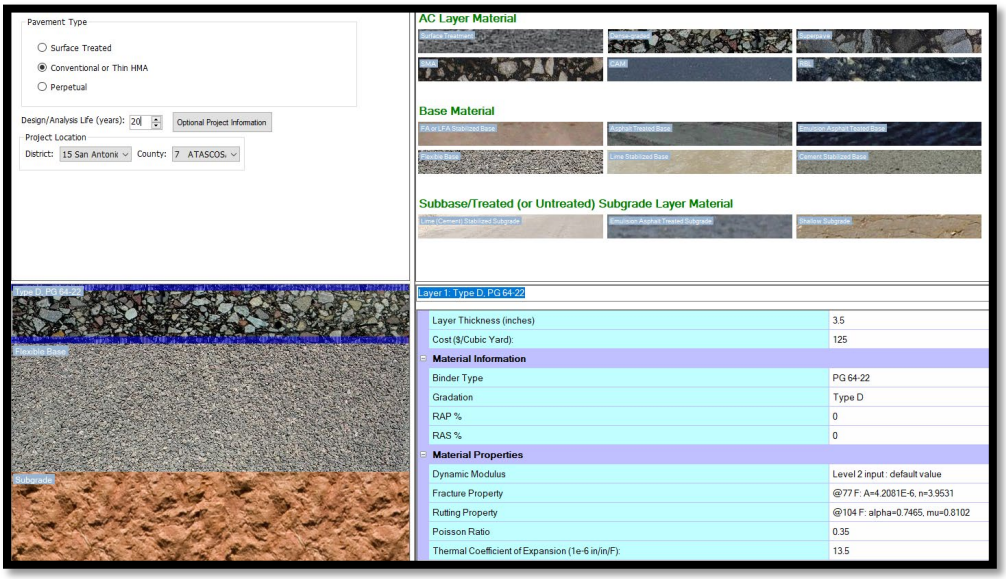

Figure 6.2 TxME Layer Configuration Information for SH 16

Then, the environmental factors for each specific pavement section had to be selected. This was performed by utilizing information from the nearest weather station. Climate information such as annual temperature, annual precipitation, average number of wet days, average number of freeze/thaw cycles among other information were then generated. Figure 6.3 illustrates the typical climate information incorporated.

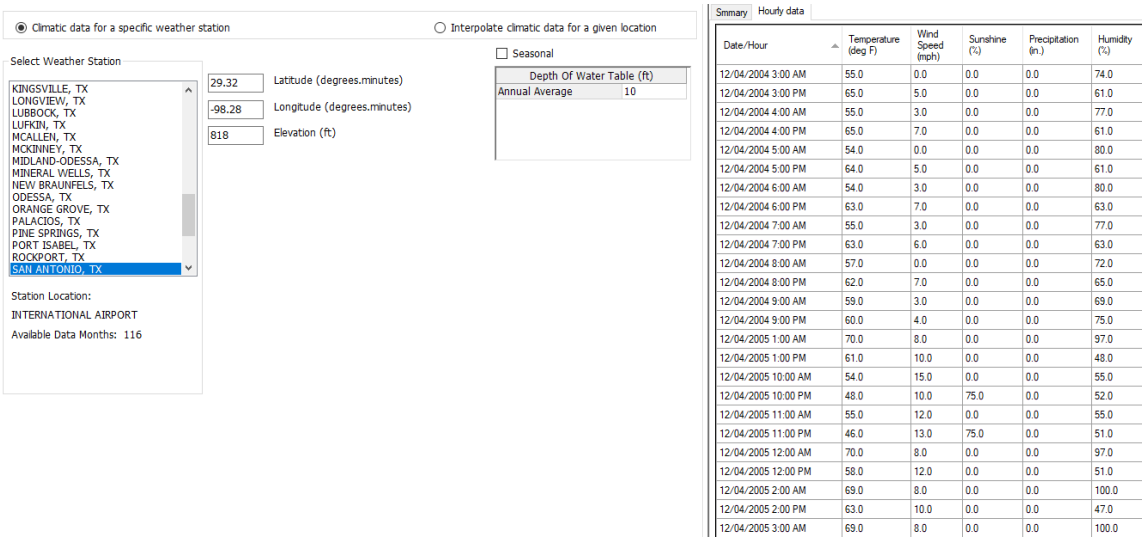

Date/Hour	Temperature (deg F)	Wind Speed (mph)	Sunshine (%)	Precipitation (in.)	Humidity (%)
12/04/2004 3:00 AM	55.0	0.0	0.0	0.0	74.0
12/04/2004 3:00 PM	65.0	5.0	0.0	0.0	61.0
12/04/2004 4:00 AM	55.0	3.0	0.0	0.0	77.0
12/04/2004 4:00 PM	65.0	7.0	0.0	0.0	61.0
12/04/2004 5:00 AM	54.0	0.0	0.0	0.0	80.0
12/04/2004 5:00 PM	64.0	5.0	0.0	0.0	61.0
12/04/2004 6:00 AM	54.0	3.0	0.0	0.0	80.0
12/04/2004 6:00 PM	63.0	7.0	0.0	0.0	63.0
12/04/2004 7:00 AM	55.0	3.0	0.0	0.0	77.0
12/04/2004 7:00 PM	63.0	6.0	0.0	0.0	63.0
12/04/2004 8:00 AM	57.0	0.0	0.0	0.0	72.0
12/04/2004 8:00 PM	62.0	7.0	0.0	0.0	65.0
12/04/2004 9:00 AM	59.0	3.0	0.0	0.0	69.0
12/04/2004 9:00 PM	60.0	4.0	0.0	0.0	75.0
12/04/2005 1:00 AM	70.0	8.0	0.0	0.0	97.0
12/04/2005 1:00 PM	61.0	10.0	0.0	0.0	48.0
12/04/2005 10:00 AM	54.0	15.0	0.0	0.0	55.0
12/04/2005 10:00 PM	48.0	10.0	75.0	0.0	52.0
12/04/2005 11:00 AM	55.0	12.0	0.0	0.0	55.0
12/04/2005 11:00 PM	46.0	13.0	75.0	0.0	51.0
12/04/2005 12:00 AM	70.0	8.0	0.0	0.0	97.0
12/04/2005 12:00 PM	58.0	12.0	0.0	0.0	51.0
12/04/2005 2:00 AM	69.0	8.0	0.0	0.0	100.0
12/04/2005 2:00 PM	63.0	10.0	0.0	0.0	47.0
12/04/2005 3:00 AM	69.0	8.0	0.0	0.0	100.0

Figure 6.3 TxME Climatic Information for SH 16

Above all, the most crucial information for performing the service life analysis was the incorporation of the traffic information generated in the axle load spectra section (Chapter 4) of this thesis. As previously mentioned in the preceding text, this traffic information was derived from deploying portable WIM units to selected sites in the overload corridors and energy developing areas of South Texas. The collected and processed traffic information contained detailed axle load distributions for each different type of axle (i.e. Steering Axles, Single Axles, Tandem Axles, Tridem Axles, and Quad axles), along with other valuable information (e.g. Average Daily Traffic (ADT), Average Daily Truck Traffic (ADTT), truck class distributions, and axle configurations).

The traffic information was then incorporated into the TxME in three primary methods. The first method was by incorporating the traffic information as a Level 1: Axle Load Spectra, which typically results in the highest accuracy. The second method was by incorporating the traffic information as Level 2: ESALs, which is the current method TxDOT uses in its FPS 21 pavement design software. Finally, the third method used was by incorporating the default traffic values the

TxME has designated in the software. All three methods were incorporated in the numerical simulations, the differences are described in following section (Chapter 7). Figure 6.4 shows the relevant traffic information necessary to run the analysis.

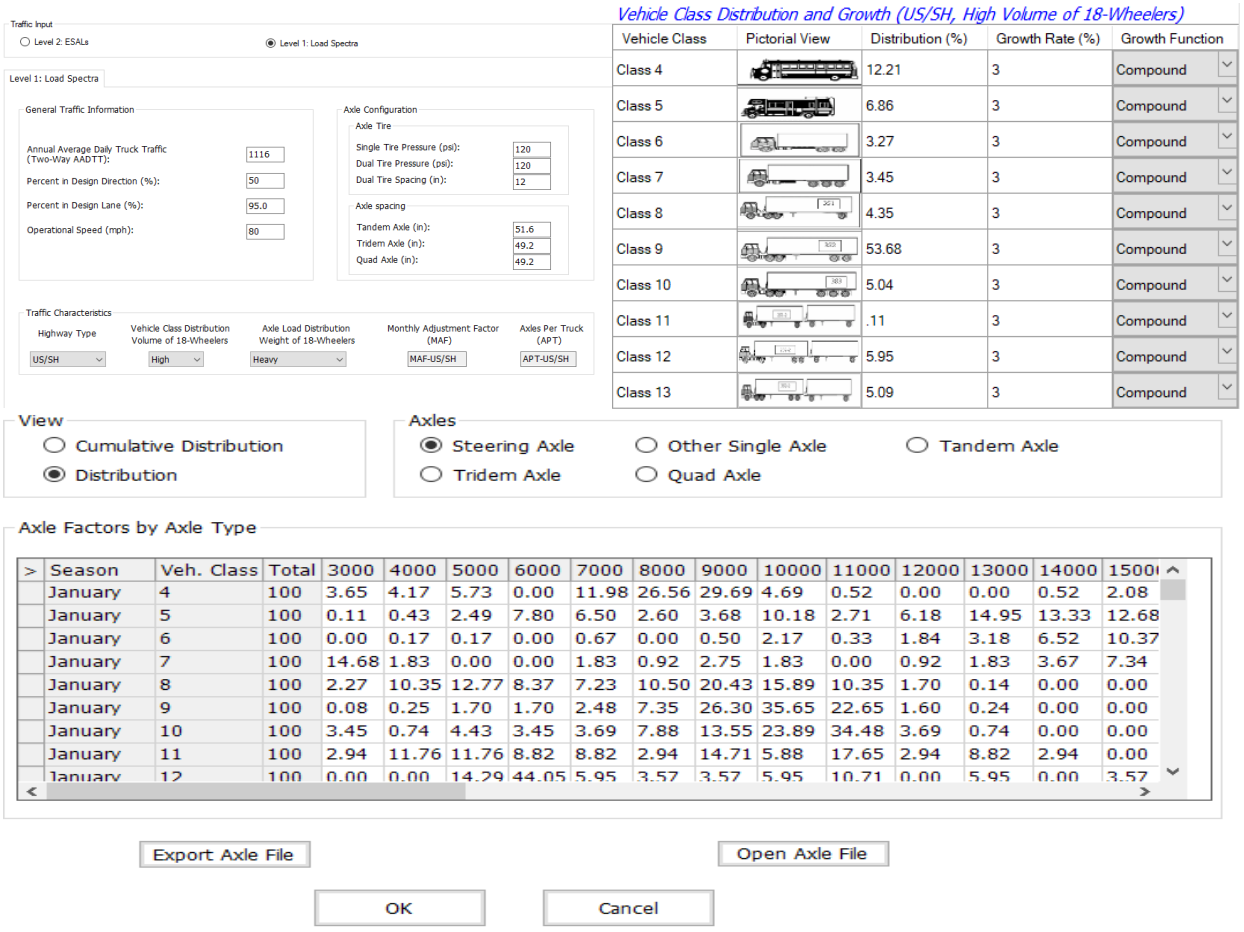

Figure 6.4 TxME Traffic Information for SH 16

6.3 Methodology for Reduction of Service Life

In addition to the different numerical analysis conducted in Chapter 7, a pavement-life reduction analysis was also performed. This analysis was performed to compare the current traffic loading conditions to that of the pre-energy development traffic loading conditions and to access the reduction in service due to the drastic increase in traffic. To perform this service life reduction analysis, the projected ESAL values for both the current and the pre-energy development traffic conditions were derived and incorporated into the TxME software.

In order to properly and accurately make this comparison, the current traffic conditions collected from the deployed portable WIM units had to be converted to ESALs. The number of

load repetitions for each axle weight and each axle type was first obtained from the axle load spectra. Then this number of load repetitions was multiplied by the modified EALFs mention previously and projected to obtain the cumulative ESALs, as shown by Equation 6.14. The cumulative ESAL values associated to the pre-energy development traffic conditions were derived from an extensive search in the available databases.

$$ESAL_{current} = \sum_{i=1}^{m} (EALF)_i n_i \quad (6.14)$$

where:

$(EALF)_i$ = *Modified EALF Values*

n_i = *Projected Number of passes of* i^{th}*-axle load group during the design period*

Then using the traffic growth rate both ESAL values were converted to equivalent values corresponding to the construction year. The ESAL values for both time periods were ultimately incorporated into the TxME and the service life results were then contrasted. The difference in service life between these two traffic loading conditions represents the induced service life reduction due to energy development operations, as shown in Figure 6.5.

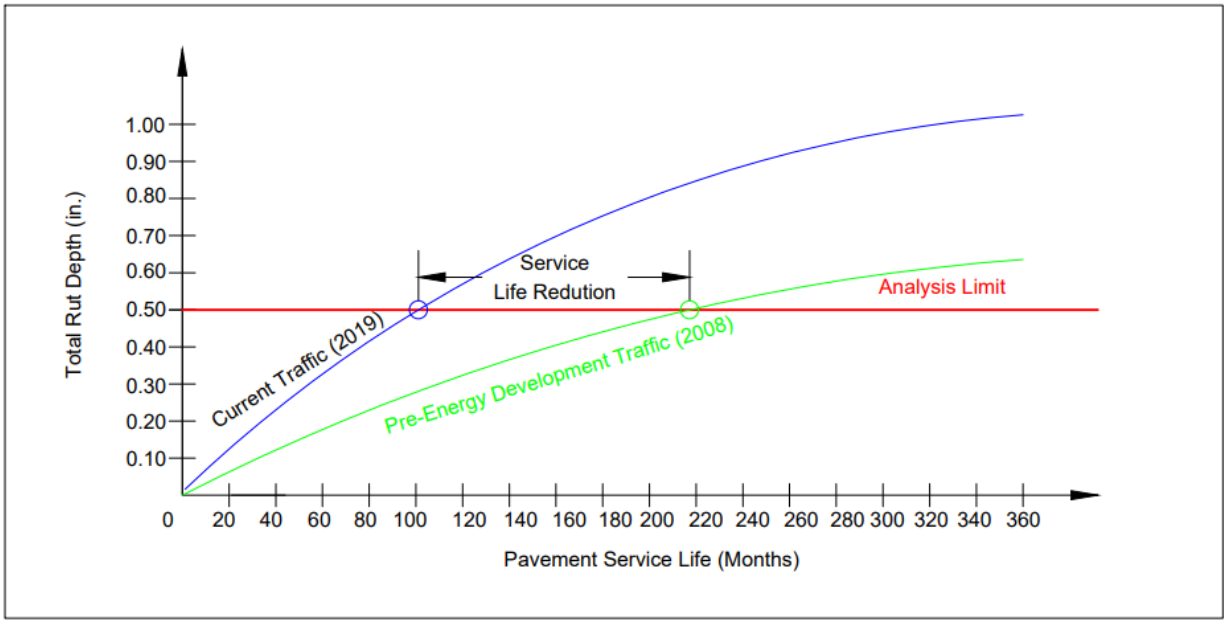

Figure 6.5 Service Life Reduction of Current and Pre-Energy Boom Example

CHAPTER 7: RESULTS AND DISCUSSION

This section illustrates the main comparisons in the predicted service life between results obtained from (1.) the developed axle load spectra (ALS), (2.) the traditional ESAL concept, (3.) the TxME default traffic input values, and (4.) the influence of the material properties. The pavement design simulations for FM roads were conducted using a 20-year design life, while for SH and US highways the simulations were conducted using a 30-year design life. The distress model's failure criteria were based on 0.50 in. total rut depth for rutting, 50% of the total lane area for fatigue cracking, and 2112 ft/mile for thermal cracking. However, since thermal cracking and fatigue cracking were not the primary modes of failure for highways under heavy loading, as seen by Figure 7.1, the results were not reported. The failure criteria that dictated the predicted service life analysis was the permanent deformation, also known as rutting.

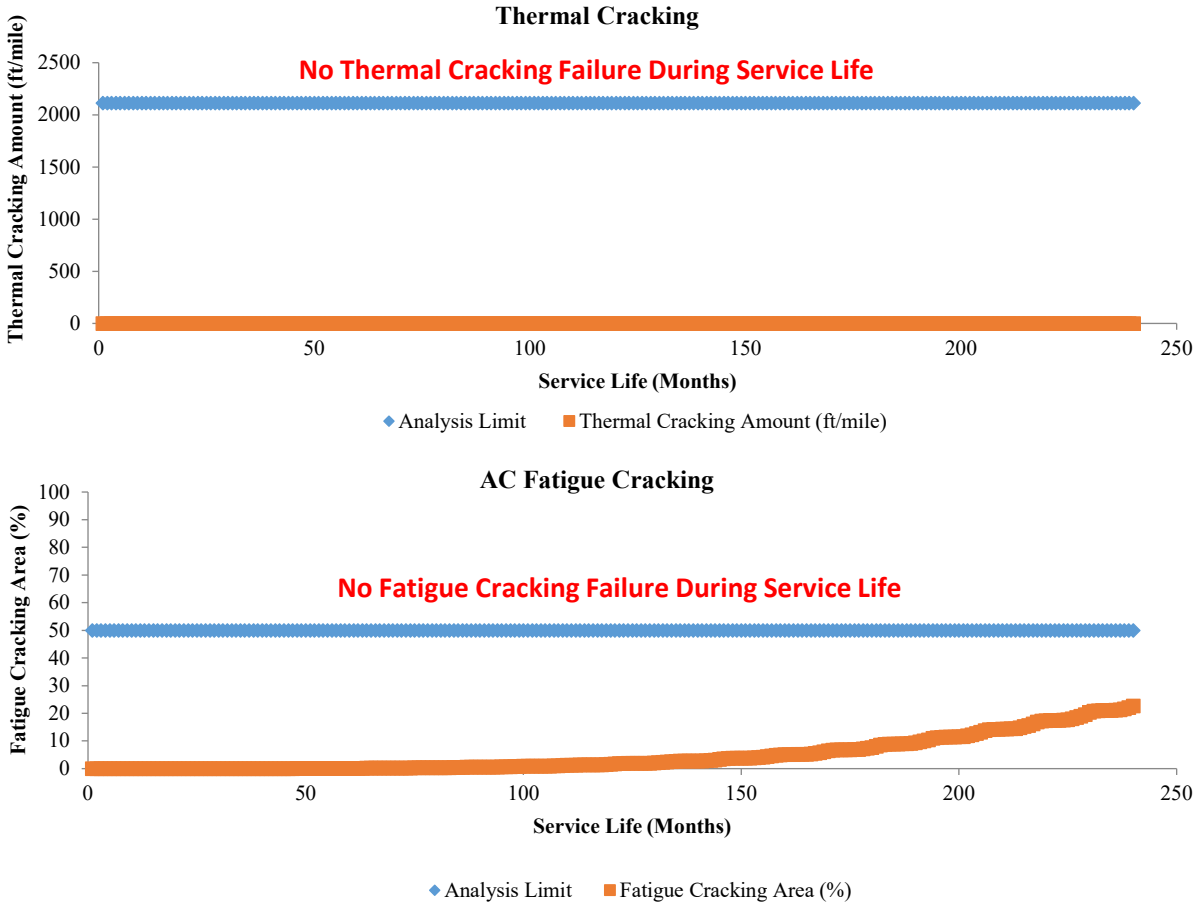

Figure 7.1(a) Thermal Cracking Failure (b) Fatigue Cracking Failure

7.1 Axle Load Spectra (ALS) vs. Equivalent Single Axle Load (ESAL)

Traffic characterization using the traditional ESAL concept is incapable of capturing the seasonal variations in damage imparted by different classes of vehicles at a specific time. In contrast, the axle load spectra in the TxME was created with one of its main focuses being the incremental damage concept for the characterization of the performance of flexible pavement structures. The incorporation of the axle load spectra in the TxME allows for the determination of incremental damage imparted by a specific vehicle class at a specific timeframe on a pavement section. In addition, it is a vital component for the calculation of the cumulative damage during service life of pavements.

The main comparison that this study aims to highlight is the distinction in the predicted pavement service life between the developed axle load spectra (ALS) for overweight corridors and energy sectors zones versus using the traditional ESAL concept. Figure 7.2 confirms that the use of the axle load spectra generally resulted in lower predicted service lives compared to using traditional ESALs. With the exception of SH 119, where the service life of this highway reached its complete design life expectancy for both ALS and ESALs. This exception is attributed to the low volume and light weight truck traffic in this highway. Moreover, from the figure, the service life of US highways is overpredicted by an average 137%, while the service of SH highways is overpredicted by an average of 151%. However, the most significant overprediction takes place in FM roadways, where the average service life is overpredicted by a staggering 229%. This substantial over prediction in service life using ESALs may interfere with the ability of pavement engineers to accurately predict the actual pavement life or implement proper maintenance strategies. This comparison shows that utilizing traditional ESALs is not the best technique to implement in order to characterize the traffic distributions of a particular area. Since ESALs are not capable of accounting for the effect of various axle load groups at a particular time in the damage quantification procedure.

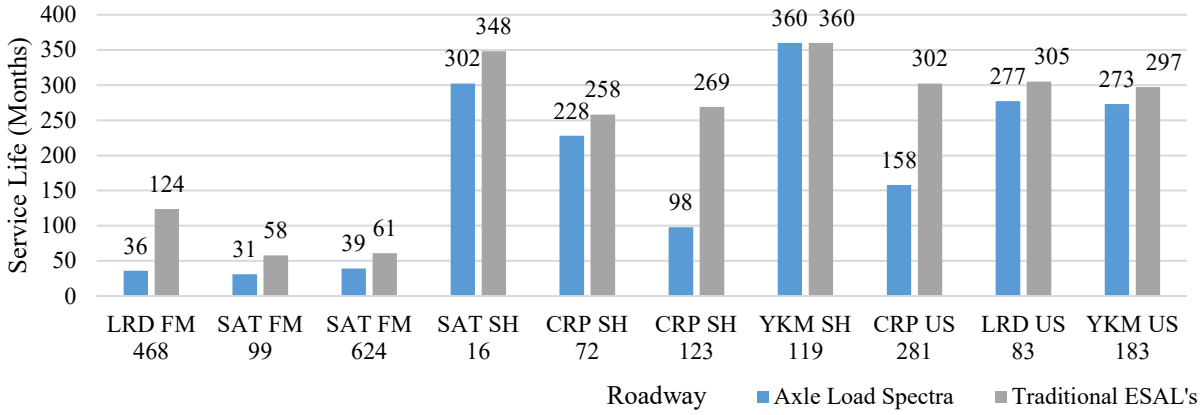

Figure 7.2 Axle Load Spectra vs. Traditional ESALs

Another comparison was made using ESALs that were derived from the Modified EALF's developed for these specific pavement sections. In contrast to the traditional ESALs, the Modified ESALs are better suited to characterize the traffic operations since they were developed using mechanistic distress models. In addition, they were tailored towards the specific axle load and axle configuration of vehicles operating in the ten selected pavement sections. Figure 7.3 illustrates the comparison in service life between the ALS and the Modified ESALs. As shown in the figure, the Modified ESALs, (ESALs that were derived from the Modified EALFs) also tend to overpredict the service life; however, this difference is not as pronounced. The service life of US highways is now barely overpredicted by an 102%, while the service of SH highways and FM roads only overpredicted by 120% and 118%, respectively.

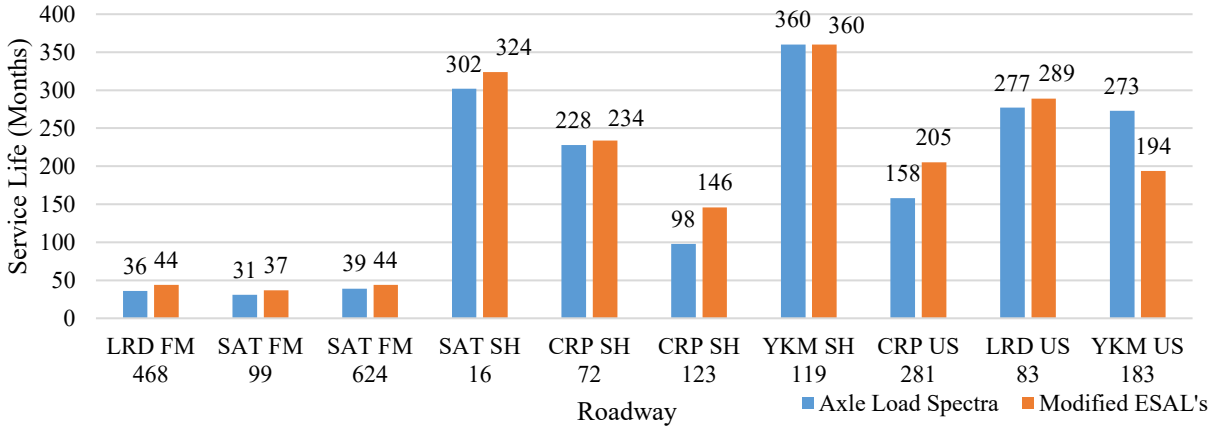

Figure 7.3 Axle Load Spectra vs. Modified ESALs

Moreover, the axle load spectra (ALS) resulted in lowest predicted service life, followed by the Modified ESALs, and the Traditional ESALs. An important observation is that the Modified ESALs led to a more accurate service life prediction when compared to the Traditional ESALs, as illustrated in Figure 7.4. This is because the ESALs derived from the Modified EALFs are better suited to estimate the damage imparted by heavy vehicles operating on these roadways. In addition, if it is not feasible to acquire axle load spectra information at a particular site, using pneumatic tube counters to collected traffic information and applying the Modified EALFs can still yield satisfactory service life predictions.

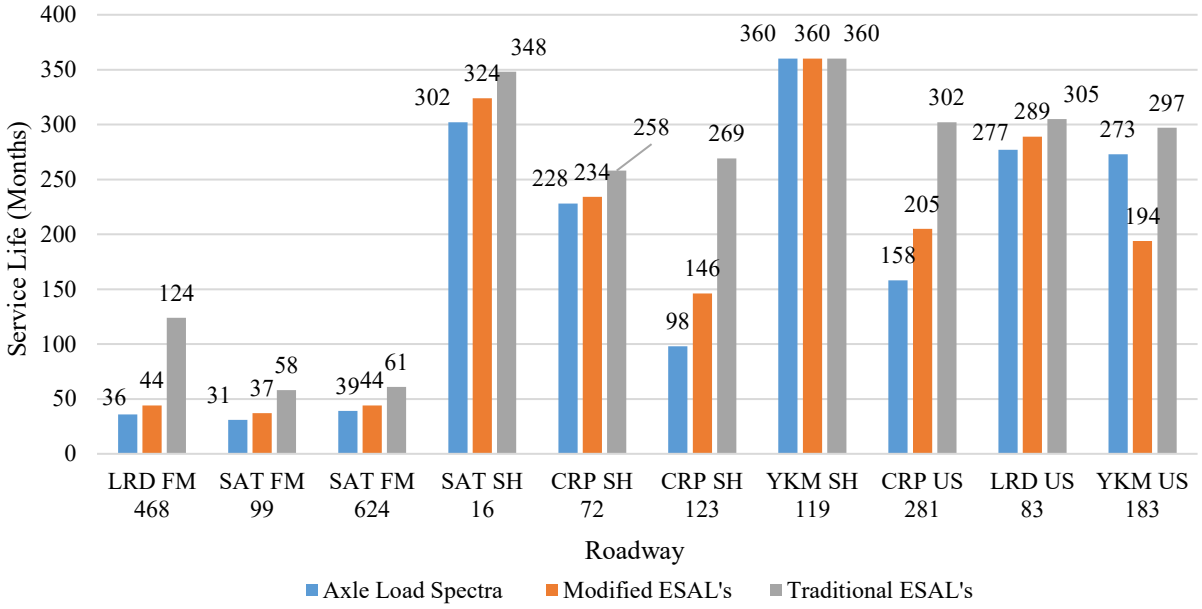

Figure 7.4 Axle Load Spectra vs. Traditional ESALs vs. Modified ESALs

7.2 Axle Load Spectra (ALS) vs. TxME Default Values

Figure 7.5 illustrates a comparison between the developed axle load spectra and the Default TxME traffic values. For this comparison there are three traffic conditions that can be implemented in the software, they are Low, Medium, and High designations of axle loads. However, the highest designation of axle loads was selected for this comparison. From Figure 7.5, it can be noted that for almost all cases the default TxME values overpredicted the service life of the selected

roadways. Once again with the exceptions of SH 119 and US 183 in the Yoakum District, which as previously stated, had low volume and light weight truck traffic. The overprediction of service life was more significant in FM roadways compared to SH and US highways. In general, the Default TxME traffic values overpredicted the service life in FM roadways by an average of 262%, SH highways by 164%, and US highways by 140%.

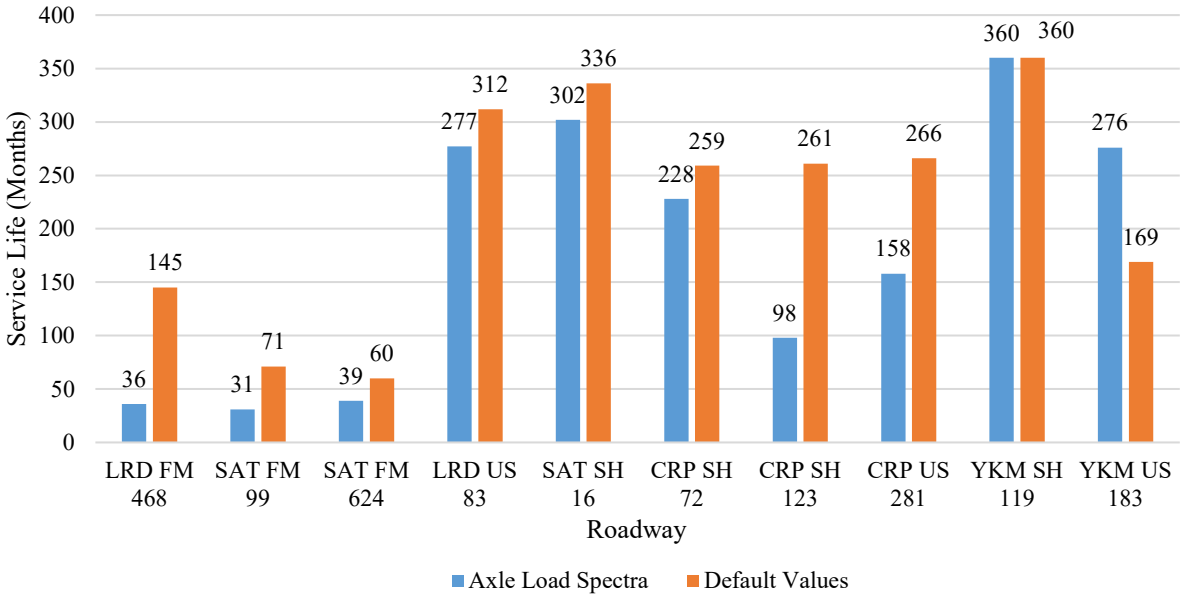

Figure 7.5 Axle Load Spectra vs. TxME Default Traffic Values

It is also important to note that for highways with significant overweight traffic, the overprediction of the Default TxME traffic values was more significant. Such is the case of FM 468, where the default values overpredicted the service life by over 400%. Figure 7.6 highlights the rutting analysis comparison of FM 468, where rutting failure occurred at 36th month for the axle load spectra analysis, meanwhile failure in rutting did not occur until the 145th month for the Default TxME values analysis. This underlines the importance of selecting accurate site-specific traffic information as opposed to simply using default software values.

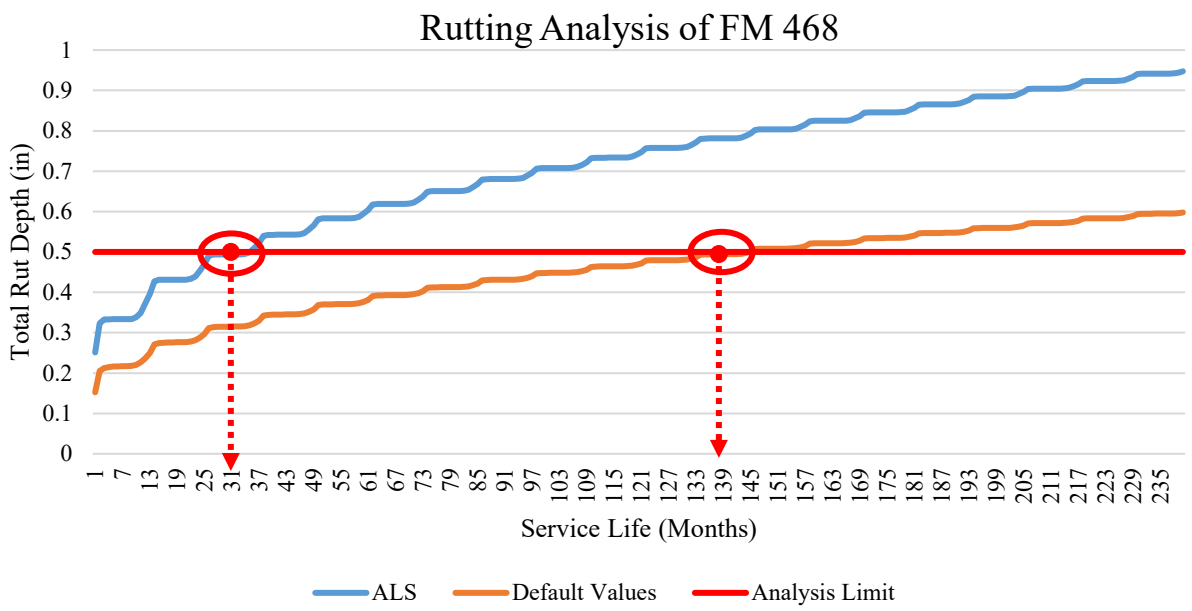

Figure 7.6 Rutting Analysis Comparison between ALS and TxME Default Traffic Values

7.3 Axle Load Spectra (ALS) vs. Influence of Material Properties

The influence of material properties in pavement design are also imperative parameters that are often overlooked by pavement design engineers. It is important that pavement designers consider a range of modulus values for the different pavement layers in their analysis. Figure 7.7 illustrates a comparison of the service life of different highways considering the different modulus values in the summer time and winter time. The comparisons are made by using the back-calculated layer modulus obtained from the FWD testing conducted in both summer and winter time. The average of the modulus values was used as the reference to compare the summer and winter modulus fluctuations. When only using the winter modulus, the service life was overpredicted by an average of 157% for FM roadways, 116% for SH highways, and 120% for US highways. On the other hand, when only using the summer modulus, the service life of FM highways was underpredicted by an average of 53% for FM roadways, 91% for SH highways, and 92% for US highways.

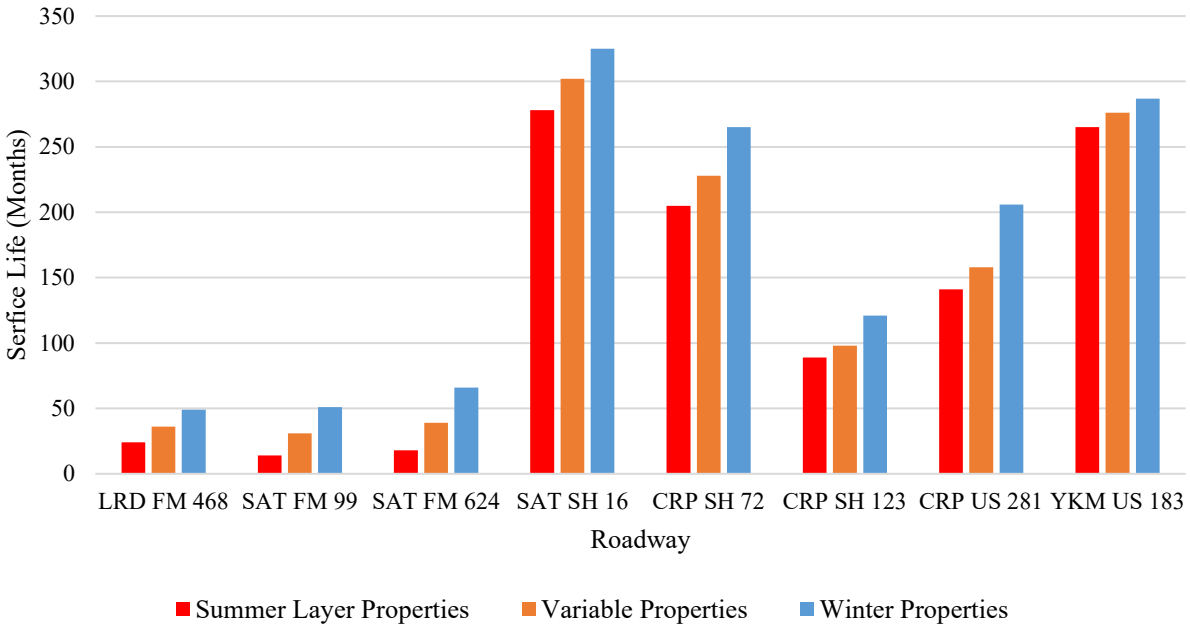

Figure 7.7 Influence of Modulus Values Using ALS in TxME

Figure 7.7 illustrates the result for comparing summer and winter modulus on FM 99 in the San Antonio District. From the figure, it can be observed that pavement designs using only the winter moduli resulted in longer predicted service lives. Whereas in the cases of only using the summer moduli, the service lives of the pavement designs were significantly lower. This is the result of modulus values being higher in the winter time when the pavement layers are stiffer, meanwhile the modulus values are lower in the summer because of the softening of the pavements layer due to an increase in temperature. As a result, the damage imparted by a heavy loaded Class 9 truck during the summer is more damaging to the pavement structure. Figure 7.8 also illustrates the months at which each simulation reaches the failure limit for FM 99. In this example, the winter modulus overpredicts the service life by 165%, while the summer modulus underpredicts the service life by 65%. Thus, these results highlight the significant role that modulus values plays in service life predictions.

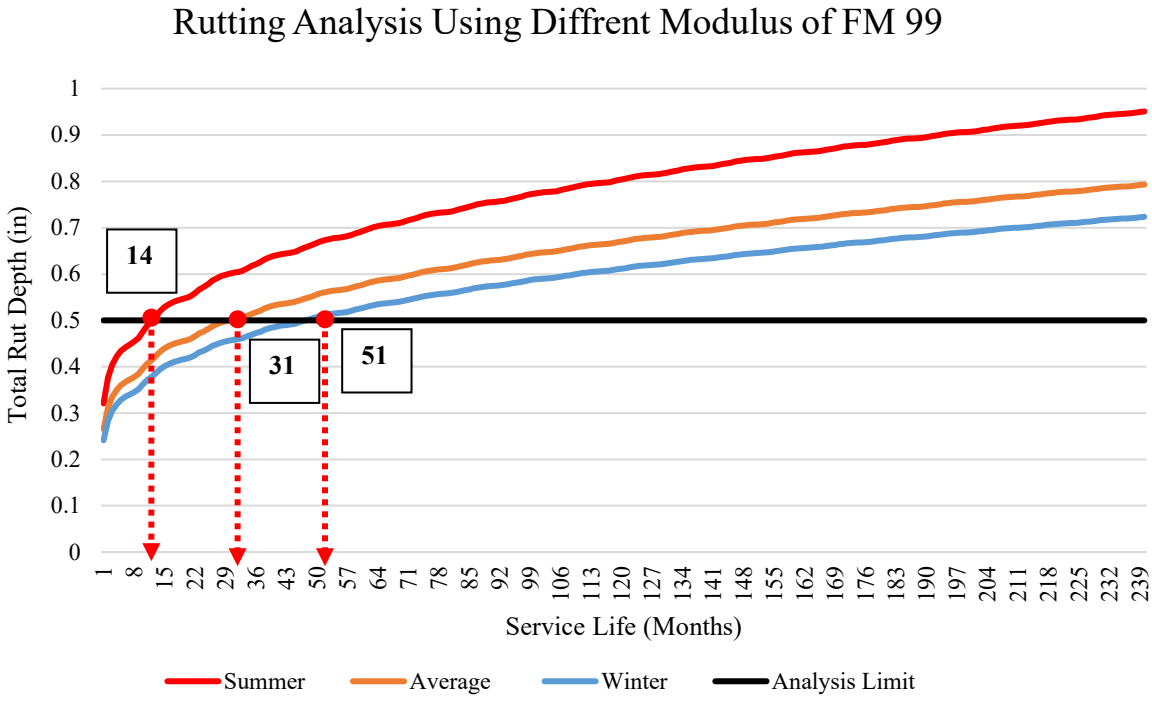

Figure 7.8 Rutting Analysis Comparison between Different Modulus Values

7.4 Influence of Pavement Type (US, SH, FM)

Figure 7.9 illustrates a comparison of the primary pavement design approaches that this study focuses on including, developed axle load spectra, the Modified ESALs, and the TxME Default values. From the figure, the general pattern shows that service life is considerably overpredicted by the Default TxME values, followed by the Modified ESAL values. The three different highway-types are prone to this fluctuation of service life due different design approaches. However, FM roads and some SH highways are most notably affected. The premature failure of FM roads can be attributed to high traffic volume of heavily loaded trucks coupled with a thin surface treated pavement structure. On the other hand, SH and US highways are not as severely affected because they have a more robust and thicker pavement layer configuration which leads to a higher prediction in service life.

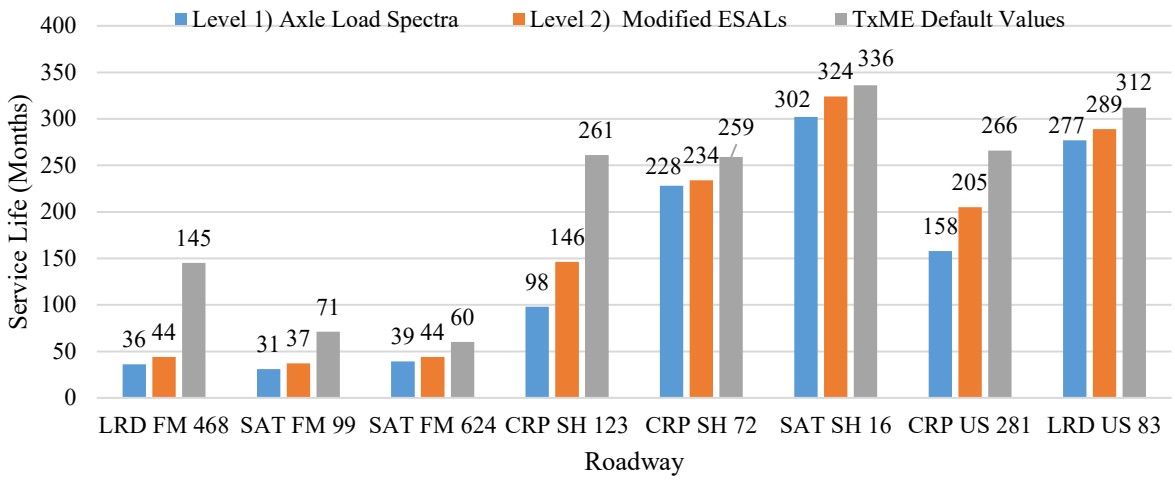

Figure 7.9 Influence of Pavement Type on Service Life

Moreover, Figure 7.10 illustrates a comparative rutting analysis failure of three different highway types (FM, SH, and US) which are also the most heavily trafficked in the network, as illustrate in Table 7.1. The figure shows that FM 468 fails at 36 months, followed by SH 123 at 98 months, and US 281 at 158 months. The difference of service life between these three highway types ranged from 60 to 62 months. Unsurprisingly, the FM roads failed first due to the relatively low structural capacity compared to the other two types of highways. FM roadways with less robust pavement structures were found to be more sensitive to the increasing traffic loads, compared to SH and US highways because they were never designed to carry such high volume of OW traffic.

Table 7.1 Current Traffic Information for all Ten Selected Sites.

District	Roadway	Current Traffic (2019)		
		ESAL (Million)	AADTT	ADT
Laredo	US 83	8.7	1636	6300
	FM 468	17.5	839	2150
San Antonio	FM 624	3.8	289	875
	FM 99	4.8	267	702
	SH 16	6.5	1116	5072
Corpus Christi	US 281	20	1815	7000
	SH 72	7	1763	5700
	SH 123	28.5	1976	10400
Yoakum	US 183	3.8	1432	8420
	SH 119	2	659	2530

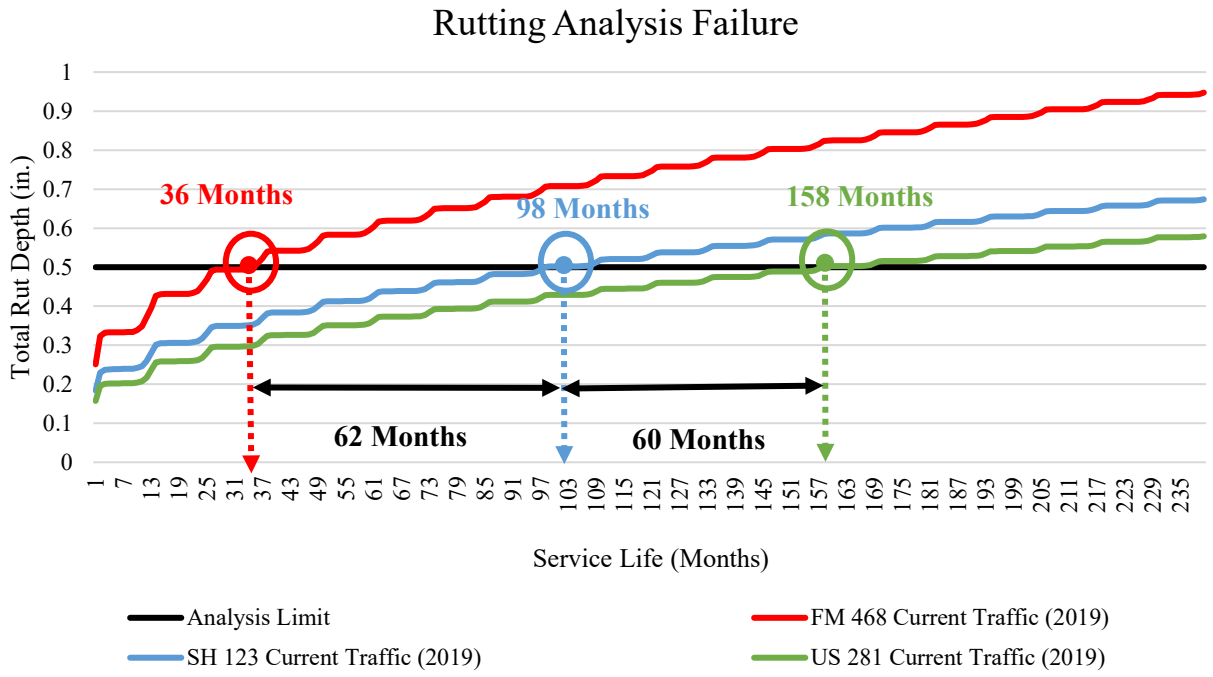

Figure 7.10 Service Life Reduction of Different Highway Types

7.5 Reduction of Service Life

Since the onset of energy development activities in 2008, enormous amounts of truck traffic were generated the Eagle Ford Shale Region due to the movement of sand, water, chemicals, and heavy equipment for the extraction of crude oil and natural gas. This movement in resources resulted in a drastic increase of truck traffic passing through the highway network that was not originally designed to sustain the new volumes and loads associated with the traffic. As a result, the new generated traffic operations detrimentally impacted the transportation infrastructure in the network and significantly reduced the pavement life.

Figure 7.11 illustrates the drastic traffic increase of the selected highways impacted by energy development activities. This plot provides the comparative cumulative 18-Kip ESALs of the pre-energy development traffic in 2008, and the current projected 2019 ESALs from the data collected in the axle load spectra. The average traffic increase in the past decade for FM, SH, and US highways was 1440%, 478%, and 239% respectively. The most significant increases occurred

in the Corpus Christi District on US281 where it underwent a 331% increase meanwhile SH123 underwent a 903% increase. However, no highway compared to FM 468 of the Laredo District, which experienced a 2480% increase in cumulative 18 Kip ESALs.

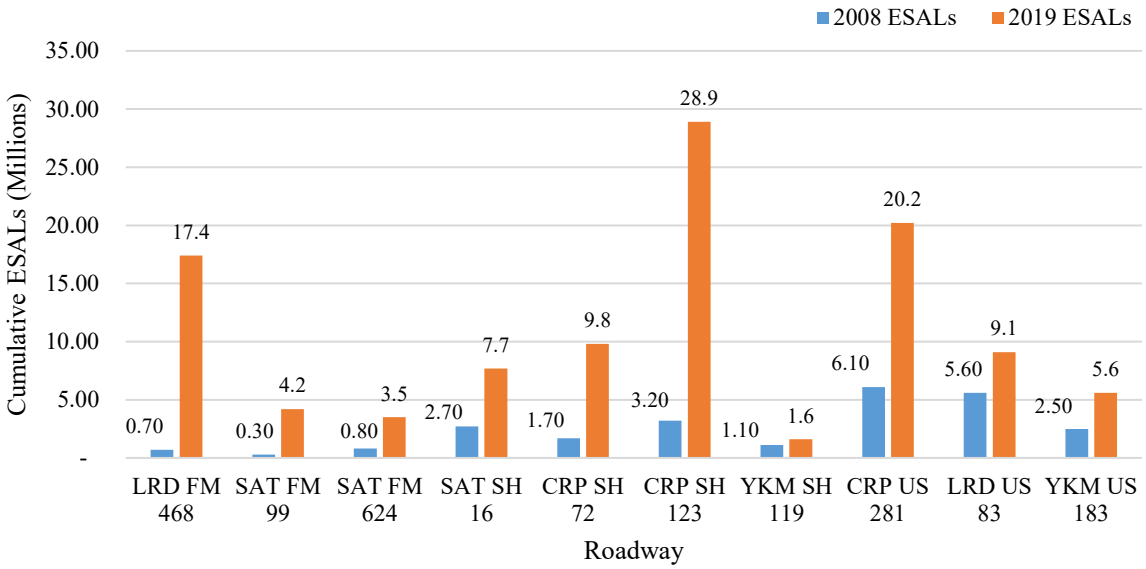

Figure 7.11 Cumulative 18-kip ESAL values (20-Year Design Life)

The service life of these highways is not only affected by an increase in traffic volume, but also in the increase in axle weights and gross vehicle weights. This combination of increased traffic volume and axle loads was damaging highways designed to carry legal gross vehicle weights of up to 80,000 lbs. More importantly, heavily loaded trucks used by the energy companies were also travelling over Load-Zoned (LZ) roads, which were designed to accommodate vehicles that weigh less than 58,420 lbs. Thus, these FM roads were greatly affected by the significant increase in heavy truck traffic, where the loss of pavement serviceability is more pronounced compared to other highways in the network.

The conducted pavement conditions surveys confirmed that FM roads throughout the network were severely distressed and had already reached rutting failure according to our 0.50 in. failure criteria. Figure 7.12 illustrates the pavement conditions of FM 468, FM 99, and FM 624 where it is evident that these pavements are in a very deteriorate state and have sustained

significant damage The primary damage associated with these roads are deep rutting, severe flushing, and pot hole formation among others, which are essentially load induced distresses.

Figure 7.12 Pavement Conditions of FM 468, FM 99, and FM 624

As mentioned in the preceding section of this report, the reduction in service life comparison was conducted by converting the data collected from the portable WIM units to ESALs using the modified EALFs and by extracting the 2008 ESALs historical databases. Then both $ESAL_{Current}$, and $ESAL_{Pre\text{-}Energy\ Development}$ were converted to the construction year of the highway using the known traffic growth rates. The difference between these two-analysis resulted in the induced service life reduction.

The results for the reduction of service life for FM 468 are illustrated in Figure 7.13. This plot illustrates the difference in rutting performance of FM 468 for both current and pre-energy development traffic. Based on the analysis, rutting failure for the pre-energy development occurs at month 195. On the other hand, based on the 2019 traffic conditions, rutting failure occurred at the 36 months. This is a reduction of 159 months, that is 13.25 years in service life reduction of the pavement attributed to the onset of the energy developing activities in the region. The results

were verified with the pavement conditions surveys that were conducted in July of 2018. The survey of FM 468 revealed rutting in excess of 0.50 in. nearly 3 years from reconstruction in 2015, which is what the current traffic analysis predicted (36 months) of service life.

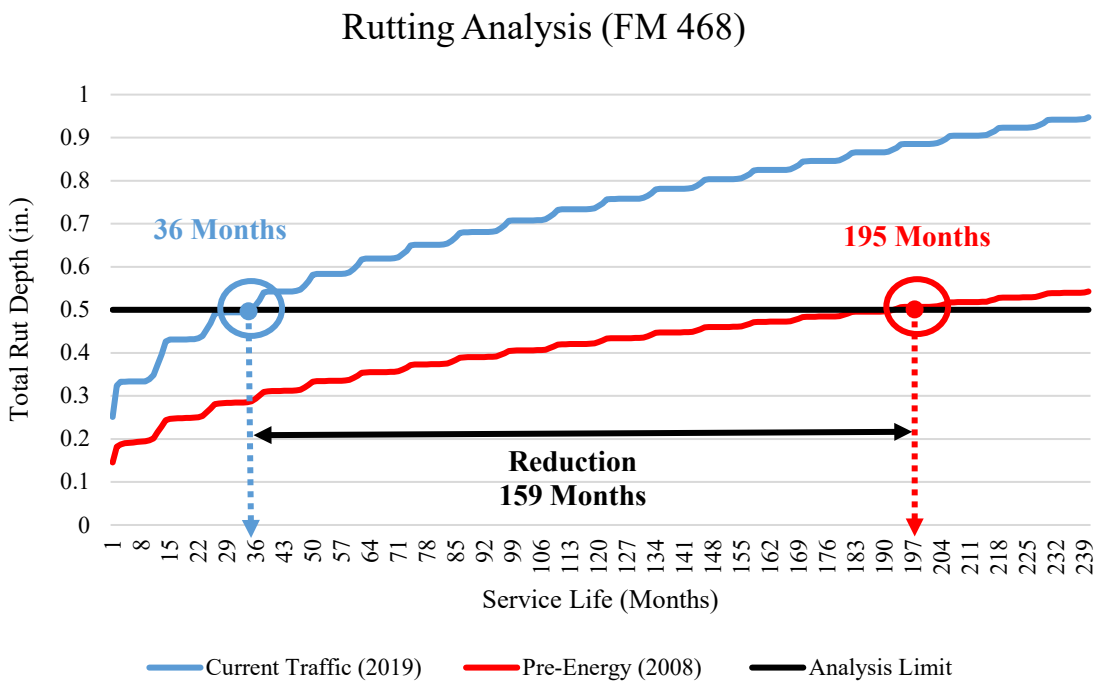

Figure 7.13 Reduction of Service Life in Laredo FM 468

Figure 7.14 illustrates similar pavement life reduction analysis conducted for all of the selected roadways in the overload corridors and energy sectors of South Texas. From the plot, energy developing activities in the Yoakum District have consumed 85 months of service life for US 183 and 28 months of the service life in SH119. In the San Antonio District, the pavement life reduction was 75, 56, and 46 months for FM 99, FM 624, and SH 16 respectively. However, from all evaluated sites the Laredo and Corpus Christi Districts suffered the greatest reduction of pavement serviceability. From the plot, it is evident that the highways with the greatest reduction in pavement life were FM 468, SH 123, and US 281 with a reduction of 159, 131, and 108 months respectively. This large reduction of pavement service life is attributed to the drastic increase in truck traffic volume over the past decade as mentioned previously in Figure 7.11. Therefore, one

can conclude that the reduction in pavement service life is closely tied to the traffic volume fluctuations that a pavement structure can experience over its service life.

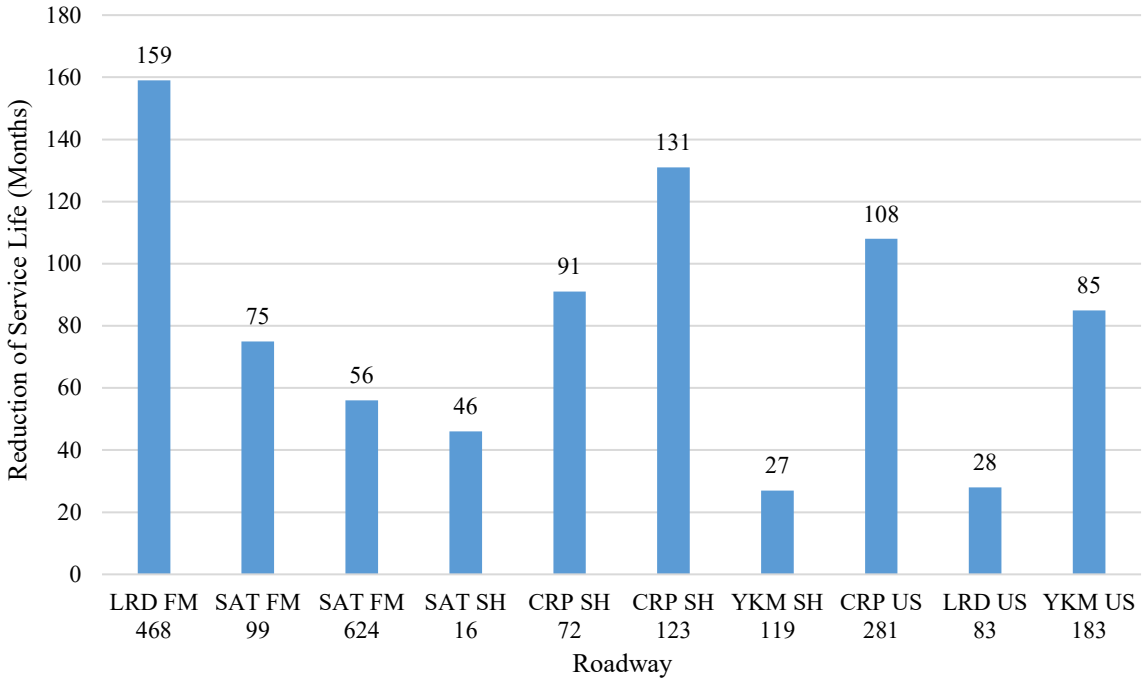

Figure 7.14 Service Life Reduction Results of All Selected Roadways

CHAPTER 8: CONCLUSIONS AND RECOMMENDATIONS

The objective of this study was to characterize the traffic operations in overweight corridors and energy development regions of South Texas in order to properly quantify the damage induced by overweigh vehicles. To achieve this objective, the Axle Load Spectra (ALS) database was developed through deployment of portable WIM devices in ten selected highways. The collected data from portable WIM units, FWD, and GPR were incorporated into TxME to run numerical analysis that predict the service life of each highway pavement. The different methods used to incorporate traffic information (i.e. Axle Load Spectra, ESALs, and Default TxME traffic values) showed significant differences in the predicted service life of representative highways.

8.1 Key Findings

The major findings from the report and numerical analysis are summarized below:

1. The Portable WIM unit utilized in this study provides a simple and inexpensive method to collect specific weigh-in-motion data in rural locations and produce reliable and accurate results.
2. The deployed Portable WIM units collected satisfactory data that is suitable for the development of the axle load spectra for energy developing areas in the Eagle Ford Shale and any other areas.
3. The collected WIM data showed that FM roads had traffic that was up to 64% overweight, while state highways and US highways had traffic that was up to 36% and 45% overweight, respectively.
4. Despite the fact that these roads were not designed to withstand heavy loads, gross vehicle weights in excess of 250,000 lb. were recorded for FM roads, and up to 364,000 lb. for SH roads.
5. Utilizing traditional ESALs in the service life analysis overpredicts the service life of US, SH, and FM roadways by an average of 137%, 151%, and a staggering 229%, respectively.
6. Utilizing the Modified ESALs derived from the developed EALFs factors also overpredicted the service life of the selected highways. However, this overprediction was less pronounce. The service life of US highways was overpredicted by an average of 102%,

while the service life of SH highways and FM roadways were overpredicted by 120% and 118%, respectively.

7. The Modified ESALs led to a more accurate service life prediction when compared to Traditional ESALs. This was because ESALs derived from the Modified EALFs were better suited to estimate the damage imparted by heavy vehicles operating on these highways.
8. If it is not possible to acquire axle load spectra information at a particular site, using pneumatic tube counters to acquire the traffic information and applying the Modified EALFs can still yield satisfactory service life predictions.
9. The Default TxME traffic values tend to overpredicted the service life in FM roadways by an average of 262%, SH highways by 164%, and US highways by 140%. It is also important to note that for highways with significant overweight traffic, the overprediction of the Default TxME traffic values was more pronounced.
10. Due to seasonal variations in material properties, only using the winter modulus values in the numerical simulations led to overprediction of the service life by an average of 157% for FM roadways, 116% for SH highways, and 120% for US highways.
11. When using the summer modulus values, service life of FM highways was underpredicted by an average of 53% for FM roadways, 91% for SH highways, and 92% for US highways. This is the result of summer modulus values being significantly lower compared to winter modulus values due to viscoelastic properties of the asphalt layer.
12. FM roads failed primarily because of their thin surfaced treated layers and relatively low structural capacity compared to SH and US highways. FM roadways with less robust pavement structures were found to be more sensitive to increasing traffic loads as opposed to SH and US highways because they were not designed to carry high volumes of OW traffic.
13. Due to drastic increases in truck traffic generated from energy developing activities, certain highways experienced a service life reduction of up to 159 months (13.25 years).

8.2 Recommendations for Future Work

The following comments are recommendations that could be applied to future work to enhance the axle load spectra and the service life predictions of current and future highways:

1. Collect additional portable WIM data in highways throughout the state that have heavy overweight traffic or are located in energy developing areas. (Permian Basin, Barnett Shale, Granite Wash, etc.)
2. Collect portable WIM data at multiple time intervals for all seasons (Fall, Winter, Spring, Summer) for better characterization of the traffic.
3. Study other energy developing areas with different climatic conditions (such as the Granite Wash and Barnett Shale) to compare the service life of those highways.
4. Collect FWD data multiple times throughout the year at each highway for better indication of actual material properties of each pavement structure.
5. Monitor the pavement service life of a newly constructed/rehabilitated road from initial construction to compare the actual pavement life to the predicted service life based on the axle load spectra.

REFERENCES

Al-Qadi, I., Wang, H., Ouyang, Y., Grimmelsman, K., & Purdy, J. E. (2016). LTBP Program's Literature Review on Weigh-in-Motion System (No. FHWA-HRT-16-024). United States. Federal Highway Administration

American Association of State Highway and Transportation Officials (AASHTO). (2008). *Mechanistic-Empirical Pavement Design Guide, Interim Edition: A Manual of Practice*. Washington, DC. Pavement Design Guide, Interim Edition: A Manual of Practice. Washington, DC.

Ashtiani, R., Morovatdar, A., Licon, C., Tirado, C., Gonzales, J., & Rocha, S. (2019). *Characterization and Quantification of Traffic Load Spectra in Texas Overweight Corridors and Energy Sector Zones* (No. FHWA/TX-19/0-6965-1), (In Press).

Bierling, D., Martin, M., See, A., Morgan, C., Bujanda, A., and Kelly, N. (2014). Energy Development Impacts on State Roadways: A Review of DOT Policies, Programs and Practices across Eight States Final Report. Transportation Policy Research Center.

Blincoe, L. J., Miller, T. R., Zaloshnja, E., and Lawrence, B. A. (2015). The economic and societal impact of motor vehicle crashes, 2010. Report No. DOT HS 812 013, National Highway Traffic Safety Administration, Washington, D.C.

Buchanan, M. S. (2004). "Traffic load spectra development for the 2002 AASHTO Design Guide," Report No. FHWA/MS-DOT-RD-04-165, Mississippi State University, Jackson, MS.

Burnos, P., & Rys, D. (2017). The effect of flexible pavement mechanics on the accuracy of Axle load sensors in vehicle weigh-in-motion systems. Sensors, 17(9), 2053.

Cardinal Scales. (n.d.). Truck Scales. Retrieved November 14, 2017, from https://cardinalscale.com/product/product-category/Truck-Scales

Chandra, D., K. M. Chua, and R. L. Lytton (1989). "Effects of Temperature and Moisture on the Load Response of Granular Base Material in Thin Pavements." Transportation Research Record 1252, National Research Council, Washington, D.C., pp 33-41.

Chang, D. W., Kang, Y. V., Roesset, J. M., & Stokoe, K. (1992). Effect of depth to bedrock on deflection basins obtained with Dynaflect and falling weight deflectometer tests. Transportation Research Record, 8-8.

Charles Gurganus (2016). Project and Pavement Performance Associated with Energy Development and Production. Research Report RR-16-02. Texas A&M Transportation Institute. Texas Department of Transportation.

Chen, D. H., & Scullion, T. (2006). Using nondestructive testing technologies to assist in selecting the optimal pavement rehabilitation strategy. Journal of testing and evaluation, 35(2), 211-219.

Chen, F. H. (1988). Foundations on Expansive Soils. Elsevier, Amsterdam, the Netherlands.

Epps, J. A., Newcomb, D., Ellis, D. and Stockton, B., "Impacts of Reduced Pavement Rehabilitation and Maintenance on Energy Development in Texas", Research Project 0-6581 Work Request No. 27, March 2013.

Epps, J. A., and Newcomb, D. E. (2016). Maintenance and Rehabilitation Strategies For Repair of Road Damage Associated with Energy Development and Production. Implementation Report IR-15-03. Retrieved October 20, 2017.

Ewing, B. T., Watson, M. C., McIntruff, T., and McIntruff, R. N. (2014). Economic Impact Permian Basin's Oil and Gas Industry, Texas Tech University College of Petroleum Engineering, Rawls College of Business, 1-80.

Faruk, A. N., Liu, W., Lee, S. I., Naik, B., Chen, D. H., & Walubita, L. F. (2016). Traffic volume and load data measurement using a portable weigh in motion system: A case study. International Journal of Pavement Research and Technology, 9(3), 202-213.

Federal Highway Administration (2014), "Traffic Monitoring Guide," Federal Highway Administration, Office of Highway Policy Information, U.S. Department of Transportation. https://www.fhwa.dot.gov/policyinformation/tmguide/tmg_2013/vehicle-types.cfm

Federal Highway Administration, U. (2016). Traffic Volume Monitoring. Traffic Monitoring Guide.

Gordon, R. L., Reiss, R. A., Haenel, H., Case, E. R., French, R. L., Mohaddes, A., & Wolcott, R. (1996). TRAFFIC CONTROL SYSTEMS HANDBOOK-REVISED EDITION 1996(No. FHWA-SA-95-032).

Haider, S. W., and Harichandran, R. S. (2007). "Relating Axle Load Spectra to Truck Gross Vehicle Weights and Volumes." *Journal of Transportation Engineering*, 133(12), 696-705.

Hopman, R. C. (n.d.). Energy Sector, Powerpoint Presentation. TxDOT.

Highway Research Board (1962), "The AASHO Road Test, Report 5, Pavement Research," Special Report 61E, Highway Research Board, National Academy of Sciences, Washington, D.C.

Hu, S., Zhou, F. and Scullion, T. (2011). Texas M-E Flexible Pavement Design System: Literature and Proposed Framework, Report No. FHWA/TX-12/0-6622-1, Texas Transportation Institute, College Station, TX.

Hu, S., Zhou, F., and Scullion, T. (2012). Texas M-E Flexible Pavement Design System: Literature Review and Proposed Framework, Report No. FHWA/TX-12/0-6622-1, Texas A&M Transportation Institute, College Station, TX.

Insurance Institute for Highway Safety, General Statistics. (2016). Retrieved October 05, 2017, from http://www.iihs.org/iihs/topics/t/general-statistics/fatalityfacts/state-by-state-overview.

Intercomp. (n.d.). LS630-WIM™ Portable Low-Speed Weigh-In-Motion Scale. Retrieved November 13, 2017, from https://www.intercompcompany.com/ls630-portable-low-speed-weigh-in-motion-scale-p-46.html

Intercomp. (n.d.). PT300DW™ Wheel Load Scales. Retrieved November 14, 2017, from https://www.intercompcompany.com/pt300dw-wheel-load-scales-p-10042.html

International Road Dynamics. (n.d.). Lineas Quartz WIM Sensor by Kistler for Weigh in Motion. Retrieved November 15, 2017, from https://www.irdinc.com/pcategory/wim-scales--sensors/lineas-quartz-wim-sensor-by-kistler.html

International Road Dynamics, Inc.(n.d.) PAT Bending Plate System® - Bending Plate WIM Scales. Retrieved November 13, 2017, from https://www.irdinc.com/pcategory/wim-scales--sensors/irdpat-bending-plate-system.html

International Road Dynamics. (n.d.). Piezoelectric RoadTrax BL. Retrieved November 15, 2017, from https://www.irdinc.com/pcategory/axle-sensors--accessories/piezoelectric-roadtrax-bl.html

Jiang, Y., Li, S., Nantung, T. E., and Chen, H. (2008). Analysis and Determination of Axle Load Spectra and Traffic Input for the Mechanistic-Empirical Pavement Design Guide, Publication FHWA/IN/JTRP-2008/07, Joint Transportation Research Program, Indiana Department of Transportation and Purdue University, West Lafayette, Indiana.

Klein, L. A. (2001). Sensor technologies and data requirements for ITS.

Kwon, T. M. (2012). "Development of a Weigh-Pad-Based Portable Weigh-In-Motion," Final Report MN/RC 2012-38, University of Minnesota Duluth, Duluth, MN.

Kwon, T. M. (2016). "Implementation and Evaluation of a Low-Cost Weigh-In-Motion System." Final Report MN/RC 2016-10, University of Minnesota Duluth, Duluth, MN.

Labarrere,J.(n.d.).BridgeWIM.RetrievedMay12,2019,fromhttp://www.iswim.org/index.php?nm=2&nsm=6&lg=en

Lawrence, K. (2001). *Sensor Technologies and Data Requirements for ITS Applications*. Artech House ITS Library, Boston, MA, USA.

Lydon, M., Taylor, S. E., Robinson, D., Mufti, A., & Brien, E. J. O. (2016). Recent developments in bridge weigh in motion (B-WIM). Journal of Civil Structural Health Monitoring, 6(1), 69-81.

Malla, R. B., Sen, A., and Garrick, N. W. (2008). "A special fiber optic sensor for measuring wheel loads of vehicles on highways." *Sensors*, 8(4), 2551-2568.

Mimbela, L. E. Y., & Klein, L. A. (2000). Summary of vehicle detection and surveillance technologies used in intelligent transportation systems.

Morovatdar, A., Ashtiani, R., Licon, C., Tirado, C., Mahmoud, E. (2020). A Novel Framework for the Quantification of Pavement Damages in the Overload Corridors. *Transportation Research Record*, (In Press).

Morovatdar, A., Ashtiani, R., Licon, C., Tirado, C. (2019). Development of a Mechanistic Approach to Quantify Pavement Damage using Axle Load Spectra from South Texas Overload Corridors. *In Geo-Structural Aspects of Pavements, Railways, and Airfields Conference, (GAP 2019),* (In Press).

NCHRP (2004), Guide for Mechanistic-Empirical Design of Pavement Structures, NCHRP Project 1-37A, National Cooperative Highway Research Program, Washington, D.C.

Oh, J., Walubita, L. F., and Leidy, J. (2015). "Establishment of Statewide Axle Load Spectra Data using Cluster Analysis." *KSCE Journal of Civil Engineering*, 19(7), 2083.

Olsen, L., and Media, A. S. (n.d.). Boom in oil and traffic deaths. Retrieved October 07, 2017, from http://www.houstonchronicle.com/local/boom-in-oil-traffic-deaths/.

Pavement Management Information System: Rater's Manual, (2016), Texas Department of Transportation

Prozzi, J. A., and Hong, F. (2005). Evaluate Equipment, Methods, and Pavement Design Implications for Texas Conditions of the AASHTO 2002, Axle Load Spectra Traffic Methodology. Research Report FHWA/TX-05/0-4510, Center for Transportation Research, The University of Texas at Austin, Austin, TX.

Prozzi, J. A., Murphy, M., Loftus-Otway, L., Banerjee, A., Kim, M., Wu, H., Prozzi, J.P., Hutchinson, R., Harrison, R., Walton, C.M., Weissmann, J., and Weissmann, A. (2012), Oversize/Overweight Vehicle Permit Fee Study, Report No. FHWA/TX-13/0-6736-2, Center for Transportation Research, University of Texas at Austin, Austin, TX.

Prozzi, J. A., Buddhavarapu, P., Kouchaki, S., Weissmann, J., Weissmann, A., Jiang, N., Savage, K., and Walton, C. M. (2017). Infrastructure-Friendly Vehicles to Support Texas Economic Competitiveness. Report No. FHWA/TX-16/0-6817-1, Center for Transportation Research, University of Texas at Austin, Austin, TX.

Quiroga, C., Tsapakis, I., and Holik, W. (2016). Descriptive Statistics and Well County Maps. Implementation Reports .

Refai, H., Othman, A., and Tafish, H. (2014). "Portable Weigh-In-Motion for Pavement Design." Final Report No. FHWA-OK-14-07, The University of Oklahoma, Norman, OK.

Sayyady, F., Stone, J., List, G., Jadoun, F., Kim, Y., and Sajjadi, S. (2011). "Axle Load Distribution for Mechanistic-Empirical Pavement Design in North Carolina: Multidimensional Clustering Approach and Decision Tree Development." *Transportation Research Record: Journal of the Transportation*

Research Board, (2256), 159-168.

"Summary of Drilling, Completion and Plugging Reports Processed for 2012," Railroad Commission of Texas, January 7, 2013. http://www.rrc.state.tx.us/data/drilling/txdrillingstat.pdf.

Sridhar, B. K. (2008), "Characterization and Development of Axle Load Spectra to Enhance Pavement Design and Performance on the Basis of New Mechanistic-Empirical Design Guide in Louisiana", Louisiana State University, Baton Rouge, LA.

Sebesta, S.D. (2014). Rehabilitation Recommendations for SH72 in Karnes County. TM-14-06. Texas A&M Transportation Institute. Texas Department of Transportation.

Swan, D., Tardif, R., Hajek, J., and Hein, D. (2008). "Development of Regional Traffic Data for the Mechanistic-Empirical Pavement Design Guide." *Transportation Research Record: Journal of the Transportation Research Board*, (2049), 54-62.

Tang, Y., Zhang, C., Gu, R., Li, P., & Yang, B. (2017). Vehicle detection and recognition for intelligent traffic surveillance system. Multimedia tools and applications, 76(4), 5817-5832.

Texas Transportation Researcher (1989). "Models Developed to Predict Climatic Effects on Low-Volume Roads." Vol. 25, No. 4, Texas Transportation Institute, Texas A&M University, College Station, TX, pp 5-6.

Turnstall, T., Oyakawa, J., Conti G,,Wells M., Hernandez,J ., Lee, Y., Loeffelhilz V,. Ravi N., Rodriguez J., Teng, F., Torres, C., Torrez, H., Wang, B., and Zhang, J. (2014). Economic Impact of the Eagle Ford Shale. Center for Community and Business Research, UTSA Institute for Economic Development, San Antonio, TX.

Turnstall, T., Oyakawa, J., Roberts, S., Eid, H., Abalos, R., Wang, T., Calderon, E., and Melara, K. (2013). Economic Impact of the Eagle Ford Shale. Center for Community and Business Research, UTSA Institute for Economic Development, San Antonio, TX.

Turochy, R. E., Timm, D. H., and Mai, D. (2015). Development of Alabama Traffic Factors for use in Mechanistic-Empirical Pavement Design, Report No. FHWA/ALDOT 930-793, Auburn University, Auburn, Alabama.

TxDOT. (2017). Permian Road Safety Coalition Safety Forum. Texas Department of Transportation.

TxDOT. (2016). Transportation in the Energy Sector. Texas Department of Transportation.

U. S. Energy Information Administration. (2017). Eagle Ford Region Drilling Productivity Report. Retrieved October 20, 2017, from https://www.eia.gov/petroleum/drilling/pdf/eagleford.pdf

U. S. Energy Information Administration. (2017). Permian Region Drilling Productivity Report. Retrieved October 18, 2017, from https://www.eia.gov/petroleum/drilling/pdf/permian.pdf.

Walubita, L. F., Prakoso, A., Aldo, A., Lee, S. I., & Djebou, C. (2019). Using WIM Systems and Tube Counters to Collect and Generate ME Traffic Data for Pavement Design and Analysis: Technical Report (No. FHWA/TX-18/0-6940-R1).

Walubita, L. F., Faruk, A. N., and Ntaimo, L. (2015). Intelligent Freight Monitoring: A Review of Potential Technologies. Texas A&M Transportation Institute Report 2015-8, College Station, TX.

Wang, H., Zhao, J. and Wang, Z. (2015). "Impact of Overweight Traffic on Pavement Life using Weigh-in-Motion Data and Mechanistic-Empirical Pavement Analysis." *9th International Conference on Managing Pavement Assets*, Washington, D.C.

Wu, D., Yuan, C. and Liu, H. (2017). "A Risk-based Optimization for Pavement Preventative Maintenance with Probabilistic LCCA: A Chinese Case," *International Journal of Pavement Engineering*, 11-25.

Xiao, D. X., and Wu, Z. (2016). "Using Systematic Indices to Relate Traffic Load Spectra to Pavement Performance." *International Journal of Pavement Research and Techno*logy, 9(4), 302-312.

APPENDIX A. VISUAL INSPECTION SURVEYS

- ***Laredo District – Farm-to-Market (FM) 468***

The first visual inspection survey was conducted on Farm-to-Market (FM) 468 in LaSalle County of the Laredo District. Upon initial inspection, FM 468 appeared to be in a severely distressed state exhibiting multiple distress types. The first distress present on both K1 and K6 lanes was severe flushing on both right and left wheel paths throughout the entire section, as shown in Figure A.1. The flushing rated 3, according to TxDOT's 2018 PMIS Pavement Rater's Manual, begins in the intersection with FM 469 and continues past the Dimmit County line. The second documented distress was shallow to severe rutting throughout most of the inspected section. The rutting illustrated in Figure A.2, ranged from .25in to .50in in both wheel paths and covered approximately 70% of the wheel paths area. Moreover, an area with a large patch appearing to be milled out and replaced, as shown in Figure A.3, was also reported. However, the patch already seems to be disintegrating. Alligator cracking is also developing in the wheel paths covering an area of approximately 30%. In addition, raveling and potholes were also spotted in certain places of the inspected area. Heavily loaded vehicles coupled with a thin asphalt layer are believed to be the reasons for the many distresses present and the poor ride quality of FM 468.

Figure A.1. Severe Flushing in FM 468 - La Salle County

Figure A.2. Shallow Rutting in FM 468 - La Salle County

Figure A.3. Patches in FM 468 - La Salle County

- ***Laredo District – US Highway 83***

US highway 83 displayed multiple distress types; raveling among the most significant. The raveling rated 2 was present throughout most of the inspected section, particularly in between the right and left wheel paths and towards the right shoulder. As illustrated in Figure A.4 and highlighted by the red oval one can identify areas where a significant amount of aggregate is missing. Shallow rutting was also reported in the inspected section ranging from .25in to .313in and covering approximately 40% of the wheel paths area. Additionally, as illustrated in Figure A.5, flushing rated 2 can be spotted in certain parts of the section along with alligator cracking.

Figure A.4. Raveling and Missing Aggregate in US 83 -Dimmit County

Figure A.5. Flushing and Shallow Rutting in US 83 -Dimmit County

- ***San Antonio District – State Highway (SH) 16***

In State Highway (SH) 16 shallow and deep rutting conditions in both wheel paths were observed throughout the entire pavement section. The rutting ranged from .25in to .625in and covered approximately 90% of the wheel paths area. Severe flushing rated 3, was also present on both K1 and K6 lanes and both right and left wheel paths, as shown in Figure A.6. Additionally, the raveling rated 2, can be spotted primarily on the right wheel path and towards the right shoulder, illustrated in Figure A.7. As of 2019, work to reconstruct SH 16 between Tilden and Jourdanton is under progress.

Figure A.6. Distresses Present in SH 16-Atascosa County

Figure A.7. Raveling and Rutting in SH 16-Atascosa County

- ***San Antonio District – Farm-to-Market (FM) 99***

FM 99 also appeared to be in a poor and distressed condition exhibiting shallow rutting, flushing, and pot hole formation. Shallow to severe rutting is present throughout the entire inspected section ranging from .25in to .50in. in both wheel paths and covering approximately 65% of the wheel paths area, as shown in Figure A.8. Flushing was also detected on both K1 and K6 lanes and rated at a level 2. Nonetheless, as illustrated in Figure A.9, the most significant distress was the severity of the potholes present in FM 99. Several large potholes were documented in the small inspection

area however, while driving on the rest of FM 99 the inspectors encountered numerous potholes and failures. Heavily overloaded vehicles have adversely damaged much of FM 99 and have compromised its structural integrity.

Figure A.8. Rutting and Flushing in FM 99 - McMullen County

Figure A.9. Pothole Formation in FM 99 - McMullen County

- ***San Antonio District – Farm-to-Market (FM) 624***

Similarly, FM 624 was also in a distressed condition exhibiting shallow to deep rutting, flushing, and pot hole formation. The research team documented shallow and deep rutting throughout most

of the inspected section ranging from .25in to .625in in both wheel paths and covering approximately 60% of the wheel paths area as shown in Figure A.10. Moreover, severe flushing was also documented on both K1 and K6 lanes and rated at a level 3. As illustrated in Figure A.11, several large potholes were also identified and logged.

Figure A.10. Rutting and Flushing in FM 624 - McMullen County

Figure A.11. Pothole Formation in FM 624 - McMullen County

- ***Corpus Christi District – US Highway 281***

US 281 also exhibited multiple distresses such as shallow rutting, alligator cracking, and longitudinal cracks. Shallow rutting was reported through most of the inspected section ranging

from .25 in to .375 in. in both wheel paths and covering approximately 40% of the wheel paths area as illustrated in Figure A.12. Alligator cracking was also documented primarily on the right wheel path and covering approximately 30% of the wheel paths area. However, the most significant distress was the sealed and non-sealed longitudinal cracks present throughout the R1 lane and covering an approximate area of 30%. Additionally, the longitudinal cracking has led the right shoulder to separate and begin to sink in. Figures A.13 and A.14 respectively, show the severity of the longitudinal cracks present.

Figure A.12. Rutting in US 281 – Live Oak County

Figure A.13. Longitudinal Cracks in US 281 – Live Oak County

Figure A.14. Longitudinal Cracking in Right Shoulder in US 281 –Live Oak County

- ***Corpus Christi District – State Highway (SH) 72***

Upon inspection, SH 72 appeared to be in a fair condition as illustrated in Figure A.15. Since its recent reconstruction in 2013-2014, the only observable distresses that have initiated are shallow rutting and moderate flushing. Moreover, if the current overweight traffic persists, SH 72 will soon start to develop more severe rutting.

Figure A.15. Pavement Conditions of SH 72 –Karnes County

- ***Corpus Christi District – BU 181/SH 123***

Similarly, to the other highways, the pavement distresses documented in BU 181/SH 123 were

also shallow rutting and flushing. The research team logged shallow rutting throughout most of the inspected section ranging from .25in to .375in primarily on the right wheel path and covering approximately 50% of the wheel paths area as shown in Figure A.16. Flushing was also spotted as illustrated in Figure A.17 and rated at a level 2.

Figure A.16. Shallow Rutting in BU 181/SH 123 –Karnes County

Figure A.17. Flushing in BU 181/SH 123 –Karnes County

- ***Yoakum District – SH 119***

SH 119 in the Yoakum District appeared to be in a structurally sound and fair condition as shown in Figure A.18. Since its recent lane widening, the only distress that has started to develop is shallow rutting. Despite drilling operations and pipe line construction, SH 119 has remained in an adequate condition.

Figure A.18. Pavement Conditions of SH 119 - Dewitt County

- ***Yoakum District – US 183***

The final visual inspection survey was conducted on US highway 183, the major pavement distress documented was the seal and non-sealed longitudinal cracking throughout both K6 and K1 lanes, illustrated in Figure A.19 and A.20 respectively. The longitudinal cracks covered an approximate area of 95%. In addition, shallow rutting was also recorded ranging from .25in to .375in and covering approximately 30% of the wheel paths area.

Figure A.19. Pavement Conditions of US 183 - Gonzales County

Figure A.20. Longitudinal Cracks of US 183 - Gonzales County

APPENDIX B. ONLINE SURVEY QUESTIONNAIRE

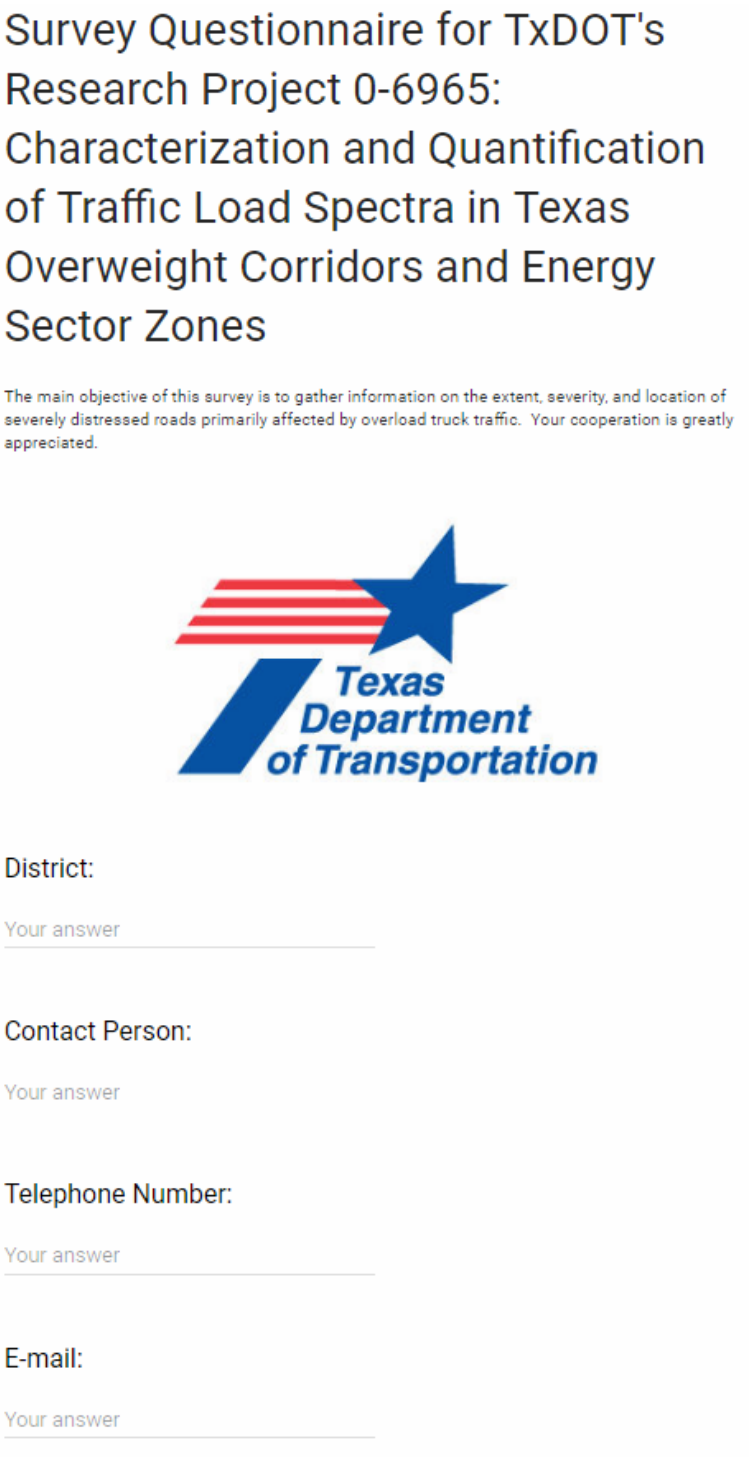

Figure B.1 First Page of Survey Questionnaire

Questionnaire

1. Are the transportation infrastructure facilities in your district adversely affected by overweight vehicles due to energy development activities?

- ○ Yes
- ○ No

2. How do you rank the severity of the damages imparted by overweight vehicles associated with energy development operations in your district?

	1	2	3	4	5	6	7	8	9	10	
Minimal	○	○	○	○	○	○	○	○	○	○	Severe

3. What are the typical pavement distresses/damages due to energy production activities in your district?

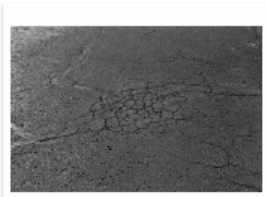

☐ Fatigue (Alligator) Cracking

☐ Edge Cracks

☐ Longitudinal and Transverse Cracking

☐ Reflection Cracking

☐ Slippage Cracks

☐ Rutting

☐ Pot holes

☐ Raveling

☐ Spalling

☐ Punchout

☐ Faulting

☐ Polished Aggregate

☐ Transverse Cracks (CPCD Pavements)

☐ Shattered Slabs and Corner Breaks (CPCD Pavements)

☐ Other:

☐ Not Applicable

Figure B.2 Second Page of Survey Questionnaire

4. Do you have an active Weigh-In-Motion (WIM) station available in your District?

- ○ Yes
- ○ No

5. If yes, how close is the Weigh-In-Motion (WIM) station from severely distressed roads?

- ○ 5 miles
- ○ 10 miles
- ○ 20 miles
- ○ 30 miles
- ○ Not Applicable

6. What are the technologies/equipment that are used to collect traffic information in your district.

- ☐ Cameras
- ☐ Pneumatic Tube Counters
- ☐ Automated Vehicle Classifiers (AVC)
- ☐ Inductive Loops Detectors (ILD)
- ☐ WIM Stations
- ☐ Portable WIM Devices
- ☐ Infrared sensors
- ☐ Microwave Radars
- ☐ Ultrasonic Sensors
- ☐ Acoustic Array Sensors
- ☐ In-road Pucks Such as Groundhogs
- ☐ Other: _____

7. What is the frequency of Over-Size/Over-Weight (OS/OW) truck traffic experienced in your District highway network?

	1	2	3	4	5	6	7	8	9	10	
Minimal	○	○	○	○	○	○	○	○	○	○	Significant

Figure B.3 Third Page of Survey Questionnaire

8. Based on your observations, how do you characterize the trend of Over-Size/Over-Weight (OS/OW) truck traffic in your District:

- ◯ Increasing
- ◯ Decreasing
- ◯ Stayed the Same

9. Please indicate highways within your District with high volume of OS/OW truck traffic.

Your answer

10. Please indicate highways and roads within your District that are severely distressed and need substantial repair/maintenance.

Your answer

11. Rate energy development impact on the transportation infrastructure network in your district.

	1	2	3	4	5	6	7	8	9	10	
Minimal Impact	◯	◯	◯	◯	◯	◯	◯	◯	◯	◯	Severe Impact

12. Rate the energy development impact level in your district State Highways (SH).

	1	2	3	4	5	6	7	8	9	10	
Minimal Impact	◯	◯	◯	◯	◯	◯	◯	◯	◯	◯	Severe Impact

13. Rate the energy development impact level in your district Farm to Market (FM) roads.

	1	2	3	4	5	6	7	8	9	10	
Minimal Impact	◯	◯	◯	◯	◯	◯	◯	◯	◯	◯	Severe Impact

Figure B.4 Fourth Page of Survey Questionnaire

14. What are the typical pavement sections at your District? Mark all that Apply

- [ ] Continuously Reinforced Concrete Pavement (CRCP)
- [ ] Jointed Reinforced Concrete Pavement (JRCP)
- [ ] Concrete Pavement Contraction Design (CPCD) or Jointed Concrete Pavement(JCP)
- [ ] Thick Asphaltic Concrete Pavement (greater than 5-1/2")
- [ ] Intermediate Thickness Asphaltic Concrete Pavement(2-1/2" to 5-1/2")
- [ ] Thin Surfaced Flexible Base Pavement (less than 2-1/2")
- [ ] Asphalt Surfacing with Heavily Stabilized Base
- [ ] Asphalt Surfacing Flexible Base over Stabilized Sub-Base Pavement
- [ ] Overlaid and/or Widened Old Flexible Pavement
- [ ] Inverted Flexible Pavement
- [ ] Other:

15. Inverted pavement design is consisted of an asphalt layer, then an unbound base layer supported by stabilized base layer (See Picture Below). Several districts use this design concept to mitigate the issues associated with reflective cracking. Please indicate if you benefited from this design concept in your district.

- ○ Yes
- ○ No

16. If so, how would you rate the performance of this design?

1	2	3	4	5	6	7	8	9	10
○	○	○	○	○	○	○	○	○	○

17. Do you mind if we contact you for more information?

- ○ Yes
- ○ No

Figure B.5 Fifth Page of Survey Questionnaire

VITA

Carlos Licon was born and raised in El Paso, Texas where he attended Captain John L. Chapin High School and completed the Pre-Engineering Magnet Program in 2013. He then attended Beloit College but transferred to the University of Texas at El Paso where he obtained his Bachelor of Science in Civil Engineering in the Fall of 2017. Immediately after graduating, Carlos enrolled in the master's graduate program in Civil Engineering at UTEP where he worked as a graduate research assistant under the guidance of Dr. Reza Ashtiani.

At UTEP, Carlos primary worked on a research project for the Texas Department of Transportation (TxDOT). During his time at UTEP, Carlos was as Stars Scholarship Fund recipient, a Hispanic Scholarship Fund recipient, and a Dwight D. Eisenhower Transportation fellow that granted him the ability to attend the Transportation Research Board (TRB) annual meeting in 2019. Ultimately, he completed his Master of Science in Civil Engineering in the Summer of 2019.

Contact Information: Carloslicon50@outlook.com

This thesis was typed by Carlos Licon Jr.